P-06-226

Forsmark site investigation

Fracture mineralogy

Results from KFM06B, KFM06C, KFM07A, KFM08A, KFM08B

Björn Sandström, Earth Sciences Centre,
Göteborg University

Eva-Lena Tullborg, Terralogica AB

December 2006

Svensk Kärnbränslehantering AB
Swedish Nuclear Fuel
and Waste Management Co
Box 5864
SE-102 40 Stockholm Sweden
Tel 08-459 84 00
+46 8 459 84 00
Fax 08-661 57 19
+46 8 661 57 19

ISSN 1651-4416
SKB P-06-226

Forsmark site investigation

Fracture mineralogy

Results from KFM06B, KFM06C, KFM07A, KFM08A, KFM08B

Björn Sandström, Earth Sciences Centre,
Göteborg University

Eva-Lena Tullborg, Terralogica AB

December 2006

Keywords: Fracture mineralogy, Geological evolution, Low temperature minerals, Stable isotopes, Calcite, Geochemistry, AP PF 400-06-077.

Abstract

Detailed fracture mineral investigations have been carried out on samples from drill cores KFM06B, KFM06C, KFM07A, KFM08A and KFM08B from the Forsmark site investigation. Open as well as sealed fractures have been sampled. The main objectives with this study are to identify fracture minerals and to distinguish different fracture mineral generations, their parageneses, relative ages and if the different fracture mineral parageneses occur in prefered fracture orientations. Mineralogical and geochemical information, as well as paleohydrogeological evidences, e.g. based on calcite geochemistry and uranium series disequilibrium (USD) have been obtained for the hydrogeochemical modelling.

The analyses presented in this report include microscopy, electron microscopy (SEM-EDS), X-ray diffraction (XRD) and chemical analyses of fractures filling material. Furthermore stable isotope analyses ($^{87}Sr/^{86}Sr$, $\delta^{18}O$, $\delta^{13}C$ in calcite, $\delta^{18}O$ in quartz, $\delta^{34}S$ in pyrite and $^{87}Sr/^{86}Sr$ in the wall rock) have been carried out to obtain information of paleohydrogeological and formation conditions during the precipitation of the fracture minerals. Uranium series analyses (USD) provide information of potential mobilisation or deposition of uranium during the last 1 Ma.

The most common fracture minerals in the area are chlorite, calcite, laumontite, quartz, adularia (low-temperature K-feldspar), prehnite, epidote, hematite, pyrite and clay minerals. Amongst the clay minerals, corrensite is the most common. Other identified clay minerals are illite, smectite, saponite and mixed-layer illite/smectite.

From the examined drill cores and data presented in previous fracture mineralogy reports /Sandström et al. 2004, Sandström and Tullborg 2005/, 4 different generations of fracture mineralizations have been distinguished: 1) quartz-epidote-chlorite, 2) adularia-albite-hematite-prehnite-laumontite-calcite-chlorite/corrensite, 3) quartz-calcite-adularia-albite-pyrite-asphaltite 4) calcite-clay minerals. Generation 1 is separated in time from Generation 2. Generation 2 represents a complex and probably prolonged period of hydrothermal alteration and precipitation of hydrothermal minerals in the area. Subsequently, after a period of dissolution of the older fracture fillings, Generation 3 minerals have precipitated at low temperatures. The precipitation of clay minerals and calcites in Generation 4 has probably occurred during a long period until present. Generation 1 is preferably found in subhorizontal or steep NW striking fractures, Generation 2 in steep NE to N striking fractures, while the later generations are found in most orientations but preferably in horizontal to subhorizontal fractures.

Geochemical analyses have been carried out in order to get an overview of the main and trace element concentrations in the fracture fillings. The results are compared with previous analyses in /Sandström and Tullborg 2005/. One of the reasons for doing “bulk fracture filling” analyses is to ensure that no extreme trace element concentrations are present, e.g. in minor phases not spotted in the the mineral identification. Uranium is an element that shows varying and in some cases very high contents in previous analyses (0.5 to 2,300 ppm). The present analyses are all in the intervall 2.7 to 164 ppm. However, U/Th ratios are generally higher in the fracture fillings compared with the host rock, indicating uranium mobility.

Uranium series analyses (USD) indicate a possible uranium redistribution during the last 1 Ma, more significantly in the uppermost 150 m of the bedrock although some of the samples taken from deeper levels also indicate a possible late mobilisation of uranium.

Sammanfattning

Denna rapport presenterar resultaten från den detaljerade sprickmineralogiska undersökningen av borrkärnorna KFM06B, KFM06C, KFM07A, KFM08A och KFM08B från Forsmarks platsundersökning. Både öppna och läkta sprickor har provtagits. Syftet med studien är att identifiera sprickmineral samt att ta fram en relativ geokronolokisk sekvens av sprickmineralgenerationer, deras parageneser och om de olika mineralparageneserna förekommer i vissa dominerande riktningar. Vidare ges geokemisk information om sprickfyllnader och paleohydrogeologisk information baserad på bl.a. stabila isotoper, kalcit-geokemi och uranserieanalys till den hydrogeokemiska modelleringen.

Resultaten som presenteras i denna rapport har tagits fram med hjälp av bl.a. mikroskopering, svepelekronmikroskopering (SEM-EDS), XRD och kemanalyser av sprickfyllnader. Analyser av stabila isotoper ($^{87}Sr/^{86}Sr$, $\delta^{18}O$, $\delta^{13}C$ i kalcit, $\delta^{18}O$ i kvarts, $\delta^{34}S$ i pyrit och $^{87}Sr/^{86}Sr$ i sidoberget) har genomförts för att få fram information om paleohydrogeologiska förhållanden vid utfällningen av sprickmineralen. Uran-serieanalys (USD) ger information om potentiell mobilitet hos uran de sista 1 Ma.

De vanligaste sprickmineralen i området är klorit, kalcit, laumontit, kvarts, adularia (låg-temperatur Kalifältspat), prehnit, epidot, hämatit, pyrit och lermineral. Det vanligast förekommande lermineralet är korrensit, andra förekommande lermineral är illit, smektit, saponit och blandskikt av illit och smektit.

Från de undersökta borrkärnorna har fyra generationer av sprickmineraliseringar tagits fram; 1) kvarts-epidot-klorit, 2) adularia-albit-hämatit-prehnit-laumontit-kalcit-klorit/korrensit, 3) kvarts-kalcit-adularia-albit-pyrit-asfaltit, 4) kalcit-lermineral. Generation 1 och 2 är klart separerade i tid och Generation 2 representerar troligen en komplex och antagligen utdragen period av hydrotermal aktivitet och utfällning av hydrotermala mineral. Generation 2 avlöses av en upplösning av äldre sprickfyllnader och sedan kristallisation av Generation 3-mineral vid låga temperaturer. Utfällning av lermineral och kalcit som hör till Generation 4 har troligen förekommit under en lång period fram tills idag. Generation 1 återfinns mest i subhorisontella eller branta NW-strykande sprickor, Generation 2 i branta sprickor med NE till N strykning medan senare generationer återfinns i de flesta riktningarna men mestadels i horisontella till subhorisontella.

Geokemiska analyser av sprickfyllnader har genomförts för att belysa tillgängligheten av olika huvud- och spårlement längs flödesvägarna. Analyserna har jämförts med tidigare erhållna resultat från /Sandström och Tullborg 2005/. Syftet med analyserna har också varit att upptäcka eventuella mindre faser som är rika på spårelement och som kanske inte har varit möjliga att identifiera med tunnslip eller röntgendiffraktometri (XRD). Från tidigare analyser vet vi att uranhalterna har varierat mycket i sprickfyllnaderna (0,5 till 2 300 ppm). I de prover som analyserats och avrapporteras här är intervallet mindre (2,7 till 164 ppm). Det är dock tydligt att de flesta proverna visar en högre U/Th kvot än sidoberget vilket, vilket indikerar en mobilitet hos uranet.

Uranserieanalys (USD) visar att många av de analyserade sprickorna har utsatts för en möjlig omdistribution av uran de senaste 1 Ma, tydligast är detta i de övre 150 metrarna även om vissa prover från större djup också tyder på en möjlig mobilitet av uran.

Contents

1 Introduction

This document reports the results gained by the detailed fracture mineralogy investigation, which is one of the activities performed within the site investigation at Forsmark. The work was carried out in accordance with activity plan AP PF 400-06-077. In Table 1-1 controlling documents for performing this activity are listed. Both activity plan and method descriptions are SKB's internal controlling documents. This document presents the result from boreholes KFM06B, KFM06C, KFM07A, KFM08A and KFM08B. The locations of the boreholes studied are shown in a map together with the bedrock geology of the Forsmark area (Figure 1-1).

Mapping of fractures and fracture minerals is carried out on all cored boreholes within the site investigation program and this information serves as a basis for the fracture mineral study. However, identifying fracture minerals macroscopically can be very difficult, especially considering clay minerals and other very fine grained mineral coatings. X-Ray Diffractometry, SEM-EDS analyses and conventional petrological microscopy are therefore used in the detailed fracture mineralogical study to identify difficult or fine-grained fracture minerals in order to support the drill core mapping geologist.

Calcites have been sampled since they provide paleohydrogeological information. A major intention with the fracture mineralogy study has been to establish a relative sequence of low-temperature events in the bedrock. The knowledge of this sequence has grown concurrently as more drill cores have been investigated and analysed and the sequence presented in this report is an updated version of the one presented in /Sandström et al. 2004, Sandström and Tullborg 2005/. The different generations are also correlated to the fracture sets defined by /La Pointe et al. 2005/ by combining the knowledge gained from the detailed fracture study with the quantitative data collected during the drill core mapping which has been extracted from the SKB primary data base SICADA.

Analyses of the $^{87}Sr/^{86}Sr$ ratio in rock samples of both fresh and hydrothermaly altered rock samples have been carried out to provide background information for the groundwater sampling as well as the radiometric dating of fracture minerals. Uranium series analyses (USD) provide informations of potential mobilisation or deposition of U during the last 1 Ma.

The flow loggs have been used as a tool for selection of samples of hydraulically conductive fractures, preferably for geochemical analyses

The results are stored in the primary data base (SICADA) and are traceable by the activity plan number.

In addition to the results from the above mentioned boreholes KFM06B, KFM06C, KFM07A, KFM08A and KFM08B also a number of isotope analyses carried out on samples from previous boreholes KFM01A to KFM06A are included in this report. The full description of these samples, including thin sections and SEM-surfaces is however not repeated in the present report. Instead, these are shown in Appendix 1 in P-Report P-04-149 /Sandström et al. 2004/ for boreholes KFM01A, KFM02A, KFM03A and KFM03B and in Appendix 1 in P-Report P-05-197 /Sandström and Tullborg 2005/ for boreholes KFM01B, KFM04A, KFM05A and KFM06A.

Table 1-1. Controlling documents for performance of the activity.

Activity plan	**Number**	**Version**
Sprickmineralogiska undersökningar	AP PF 400-06-077	1.0
Method descriptions	**Number**	**Version**
Sprickmineralogi	SKB MD 144.000	1.0

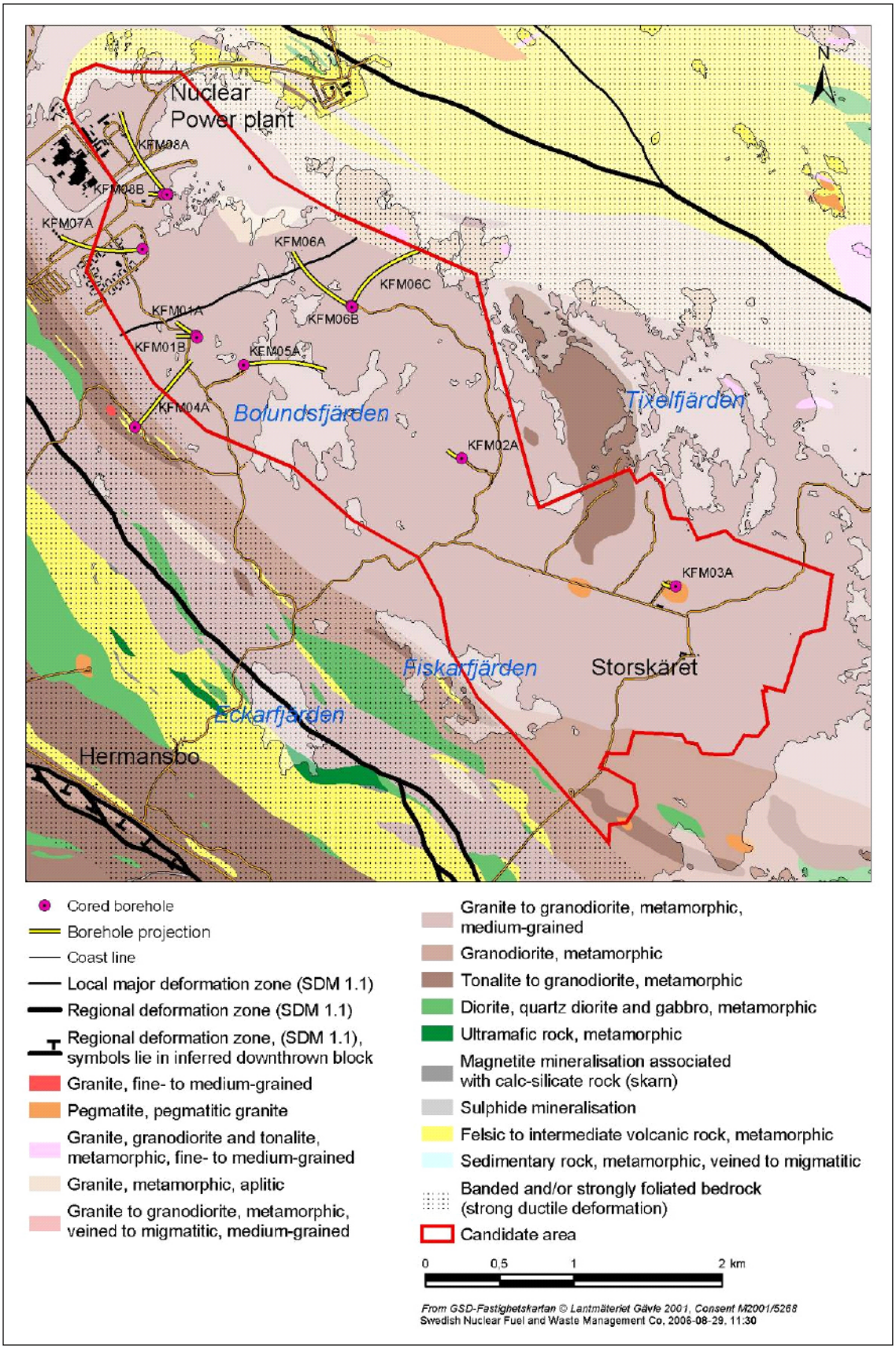

Figure 1-1. *Geological map over the Forsmark site investigation area with projections of the boreholes dealt with in this report /SKB GIS database 2006/.*

2 Objective and scope

The basic idea behind the fracture mineral study is to:

- Identify fracture minerals.
- Distinguish different fracture mineral generations, their parageneses and determine their relative ages.
- Relate the different fracture generations to the geological model of structures, i.e. to the deformation zones and fracture orientation sets.
- Provide mineralogical and geochemical information for the hydrogeochemical modelling.
- Contribute paleohydrogeological information, e.g. based on calcite geochemistry and uranium series disequilibrium (USD) data to the hydrogeochemical modelling.
- Support background information for the selection of samples within the Transport Programme (measurements of porosity, Kd, diffusivity etc).

3 Equipment

3.1 Description of equipment/interpretation tools

- Rock saw.
- Steel knife.
- Tweezers.
- Hand lens.
- Digital camera (Olympus C3020 Zoom).
- Petrographic Microscope (Leica DMRXP).
- Stereo microscope (Leica MZ12).
- Digital microscope camera (Leica DFC 280).
- Scanner (Epson 4180 Photo) and polarizing filters.
- Computer software (Corel Draw 9, Microsoft Word 2003, Microsoft Excel 2003, BIPS Image Viewer 2.51, GeoPlot 1.2).
- Analytical balance (Sartorius 2004 MP).
- Scanning electron microscope (Hitachi S-3400N) with EDS-detector (INCADryCool).
- Mass spectrometer (VG Prism Series II).

The equipment listed above is located at the Earth Sciences Centre, Göteborg University, Sweden. For instruments used at other laboratories, see section 4.5.

4 Execution

4.1 General

Fracture filling samples suitable for microscopy were selected from the drill cores KFM06B, KFM06C, KFM07A, KFM08A and KFM08B. In a few cases, samples were selected from previous drill cores to supplement where geochemical analyses were missing. In total, 115 samples were chosen from representative fractures for different analyses. The selection of the samples was more based on the information expected to be yielded from each sample than to get a statistic overview of the drill cores (see section 4.2).

- The thin-sections have been used to identify mineral parageneses of different fracture filling generations. The division into different generations has been based on textural and mineralogical observations, e.g. cross-cutting relations and dissolution/replacement textures. Ductile, semi-ductile and brittle deformations have been noted as well. Chemical compositions have been used in order to separate different generations of e.g. chlorite and calcites.
- The stable C, O and Sr isotope composition in calcite and S isotope composition in pyrite have been used to distinguish generations and to estimate formation conditions for the different mineral generations.
- The data of fracture orientations extracted from SICADA have been used to obtain a statistical basis from which the fracture mineralogy can be correlated to different fracture orientation sets. The dialogue with the drill core logging geologists has been important during the interpretation of the SICADA data.
- Uranium series analyses (USD) have been carried out to provide information of potential mobility of uranium during the last 1 Ma.

4.2 Selection of samples

Samples have been selected on different grounds:

- For mineralogical identification; the sampling has usually been initiated by the geologists carrying out the drill core logging. XRD and SEM-EDS analyses are performed on many of these samples, but they are also used for thin section preparation and subsequent microscopy.
- Samples selected for mineralogical studies (thin section preparation and surface samples); these samples often show a complex mineralogy and are usually chosen to represent several generations of fracture mineralization. Cross-cutting relations are preferably sampled for the construction of the sequence of fracture mineralizations.
- Fractures filled or coated with calcite are sampled since they can provide paleohydrogeological information. Some of these samples are analysed for stable isotopes, ($\delta^{13}C$, $\delta^{18}O$ and $^{87}Sr/^{86}Sr$) and trace elements.
- Quartz was sampled for $\delta^{18}O$ analyses.
- Pyrite in both open and sealed fractures have been sampled and analysed for $\delta^{34}S$.
- Hydraulically conductive fractures are sampled based e.g. on the flow logging. Priority is given to fractures within the sections sampled for groundwater chemistry.

A problem encountered in the fracture filling studies is the small sample volumes. The representativity of the samples can therefore not be quantified which needs to be considered in the subsequent interpretations.

4.3 Preparations

All samples were photographed before any analyses were carried out.

4.4 Data handling/post processing

The orientation data of different fracture minerals were extracted from SICADA (datafile p_fract_core) and processed using Microsoft Excel and GeoPlot 1.2.

4.5 Analytical work

Thin-sections with a thickness of 30 µm were prepared and analysed with optical microscope and scanning electron microscope (SEM) equipped with an energy dispersive spectrometer (EDS). In order to study minerals grown in the open space in some fractures, fracture surfaces were also prepared and examined by SEM-EDS. Additional fracture surfaces were only briefly examined with stereomicroscope. The SEM-EDS analyses were conducted at Earth Sciences Centre, Göteborg University, with a Hitachi S-3400N equipped with an INCADryCool EDS detector.

The XRD analyses were performed by Dr. Sven Snäll and Dr. Erik Jonsson at SGU in Uppsala. The method is described in /Petersson et al. 2004/.

Fracture calcites were hand picked by tweezers or scraped by a steel knife and analysed for stable carbon, oxygen and for strontium isotope composition. The stable carbon and oxygen isotope analyses were carried out at Earth Sciences Centre, Göteborg University. The method is described in /Sandström et al. 2004/. The Sr isotope analyses were performed at the Institute for Energy Technology in Norway (IFE), and the technique is described in /Sandström et al. 2004/.

Analyses of oxygen isotope ratios on quartz samples were carried out by Prof. Tony Fallick at the Scottish Universities Environmental Research Centre (SUERC) and were measured by the laser fluorination technique described by /Sharp 1990/ as modified for ClF_3 by /Macaulay et al. 2000/. Released oxygen was converted to CO_2 after passage through a mercury diffusion pump and stable isotope ratios measured on CO_2 using an on-line Micromass Prism 2 dual-inlet, triple-collector mass spectrometer. Using this procedure NBS28 gives +9.6‰ for $\delta^{18}O$ relative to VSMOW and analytical precision for isotopically homogeneous samples is better than ± 0.2‰ (1σ).

Pyrite samples were analysed for stable sulphur isotope ratios by Prof. Tony Fallick at SUERC and by IFE, Norway. The analytical techniques are described in /Drake and Tullborg 2006/ and /Sandström et al. 2004/ respectively.

Chemical analyses of powdered fracture filling material were made by Analytica AB in Luleå. The analytical technique is described in /Petersson et al. 2004/.

The U-serie analyses have been carried out at SUERC according to the following procedure: The sample material is furnaced at 600°C (in increments of 100°C if material is highly organic) and washed in a crucible with H_2O and poured into a beaker, 9 M HCl and spike is added (the spike is leaved to equilibriate to room temperature before adding and than allowed to equilibriate within the sample). Aqua regia ($1HCl:1HNO_3$), H_2O_2 and HF digestions are carried out and leached with 4 M HNO_3. An $Fe(OH)_3$ scavenge is carried out using NH_3. The precipitate formed is washed thoroughly and dissolved in conc. HCl and transferred to a clean beaker. The solution is dried down and taken up in ~ 50 ml 9 M HCl and a DIPE (di-isopropylether) and an extraction is conducted to remove any Fe within the sample. The first (chloride) column is pre-conditioned with ~ 20 ml of 1.2 M HCl and 9 M HCl respectively. The sample is then

introduced to the column in 9 M HCl and the Th fraction is collected by washing with (2×25 ml) 9 M HCl. The U fraction is eluted with 150 ml 1.2 M HCl and then taken to dryness (further DIPE extraction can be carried out at this stage if required; indicated by a yellow/orange colour in the solution) and prepared for electrodepositioning. The Th fraction is taken to dryness and then taken back up in 4 M HNO_3 (approx 50 mls) and an aluminum precipitation is accomplished with NH_4OH. The precipitate formed is washed well and dissolved in the minimum conc. HNO_3. The solution is dried down and taken back up in 8 M HNO_3 (approx 50 mls) ready for the second (nitric) column. The second column is pre-conditioned with ~ 20 ml 1.2 M HCl and 8 M HNO_3 respectively and the sample is introduced to the column in 8 M HNO3, and rinsed with 2×25 ml aliquots 8 M HNO_3. The Th fraction is then eluted with 100 ml 9 M HCl and taken to dryness and prepared for electrode positioning.

Rock samples were analysed on their $^{87}Sr/^{86}Sr$ ratio by Dr. Göran Åberg at IFE, Norway, according to the following procedure: Between 50 and 100 mg granitic sample was transferred to a 5 ml Savillex Teflon beaker with lid, added by 3 ml conc. HF and 0.5 ml conc HNO_3. The lid was screwed on loosely and the beaker was put on a hotplate at c 90°C overnight. After the samples were dissolved, the clear solution was evaporated to dryness. 3 ml of 6 M HCl was added to each sample and the lid was screwed loosely on. The beaker was put back on the hotplate at 90°C until next day. The clear solution was evaporated to dryness and then dissolved in 200 µl ultrapure 3 M HNO_3, centrifuged and loaded onto ion-exchange columns packed with a Sr-Spec crown-ether resin from EIChrom, which retained Sr and allowed most other elements to pass. After rinsing out the remaining unwanted elements from the columns, Sr was collected with ultrapure water (Millipore). The collected Sr-fractions were then evaporated to dryness and loaded onto pre-gassed Re filaments on a turret holding 12 samples and a NIST/NBS 987 Sr standard. The isotopic composition was determined by thermal ionization mass spectrometry (TIMS) on a Finnigan MAT 261 with a precision of c 20 ppm and a Sr blank of 50–100 pg.

4.6 Nonconformities

The activity has been performed according to the activity plan without any nonconformities.

5 Results

The original results from the present study are presented in appendices to this report and stored in the primary data base (SICADA). The data are traceable in SICADA by the Activity Plan number (AP PF 400-06-077). The appendices are:

Appendix 1: Sample description (Appendix 1 is stored as a file in SICADA file archive)

Appendix 2: Pyrite, sulphur isotopes

Appendix 3: Calcite, stable isotopes

Appendix 4: Quartz, oxygen isotopes

Appendix 5: XRD analyses of fracture fillings

Appendix 6: Chemical analyses of fracture fillings

Appendix 7: Uranium series analyses

Minor revision of the fracture generation sequence has been done since the previous fracture report /Sandström and Tullborg 2005/. The number of generations has been reduced due to the combination of previously separated generations based on additional data.

5.1 Minerals identified

Albite (Na-Plagioclase) ($NaAlSi_3O_8$) is often found in fracture fillings together with hydrothermal K-feldspar (adularia). The fillings can be brick-red due to hematite staining.

Allanite $(Ca,Mn,Ce,La,Y,Th)_2(Fe^{2+},Fe^{3+},Ti)(Al,Fe^{3+})_2O.OH[Si_2O_7][SiO_4]$ has been found in two fractures were it occurs as a thin beige coating in open fractures.

Analcime ($NaAlSi_2O_6 \cdot H_2O$) has colourless, usually trapetzohedral crystals (like garnet). Analcime is stable at temperatures up to 200°C in the presence of quartz, but can in other assemblages exist at temperatures up to 600°C /Liou 1971/. In Forsmark, relatively large crystals have been found in some fractures (in the order of 5 to 10 mm).

Apophyllite ($(K,Na)Ca_4Si_8O_{20}F \cdot 8H_2O$) is a hydrothermal sheet silicate with white to silvery surface. It is detected in some fractures at Forsmark. Based on a few SEM-EDS analyses it seems to be relatively pure K-Ca-apophyllite.

Asphaltite ("bergbeck" in Swedish). The term is here used in a broad sense, meaning black, highly viscose to solid hydrocarbons with low U and Th contents.

Baryte ($BaSO_4$) occurs in Forsmark as small grains and as small inclusions in galena.

Calcite ($CaCO_3$) occurs abundantly in Forsmark in different assemblages and with different crystal shape. The calcite generally shows low contents of Mg, Mn and Fe.

Chalcopyrite ($CuFeS_2$) occurs in Forsmark as small grains together with pyrite, galena and sphalerite.

Chlorite $((Mg,Fe,Al)_3(Si,Al)_4O_{10}(OH)_2)$ occurs abundantly in Forsmark as a usually dark-green mineral found in several associations. XRD identifies the chlorite as clinochlore but large variations in FeO/MgO ratios are indicated from SEM-EDS analyses (from 6 down to < 1).

The occurrence of K, Na and Ca in many of the chlorite samples indicates possible ingrowths of clay minerals, mostly corrensite. The Mn and Ti contents in the chlorites are usually low but a few samples have TiO_2 values between 1 and 1.5%.

Epidote ($Ca_2Al_2Fe(SiO_4)(Si_2O_7)(O,OH)_2$) occurs as a green filling in sealed fractures. According to the SEM-EDS analyses, the Fe-oxide content varies between 8 and 14% given as FeO. In reality, however, Fe in epidote is genererally Fe^{3+}. The lower temperature limit for epidote is ~ 250°C /Bird et al. 1984/.

Fluorite (CaF_2). Violet fluorite is found in a few mostly sealed fractures.

Galena (PbS) is mainly found on fracture surfaces and has cubic or octahedral crystals. The mineral occurs together with pyrite in Forsmark and some galena crystals have small inclusions of baryte.

K-feldspar ($KAlSi_3O_8$) is usually adularia (the low-temperature form) but is also found as wall rock fragments in breccias showing typical microcline twinnings. Like in albite the colour can be brick-red due to hematite staining, but also greenish varieties occur in fine-grained mixtures with quartz.

Hematite (Fe_2O_3) is common in the Forsmark fractures but the amount is relatively low (does not often turn up in the diffractograms). However, micro-grains of hematite cause intense red-staining of many fracture coatings. Small spherical aggregates of hematite have also been found in a few fractures.

Laumontite ($CaAl_2Si_4O_{12} \cdot 4H_2O$) is a common zeolite mineral in the Forsmark area. It shows a prismatic shape and is brittle. The mineral is white, but at Forsmark the mineral has a red staining due to micro-grains of hematite, although white varieties are observed as well. Zeolites have open structures suitable for ion exchange. Laumontite is stable at temperatures somewere between ~ 150° and 250°C /Liou et al. 1985/.

Pitchblende (UO_2) is an usually massive, granular form of uraninite, in Forsmark so far only found in one fracture together with hematite and chlorite.

Prehnite ($Ca_2Al_2Si_3O_{10}(OH)_2$) occurs as a light greyish green to grey or white, hydrothermal mineral. The Fe content varies between 1 and 5.5 weight % (given as FeO). Like in epidote, most of the Fe is Fe^{3+}. The stability field for prehnite is somewhere between 200° and 280°C at pressures below 3.0 kbar /Frey et al. 1991/.

Pyrite (FeS_2) is found in many fractures as small euhedral, cubic crystals grown on open fracture surfaces and in sealed fractures.

Quartz (SiO_2) has been identified in many of the analysed samples, often as very small and occasionally hematite stained, euhedral crystals covering the fracture walls. They often have a greyish sugary appearance but can also be transparent and then appear to have the colour of the wall rock.

Sphalerite (ZnS) has been found in a few fractures and is often associated with galena.

Clay minerals

Corrensite ($(Mg,Fe)_9(Si,Al)_8O_{20}(OH)_{10} \cdot H_2O$) is a chlorite-like mixed-layer clay with layers of chlorite and smectite/vermiculite, usually with a ratio of 1:1. Based on XRD analyses, some of the corrensite samples show irregular ordering in the layering, indicating either that they have not reached perfect corrensite crystallinity or that they are altered. Corrensite is the clay mineral most frequently found, and as mentioned above often found together with chlorite. This is a swelling type of clay like mixed-layer illite/smectite and saponite (see below).

Illite ($(K, H_2O)Al_2[(Al,Si)Si_3O_{10}](OH)_2$) occurs as micro – to cryptocrystalline, micaceous-flakes, and is usually light grey in colour.

Mixed-Layer clays. Mixed-layer clay with layers of illite and smectite has been identified in some fractures. XRD analyses show a 3:2 ratio of illite/smectite.

Saponite ($Mg_3(Si_4O_{10})(OH)_2 \cdot nH_2O$). This is a variety of swelling smectite.

5.2 Sequence of fracture mineralizations

Table 5-1 shows the compilation of relative sequences of fracture mineralizations in the drill core samples. From this compilation, together with data from /Sandström et al. 2004/ and /Sandström and Tullborg 2005/ it is obvious that minerals like quartz, adularia, chlorite and calcite occur as several generations. It it also concluded that epidote belongs to the oldest generation in the thin sections studied, whereas lower temperature minerals like e.g. zeolites and clay minerals are found in younger generations. From the KFM06B, KFM06C, KFM07A, KFM08A and KFM08B results, the sequence of fracture mineral generations presented in /Sandström and Tullborg 2005/ has been strengthened although slightly modified due to more textural and isotopic data. The main change is the merge of the former Generations 3, 4 and 5 into one single Generation 3.

Table 5-1. Relative chronological relations between fracture minerals in individual samples from KFM06B, KFM06C, KFM07A, KFM08A and KFM08B. The fracture orientation sets are defined in /La Pointe et al. 2005/ and the deformation zones in /SKB 2006/. The deformation zones in KFM06C have not been modelled yet and notations from the single-hole interpretation are used in these cases (*) /Carlsten et al. 2006/.

Sample	Ep	Qz	Adu	Ab	Hm	Pre	Lau	Chl	Ca	Py	Clay	X	Fracture set	DZ
KFM06B														
55.52									1		1	1A	HZ	ZFMNE00A2
67.00									1		1	1A	HZ	ZFMNE00A2
69.00		1							1			1A	NE	ZFMNE00A2
90.60		1							1		1	1A	NE	ZFMNE00A2
98.50		1							1			1A	n.a.	No Zone
KFM06C														
103.19		1							1			1A	NE	DZ1*
103.70		2	1		1			1	2	2		2A,2G	NE	DZ1*
132.35			1		1			1	1				NE	DZ1*
154.61		1							2	2			NS	DZ1*
162.02		2							2	1,2		1F	NS	DZ1*
364.26			1		1			1	2				NE	DZ2*
442.48							1		1				NE	DZ3*
450.62							1	1	1				NE	DZ3*
451.64			1	1					1		1i	1Go	n.a.	DZ3*
453.84			1		1			2	2				NE	DZ3*
651.64		2	1	1	1			1	3		3		NE	DZ5*
663.76		2						1	2	2			NE	DZ5*
675.90		2				1		1	2	2			n.a.	DZ5*
839.43		2	1	1					1,2				NS	No Zone
939.15								1	1		1C		n.a.	No Zone

Sample	Ep	Qz	Adu	Ab	Hm	Pre	Lau	Chl	Ca	Py	Clay	X	Fracture set	DZ
KFM07A														
112.34								1		1	1		HZ	ZFMNE1203
118.18							1	1			1		NW	ZFMNE1203
120.37		1	1							1		1T	HZ	ZFMNE1203
121.47A		1			3	2		3		3	3		NS	ZFMNE1203
121.47B		3	1,3		1,3				2		3		HZ	ZFMNE1203
122.81		1						1		1	1	1S	HZ	ZFMNE1203
141.44		1	1								1		HZ	ZFMNE1203
151.90					1		1		1		2		n.a.	ZFMNE1203
155.68					1		1			1			NE	ZFMNE1203
166.07					1		1	2					n.a.	ZFMNE1203
178.46								1	1		1		NE	ZFMNE1203
183.13			1					1			1		HZ	No Zone
193.77		1							1	1	1	1B	NE	No Zone
274.95		1							1	1			EW	No Zone
402.68		1							1		2	2AI	EW	No Zone
419.19	1		4			2		1,2	3				n.a.	ZFMNE0159
500.73						1		1					HZ	No Zone
569.73			1		1					1			NE	No Zone
KFM07A														
797.83					1								NE	No Zone
804.41		3					1	2,4	4	4	4		NE	No Zone
815.27	1	1			1								NS	No Zone
876.11		1	1		1				1				n.a.	ZFMNS0100
882.49	1	1			2		2	1,2				2F	n.a.	ZFMNS0100
882.95		1	2							2			NE	ZFMNS0100
883.31		2	1						3	3			NE	ZFMNS0100
883.57							1	1			1		NS	ZFMNS0100
896.68		1						1			1i,1MLC		NS	ZFMNS0100
933.91		1,3	1,3		1			1	2		2	1T	NW	ZFMNS0100
944.58											1		NE	ZFMNS0100
969.68		1	1	1				1			1i		NS	ZFMNS0100
974.16			1		1			2	3	3	2		NS	ZFMNS0100
988.83			1	1	1				1				n.a.	ZFMNS0100
998.92		1							2		2		n.a.	ZFMNS0100
KFM08A														
107.42		2				1			2				NE	No Zone
183.77		1	1	3		2			4			1F	NE	ZFMNE1061
193.01		2	1		1				2	1			NE	ZFMNE1061
197.65		1	1	1				1			1C, 1i		HZ	ZFMNE1061
245.46		1	1						1	1		1Ana	NE	ZFMNE1061
246.11		2	2					1	2	3		3Ana	NE	ZFMNE1061
247.58							1		1				n.a.	ZFMNE1061
304.57			1					1	2		1		HZ	ZFMNE1061
410.60					1				3		2		n.a.	No Zone
411.55A								1	1		1		NS	No Zone
411.55B								1	1		1		NS	No Zone
411.55C			1		1								HZ	No Zone

Sample	Ep	Qz	Adu	Ab	Hm	Pre	Lau	Chl	Ca	Py	Clay	X	Fracture set	DZ
480.30		1								1			n.a.	ZFMNS1204
492.90			1		1			2	1		2		NE	ZFMNS1204
495.07A		1	1					1			1i		HZ	ZFMNS1204
495.07B		1						1	1	1	1i		NE	ZFMNS1204
529.50			1		1								NE	No Zone
605.08	1								1				HZ	No Zone
623.02						1		1			1		NE	No Zone
686.59		1							1		1MLC	1M	HZ	No Zone
689.08			1		1						2		HZ	No Zone
789.42A									1	1	1		EW	No Zone
789.42B						1			1		1		NS	No Zone
918.53		1		1	1		1	1	1		1i		HZ	No Zone
919.32							1	2	1		2		HZ	No Zone
940.00			1		1	1							NE	No Zone
967.44	1							1			1		n.a.	No Zone
972.65							1	1		2	1		n.a.	No Zone
975.50	1						2	2			3		n.a.	No Zone
KFM08B														
7.40									1		1	1Go	NE	No Zone
8.18								1	1		1		NE	No Zone
13.19			1					1	1		1		HZ	No Zone
14.30		2	2					1	2				NE	No Zone
16.44		1						1	1		1		NE	No Zone
20.47		1						1	1		1		NE	No Zone
21.69		1						2	1		2		HZ	No Zone
26.42								1	1	1	1		HZ	No Zone
30.72									1	1	1		EW	No Zone
41.98		1	1						1	1	1	1A	EW	No Zone
43.50		1						2	1	2		2A	NE	No Zone
43.71		1	1						2	2		2A	NE	No Zone
54.45		1	1						2	2		2A	NS	No Zone
61.10		1	1										HZ	No Zone
78.46			1						1				NE	No Zone
91.36		1							2			3A	NE	No Zone
97.37		1							1	1	1		NE	No Zone

A = asphaltite, Ab = albite, Adu = adularia, Al = allanite, Ana = analcime, B = baryte, Chl = chlorite, C = corrensite, DZ = Deformation zone, Ep = epidote, F = fluorite, G = galena, Go = goethite, Hm = hematite, i = illite, Lau = laumontite, M = muscovite, MLC = Mixed layer clay, Pre = prehnite, Py = pyrite, Qz = quartz, S = unknown sulphide, T = titanite.

5.2.1 Generation 1

The oldest generation of fracture minerals within the Forsmark site is dominated by epidote, quartz and Fe-rich chlorite. The minerals occur occasionally as semi-ductile mylonites but mostly as brittle cataclasites (Figure 5-1). In voids within the cataclasites, epidote has grown as euhedral crystals showing zonation due to variation in Fe-content.

The lower temperature limit for epidote stability is ~ 250°C, although epidote normally is found at temperatures above 300°C /Bird et al. 1984 and references therein/. Below this temperature prehnite is formed instead of epidote /Liou et al. 1983/. Based on the cooling ages of biotite

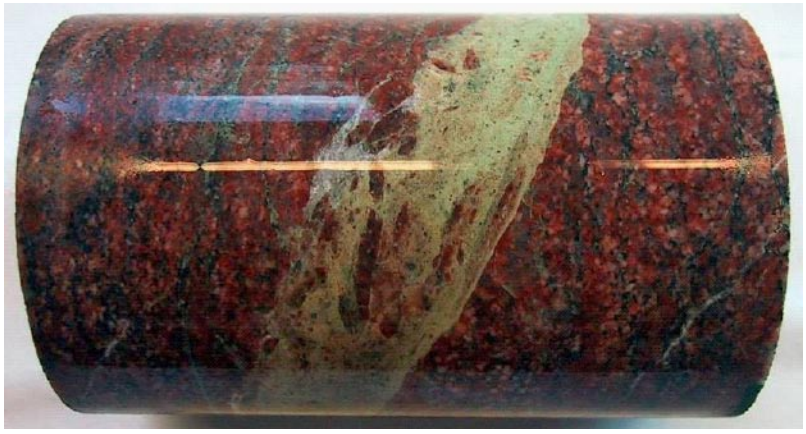

Figure 5-1. *Epidote and calcite cataclasite, KFM08A 605.08–605.16 m. The diameter of the drill core is c 5 cm.*

(~300°C) of 1,704–1,635 Ma in the area /Page et al. 2004/, a late Svekokarelian age is proposed for the formation of Generation 1 fracture minerals.

The epidote sealed fractures are preferably steeply dipping with a NW orientation parallel to the rock foliation. They may also be subhorizontal (Figure 5-2). A population of steep fractures with NE orientation can also be seen in Figure 5-2, which was not observed in the previous drill cores /Sandström and Tullborg 2005/. This could be due to the difficulty to macroscopically distinguish epidote from prehnite during the drill core mapping.

In KFM07A, altered rock has been partly replaced by epidote, locally showing a polygonal fabric (Figure 5-3 and 5-4) as well as symplectitic crystals, suggesting a metamorphic high temperature (~ 400–500°C) origin of this epidote alteration /e.g. Vernon 2004/. The relation between this rock alteration and the epidote sealed fractures/cataclasites has not been established, however the polygonal crystallization suggests formation conditions of at least some of the epidote under metamorphic conditions further indicating a Svekokarelian origin. The epidote sealed fractures are associated with wall rock alteration giving the adjacent rock a red colour. This red-colouring is due to small grains of hematite in the saussuritized plagioclase. The wall rock alteration is described in more detail in /Sandström and Tullborg 2006/.

5.2.2 Generation 2

Epidote sealed fractures of Generation 1 are cut by fractures sealed with a sequence of hydrothermal minerals (Figure 5-5) representing a complex event of hydrothermal activity which probably was active during a prolonged period. The sequence involves a first phase of hematite stained adularia, albite and quartz, followed by prehnite and subsequently laumontite. Calcite and chlorite occur coeval with all these minerals. Laumontite, calcite and chlorite are the most abundant minerals in Generation 2.

The chronological relations between the different phases within the hydrothermal sequence have been established based on cross-cutting relations and fractures where transformation of prehnite into laumontite can be seen (Figure 5-6), and the temperature stability of the different minerals has also been considered assuming a gradually lower temperature with decreasing age.

Calcite coeval with minerals of all three phases has been analysed for stable isotopes and trace elements. The $\delta^{13}C$ values of all calcites analysed from Generation 2 fall within the relatively narrow span between –2 and –7‰ PDB (Figure 5-7), typical for hydrothermal calcites /e.g. Tullborg 1997, Hoefs 2004/. No correlation between $\delta^{13}C$ and depth is shown in these calcites (Figure 5-8).

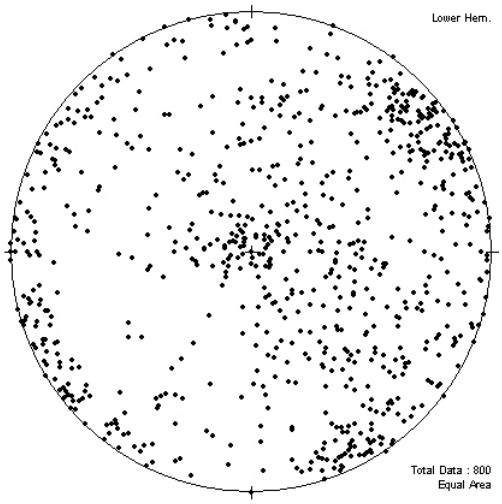

Figure 5-2. *Stereographic plot showing poles to planes of epidote filled fractures from KFM01A, KFM01B, KFM02A, KFM03A, KFM04A, KFM05A, KFM06A, KFM06B, KFM06C, KFM07A, KFM08A and KFM08B.*

Figure 5-3. *Altered rock with epidote. KFM07A 815.27–815.37 m. The diameter of the drill core is c 5 cm.*

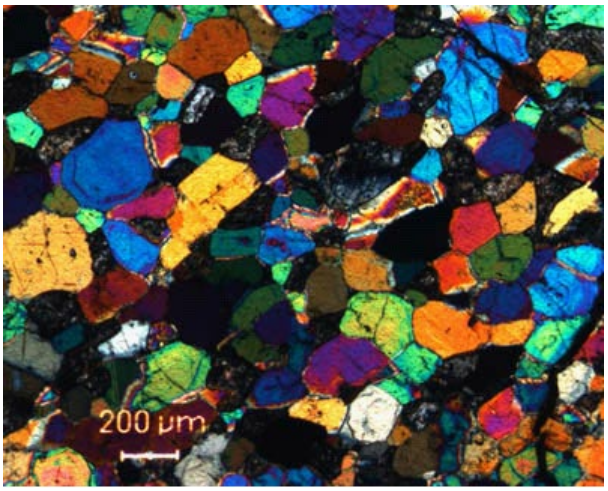

Figure 5-4. *Epidote crystals with a polygonal fabric suggesting metamorphic crystallization. KFM07A 815.27–815.37 m.*

Figure 5-5. *Epidote sealed fracture cut by a sealed fracture filled with hematite stained adularia. KFM05A 692.00–692.15 m. The diameter of the drill core is ~ 5 cm /Sandström and Tullborg 2005/.*

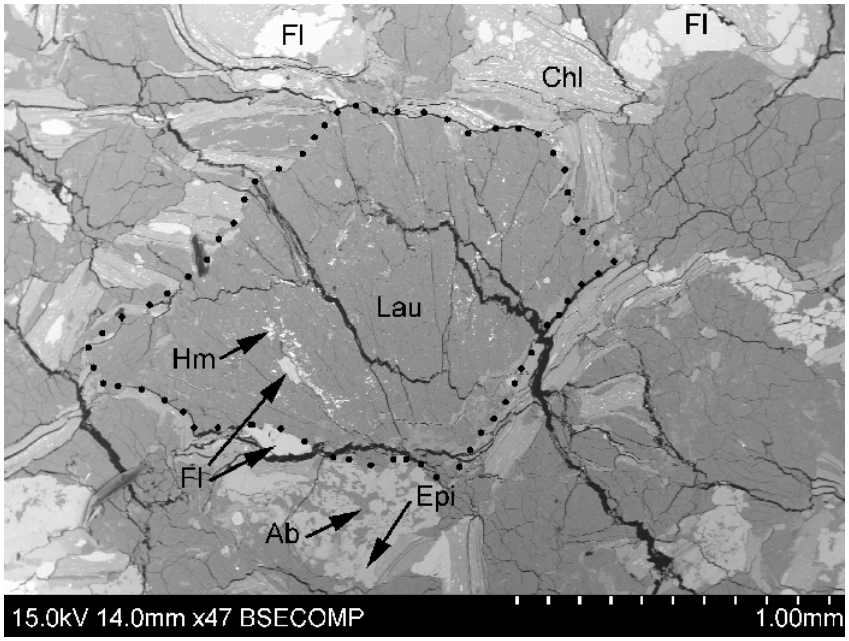

Figure 5-6. *BSE image of a laumontite pseudomorph after an older fan-like prehnite crystal. Lau = laumontite, Hm = hematite, Chl = chlorite, Fl = fluorite. KFM07A 882.49–882.83 m.*

The $\delta^{18}O$ values for these calcites vary between –8 and –24‰ PDB although most values are below –14‰ (Figure 5-7). This rather large variation is probably due to temperature variations during the precipitation. The observation that the lowest $\delta^{18}O$ values are found in calcites together with adularia while calcites occurring together with laumontite in most cases have higher $\delta^{18}O$ values supports this suggestion. Other, probably more important reasons for this variation are local variations in water/rock ratio and/or boiling of the hydrothermal fluids /Truesdell et al. 1977, Hoefs 2004/. No correlation between $\delta^{18}O$ and depth for Generation 2 calcites is shown (Figure 5-9).

Calcites found together with adularia, prehnite and laumontite show similar $^{87}Sr/^{86}Sr$ ratios ranging between 0.707 and 0.712 (Figure 5-10) supporting the interpretation of these minerals as belonging to the same prolonged geological event. The geochemistry of these hydrothermal calcites also differs from younger calcite with e.g. a higher Sr content and a smaller LREE enrichment than in calcite belonging to younger generations. Negative Ce anomalies have also been detected in many of the Generation 2 calcites /Sandström and Tullborg 2005/.

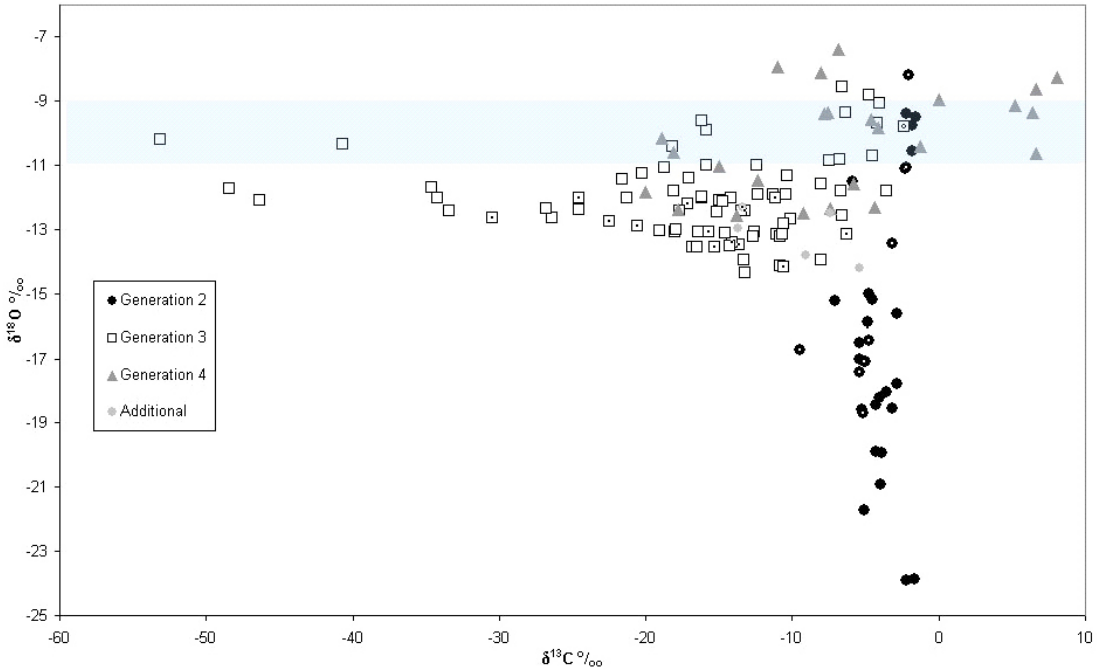

Figure 5-7. *$\delta^{13}C$ versus $\delta^{18}O$ for calcites. The samples with dots inside the symbols have been analysed for $^{87}Sr/^{86}Sr$ as well. The shaded area represents calcites in equilibrium with present day meteoric water at ambient temperatures at the Forsmark site. Data from KFM01A, KFM01B, KFM02A, KFM03A, KFM03B, KFM04A, KFM05A, KFM06A, KFM06B, KFM06C, KFM07A, KFM08A and KFM08B.*

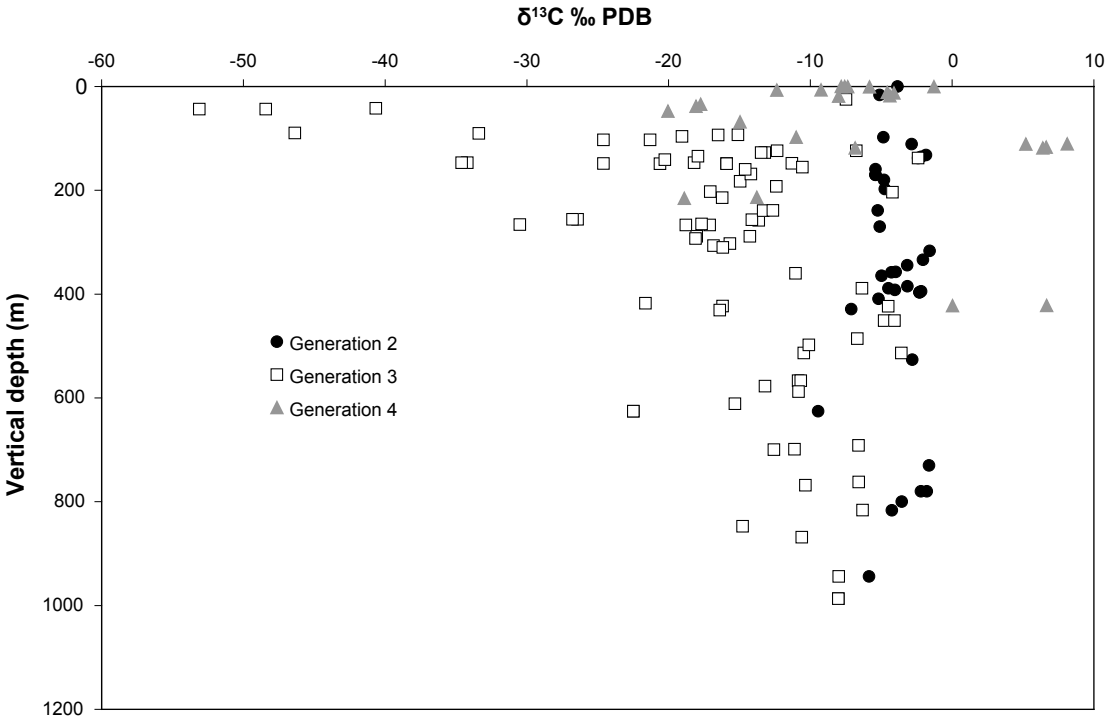

Figure 5-8. *$\delta^{13}C$ versus vertical depth.*

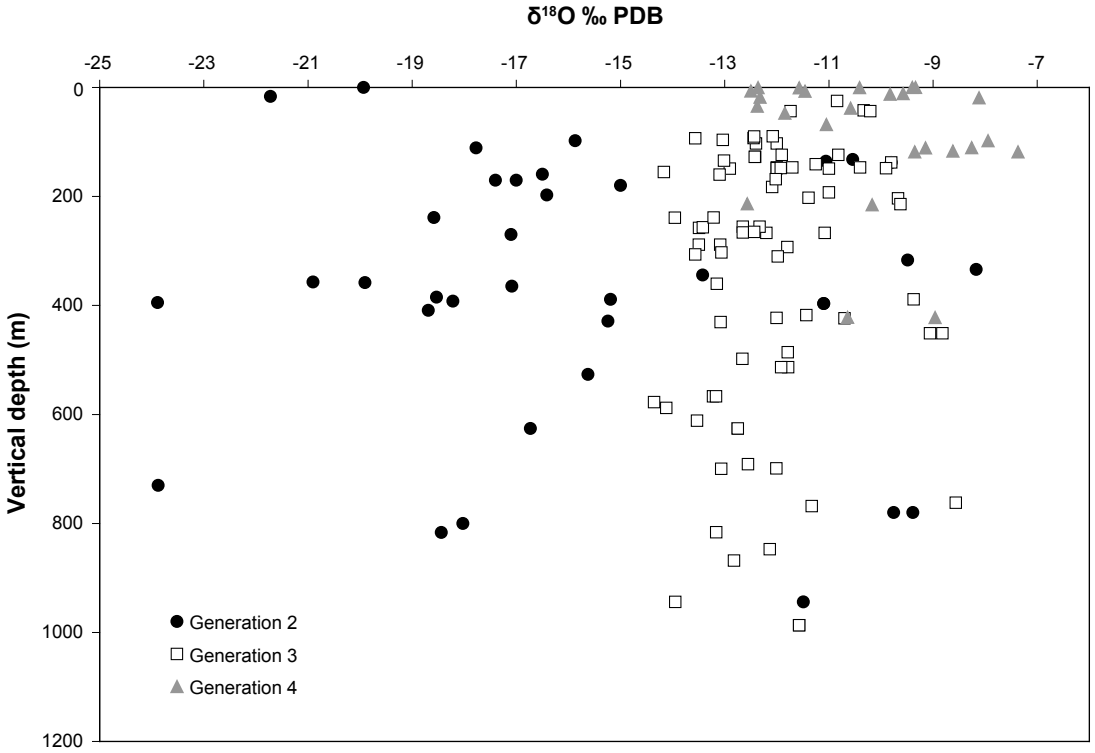

Figure 5-9. *$\delta^{18}O$ versus vertical depth.*

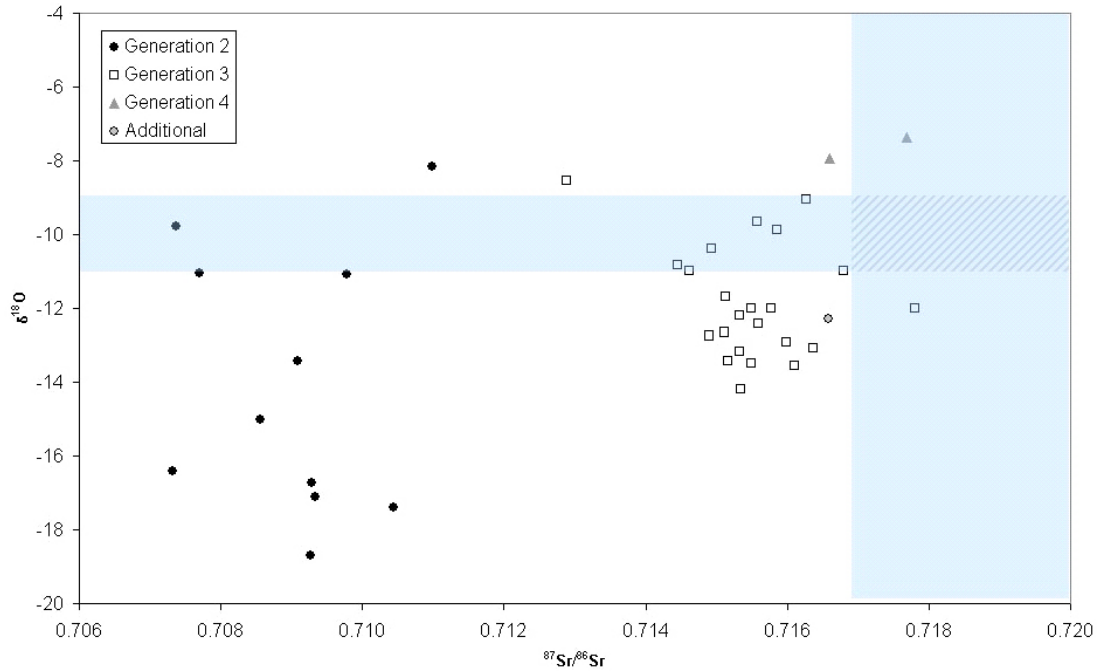

Figure 5-10. *$^{87}Sr/^{86}Sr$ ratio versus $\delta^{18}O$ in calcite. The area with shaded lines represents calcite in equilibrium with present day Meteoric water and the measured $^{87}Sr/^{86}Sr$ in groundwaters at the Forsmark site /SKB 2005/.*

Two samples of calcite found in vuggy granite (episyenite) (KFM08A 410.57 m and 411.62 m) show $\delta^{18}O$ values of –20.9 and –19.9‰ and $\delta^{18}C$ of –4.0 and –4.3‰ respectively, a typical hydrothermal signature and similar to calcite found in Generation 2 fractures. This indicates

that the formation of the vuggy granite is older than the precipitation of Generation 2 fracture minerals. This vuggy granite has been described in detail by /Möller et al. 2003/ who suggest that it was formed during post-metamorphic hydrothermal circulation.

Prehnite is stable in temperatures somewhere between 200 and 280°C at pressures below 3.0 kbars /Frey et al. 1991/, however thermodynamic data are not well known for low temperature minerals and the stabilities show large variation depending on mineral activities, and hence the temperatures should be considered with care. The stability field of laumontite is somewhere between ~ 150–250° C (the upper limit decreases when Fe_2O_3 is introduced to the system) /Liou et al. 1985/. Fluid inclusion analyses of calcite will be carried out during 2006 which hopefully will provide more precise formation temperatures for Generation 2.

Laumontite is also found as sealings in fault breccias often associated with deformation zones. These breccias are part of Generation 2 as well.

Most of the Generation 2 fractures are steeply dipping and have a NE to N orientation (Figure 5-11 and 5-12) although many subhorizontal fractures are also found. As seen in Figures 5-11 and 5-12, both adularia and laumontite sealed fractures have the same orientation. Although adularia occurs in more than this generation, the abundance and distinct brick-red colour of the hematite stained adularia in Generation 2 makes this adularia more easily detected during the drill core mapping, and is therefore dominating in the Boremap data, justifying the use of adularia as an indication of the orientation of Generation 2. The distinctly different orientation of fractures with Generation 2 minerals compared to fractures with older epidote fillings, and the fact that at the Generation 2 minerals occur as the first precipitated minerals in most of these fractures, suggest that the precipitation of these minerals was associated with a major event of new fracture formation in the bedrock. Another possibility is that older fracture minerals had been totally dissolved in the fractures before the precipitation of the Generation 2 minerals and that the fractures themselves are older than the fracture minerals.

A period of dissolution of older fracture fillings follows the precipitation of Generation 2 minerals with many open fractures with partly dissolved laumontite and calcite. Many of these open fractures have later been filled with younger fracture minerals from preferably Generation 3.

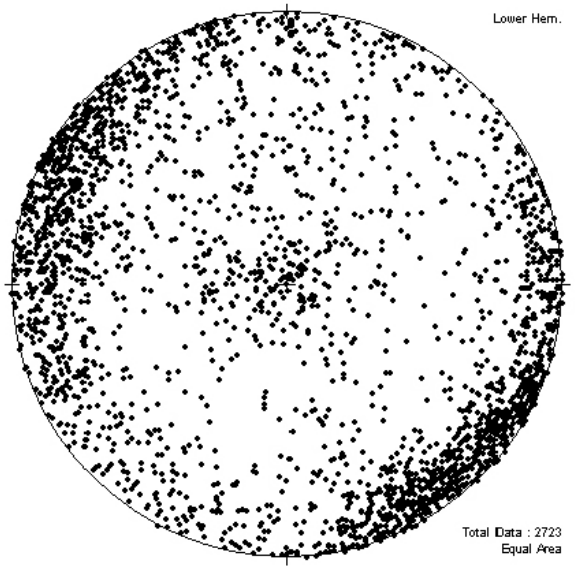

Figure 5-11. *Stereographic plot showing poles to planes with adularia filled fractures from KFM01A, KFM01B, KFM02A, KFM03A, KFM04A, KFM05A, KFM06A, KFM06B, KFM06C, KFM07A, KFM08A and KFM08B. Most fractures are steep and have a NNE to NE orientation.*

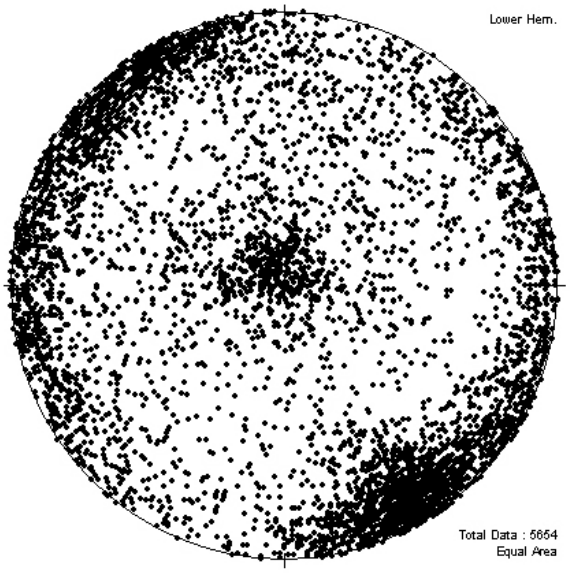

Figure 5-12. *Stereographic plot showing poles to planes with laumontite filled fractures from KFM01A, KFM01B, KFM02A, KFM03A, KFM04A, KFM05A, KFM06A, KFM06B, KFM06C, KFM07A, KFM08A and KFM08B. Most fractures are steep and have a NNE–NE-NNW orientation and also a gently dipping fracture set is present.*

5.2.3 Generation 3

Generation 3 consists of an assemblage of minerals crystallized at low temperature (~ < 150°) and is dominated by quartz, calcite and pyrite occurring both as the first minerals in fractures and as coatings on older prehnite and laumontite draped fractures (Figure 5-13 and 5-14). The minerals occur both as coatings on open fracture surfaces and as fillings in sealed fractures. Minor occurrences of adularia, corrensite, analcime, sphalerite, chalcopyrite, galena, baryte and fluorite also belong to this generation. Asphaltite occurs quite abundantly in fractures in the uppermost parts of the boreholes and is also a part of Generation 3.

Generation 3 was previously considered as three different generations (Generation 3, 4 and 5 in /Sandström and Tullborg 2005/). Additional samples with coeval relations between quartz, calcite and asphaltite as well as new isotopic data from both calcite and quartz have however given reason to revise the older model and to treat these minerals as one generation, although certainly extended in time.

Figure 5-13. *Prehnite sealed fracture and cut by a breccia sealed with a mixture of extremely fine-grained quartz and calcite together with larger calcite crystals. KFM08A 107.42–107.57 m. The diameter of the drill core is c 5 cm.*

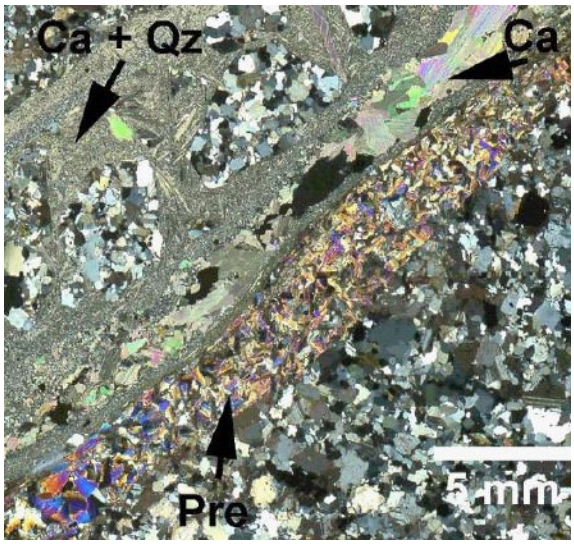

Figure 5-14. *Scanned thin section (with crossed polars) of the breccia in Figure 5-13 with a prehnite sealed fracture cut by a breccia sealed with a mixture of fine-grained matrix of quartz and calcite together with larger calcite crystals and wall rock fragments. KFM08A 107.42–107.57 m.*

The quartz in Generation 3 occurs as thin coatings of euhedral crystals in open fractures but also mingled with calcite in sealed fractures and cataclasites indicating a coeval relationship between quartz and calcite in many fractures.

The carbon isotopic composition ($\delta^{13}C$) of the calcite from Generation 3 varies between –2.4 and –53.1‰ PDB (Figure 5-7) and indicates an organic origin of the bicarbonate in the fluid responsible for the precipitation. The most extreme negative values (< –20‰) are most likely due to in situ microbial activity producing CO_2/HCO_3^- with very low $\delta^{13}C$ values which in turn is incorporated in the calcite. The variation in $\delta^{13}C$ versus depth (Figure 5-8) shows that the lowest $\delta^{13}C$ values in Generation 3 calcites are found at depths less than 300 metres. The lowest $\delta^{13}C$ values are also found in fractures which contain asphaltite as well, further supporting the interaction with organic material. In comparison, the $\delta^{13}C$ of the asphaltite is close to –30‰ /Sandström and Tullborg 2005/ indicating fractionation of the carbon isotopes during bacterial production of CO_2/HCO_3^-.

The $\delta^{18}O$ value of calcite varies between –14.5 and –8.5‰ PDB (Figure 5-7). This variation indicates either a gradual temperature shift, a change in the fluid composition or local variations in fluid-rock ratio. It is plausible that the precipitation of these calcites occurred during a long period or during different episodes, while the formation temperature graded into low temperatures (< 100°C) during the Phanerozoic. No correlation between $\delta^{18}O$ and depth is shown in Generation 3 calcites (Figure 5-9).

Fission track studies /Cederbom et al. 2000/ show that the temperature has not exceeded 100°C during Phanerozoic and (U-Th)/He ages /Page et al. 2004/ indicate that the uppermost sample is not annealed (annealing temperature ~ 60–70°C) during the Phaneorozoic whereas the samples from deeper levels show ages as young as 250 Ma. Due to the close relation between the quartz and calcite and the biogenic signature of many calcite samples, which is not expected at temperatures much above 100°C, a low temperature is suggested for most Generation 3 calcite. The presence of coeval asphaltite in these fractures also suggests a relatively low temperature precipitation. A preliminary fluid inclusion analysis of Generation 3 calcite indicates a formation temperature of ~ 80°C for the latest calcites in Generation 3.

Quartz from Generation 3 display $\delta^{18}O$ values between 18.4 and 21.9‰ SMOW. Although the oxygen isotopic fractionation between fluids and minerals at low temperature (< 200°C) is poorly known, especially for quartz, the high $\delta^{18}O$ values in both the quartz and calcite are typical for low temperature precipitation /Chacko et al. 2001/.

Pyrite occurs as small cubic crystals, often on top of quartz and calcite (Figure 5-15), but is also found coeval with theses minerals in sealed fractures. The $\delta^{34}S$ values of analysed pyrite samples vary highly between –2.8 and +31.5‰ CDT (Figure 5-16). Most hydrothermal pyrites have $\delta^{34}S$ values ranging between –3 and +1‰ /Hoefs 2004 and references therein/. Only three

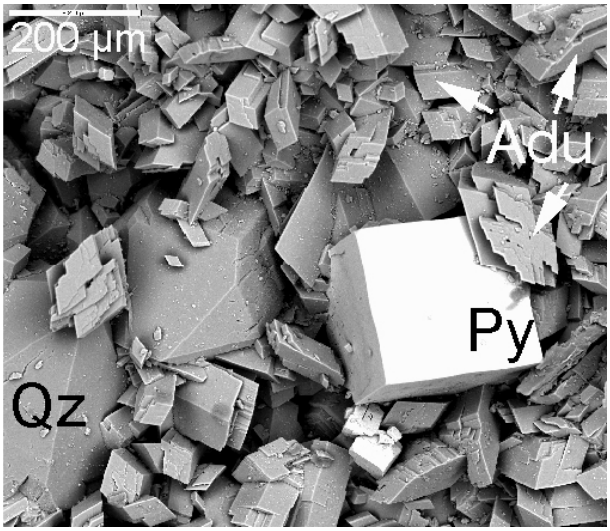

Figure 5-15. *Electron image of euhedral quartz (Qz) covered with pyrite (Py) and adularia (Adu), KF0M7A 882.95–883.05 m.*

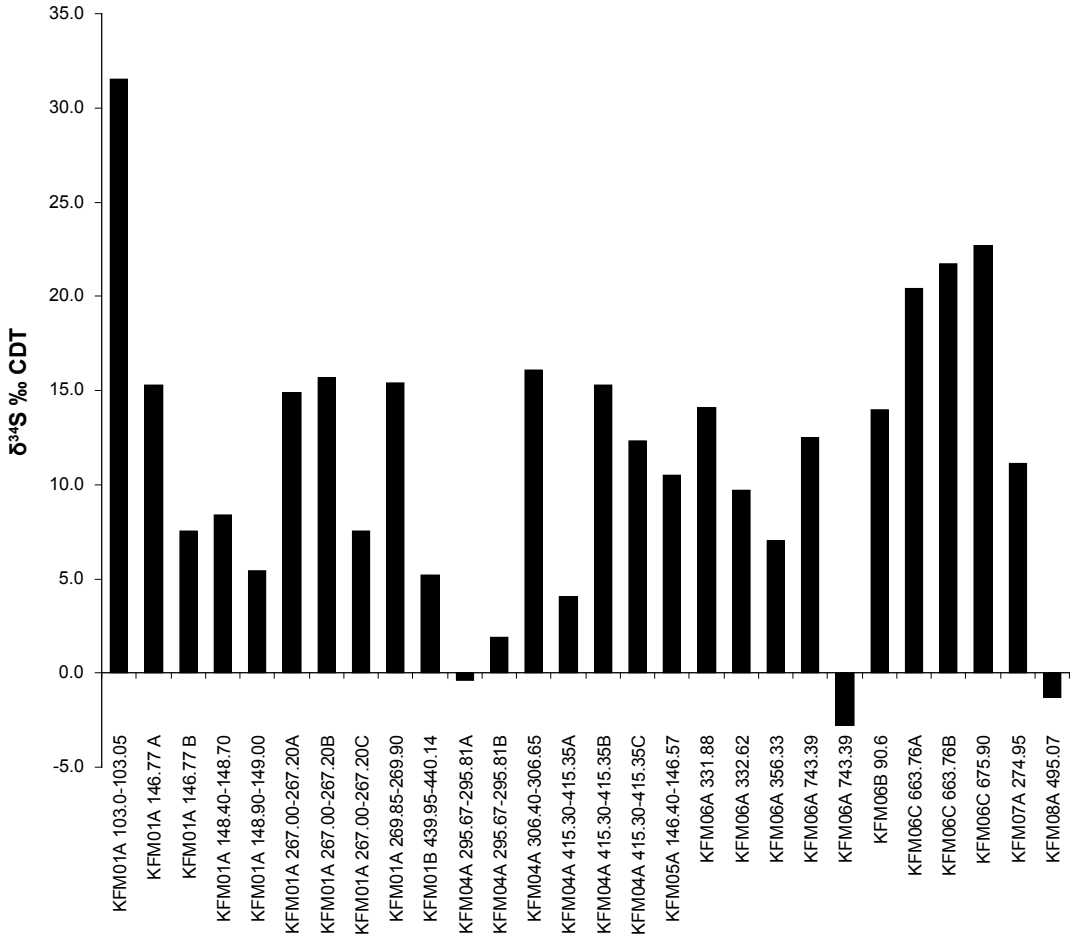

Figure 5-16. *$\delta^{34}S$ values in pyrite, data from this report and /Sandström et al. 2004/.*

samples from Forsmark have $\delta^{34}S$ values within this span, excluding a hydrothermal origin of most pyrites. The majority of the pyrite has $\delta^{34}S$ values between +5 and +31.5‰. The large variation, together with the positive values are interpreted as a result of Reyleigh fractionation under closed system conditions /cf Hoefs 2004/. This is further supported by the large variation in $\delta^{34}S$ values between different crystals on the same fracture surface (KFM01A 267.00–267.20 m). A plausible mechanism for the fractionation is bacterial reduction of sulphate origin from an overlying organic-rich sedimentary cover. The positive $\delta^{34}S$ values of the pyrite agree with the enrichment of ^{34}S found in Cambrian-Carboniferous sedimentary sulphur /Strauss 1997/. No correlation between depth and $\delta^{34}S$ values can be seen in the sampled pyrite (Figure 5-17).

Asphaltite (Figure 5-18) is found at depths down to ~ 124 m. The $\delta^{13}C$ values of the bitumen are relatively uniform with values between –29.5 and –30.1‰ PDB /Sandström and Tullborg 2005/ indicating an organic origin. These results are consistent with previous analyses of asphaltite occurrences in Sweden. Biomarker analyses of the asphaltite samples confirm an organic origin and downward migration of fluids from the organic-rich early Paleozoic Scandinavian Alum Shale is suggested as the most plausible source of the asphaltite /Sandström et al. 2006a/.

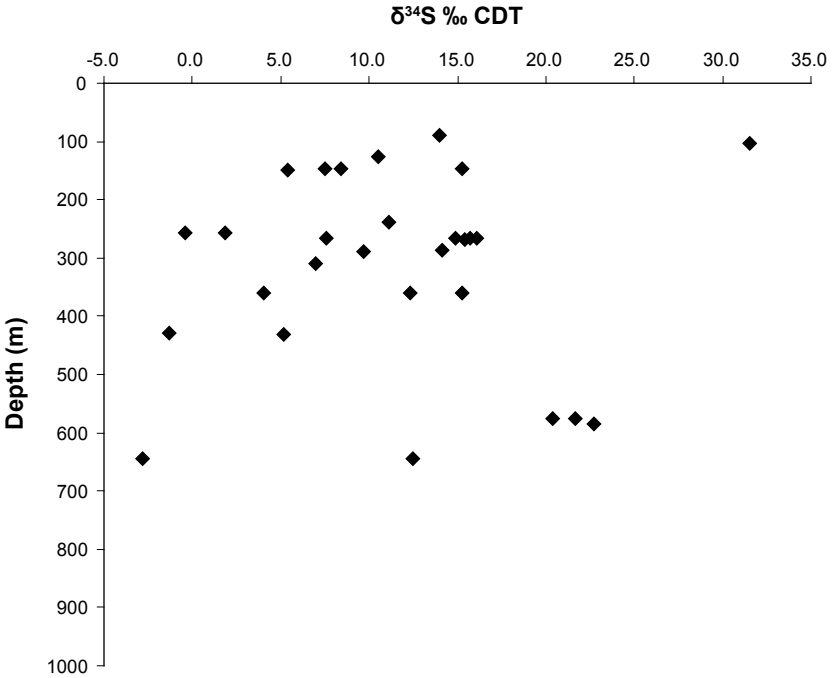

Figure 5-17. *$\delta^{34}S$ values of pyrite versus vertical depth. Data from this report and /Sandström et al. 2004/.*

Figure 5-18. *Black asphaltite in fracture together with calcite, quartz and pyrite, KFM06C 103.19–103.28 m. The diameter of the drill core is c 5 cm.*

Since pyrite almost exclusively occurs as a Generation 3 mineral, it is here used as an index mineral to show the orientation of fractures with Generation 3 minerals (Figure 5-19). Asphaltite which exclusively occurs as Generation 3 mineral has been plotted in Figure 5-20. Both pyrite and asphaltite occur in both the older NE and NW fracture orientation sets indicating reactivation of these fracture sets during the period when the Generation 3 minerals precipitated. The most common orientation of fractures with these Generation 3 minerals is however horizontal or subhorizontal. This indicates that the preferred orientation for the formation of possibly new fractures as well as the reactivation of older fractures during this period was horizontal or subhorizontal.

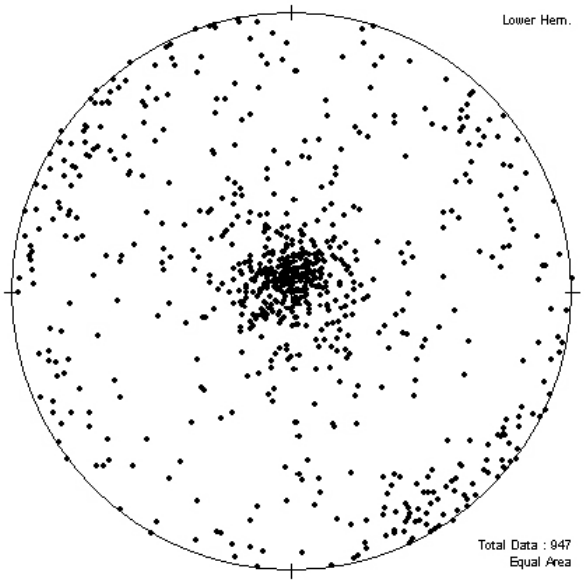

Figure 5-19. *Stereographic plot showing poles to planes of fractures with pyrite from KFM01A, KFM01B, KFM02A, KFM03A, KFM04A, KFM05A, KFM06A, KFM06B, KFM06C, KFM07A, KFM08A and KFM08B.*

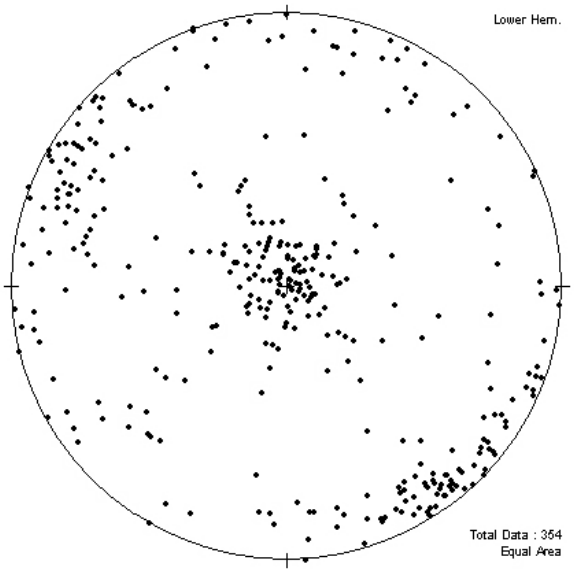

Figure 5-20. *Stereographic plot showing poles to planes of fractures with asphaltite from KFM01A, KFM01B, KFM02A, KFM03A, KFM04A, KFM05A, KFM06A, KFM06B, KFM06C, KFM07A, KFM08A and KFM08B.*

5.2.4 Generation 4

Generation 4 consists of clay minerals, chlorite and thin coatings of calcite, which preferably occur in hydraulically conductive fractures and crush zones. Although most of these fractures and zones probably have presently ongoing precipitation, some of them are most likely reactivated older fractures.

The most common clay minerals are corrensite, illite and saponite. The calcite occurs as thin coatings (Figure 5-21) in open fractures (often together with clay minerals). The $\delta^{13}C$ and $\delta^{18}O$ values of Generation 4 calcite cannot be separated from the calcite of Generation 3 although a shifting towards higher $\delta^{13}C$ and $\delta^{18}O$ values can be seen (Figure 5-7). The similarity in isotopic composition is probably due to growth of younger calcite on older crystals giving a mixed signature, but can also be due to a gradual shift in the composition of the fluids responsible of the precipitation giving zonated crystals.

The generation 4 calcites are not a distinct group. Instead these calcites probably represent different groundwater regimes. The $\delta^{18}O$ values vary between –13 and –7‰. If precipitation at ambient temperature is the case, the highest values (close to –7‰) represent precipitates from water similar to the present Baltic Sea water. Some of these calcites also show extremely high $\delta^{13}C$ values (+5 to +8‰), indicating biogenic modification in situ which may be the result of carbon isotope exchange between CH_4 and CO_2 which in turn may have produced very high $\delta^{13}C$ values in the resulting HCO_3^-. These $\delta^{13}C$ values have later been transferred into the calcites.

The Generation 4 calcites with $\delta^{18}O$ values between –13 to –9‰ can be precipitated from waters similar to present meteoric groundwater or from a slightly colder climate. These calcites are found close to the surface but also in samples from e.g. the ZFMNE00A2 zone in KFM02A (422 m) /Sandström et al. 2004/. It is not possible to confirm a postglacial age of these calcites, instead they may represent older events of similar conditions as the present. No samples of low temperature origin, showing precipitation from glacial melt water, have been found in the present set of data.

The white porous euhedral quartz belonging to Generation 4 described in /Sandström and Tullborg 2005 (section 5.2.6)/ has not been found in the drill cores dealt with in this report and the occurrences appear to be quite rare.

Figure 5-21. *Open fracture with a thin precipitate of calcite, KFM08B 97.37–97.43 m. The diameter of the drill core is c 5 cm.*

5.3 U-series analyses

Uranium series analyses (USD) have been conducted on twelve fracture coating samples ranging in depth from 28 to 803 m. The analyses have been carried out at SUERC (Scotish Universities Environmental Research Centre) by A.B McKenzie. The results are shown in Appendix 7 and Figure 5-22. The samples selected for USD analyses were all chosen to represent hydraulically conductive structures and the sample material contained mixed fracture mineral-coatings including clay minerals and/or Fe(III)-oxide.

Basically, equilibrium (activity ratio ≈ 1) between the nuclides in the uranium decay series analysed ($^{238}U/^{234}U/^{230}Th$) indicate that no mobilisation or deposition have occurred during the last 1 Ma. Plots of $^{234}U/^{238}U$ and $^{230}Th/^{234}U$ activity ratios against depth shown in Figure 5-22 indicate that many of the fracture samples analysed have been open to uranium redistribution during this time period, and the redistribution seems to be more significant in the upper part of the bedrock (0–150 m) which is an expected result. However, many of the deep samples show a small increase in $^{230}Th/^{234}U$ activity ratios indicating a possible late mobilisation. A thourough evaluation of the data will be carried out within the hydrogeochemical modelling for Forsmark version 2.2.

5.4 $^{87}Sr/^{86}Sr$ in rock samples

In order to provide background information to the groundwater sampling as well as the radiometric dating of fracture minerals, four rock samples have been analysed for $^{87}Sr/^{86}Sr$ ratios. Two fresh and one altered sample of the granitic to granodioritic rock (SKB rock code 101057) as well as one fresh sample of the granite-granodiorite-tonalite (SKB rock code 101051) have been selected for $^{87}Sr/^{86}Sr$ analysis. The results are presented in Table 5-2. The large variation in $^{87}Sr/^{86}Sr$ ratios between the different samples is surprising, although a large portion of the variation can be explained by different Rb/Sr ratios in the rock since a higher Rb content gives a higher concentration of the radiogenic ^{87}Sr isotope, which can be seen by the good correlation between $^{87}Sr/^{86}Sr$ and Rb/Sr (Figure 5-23). KFM02A 712.05 m has been re-analysed, the second

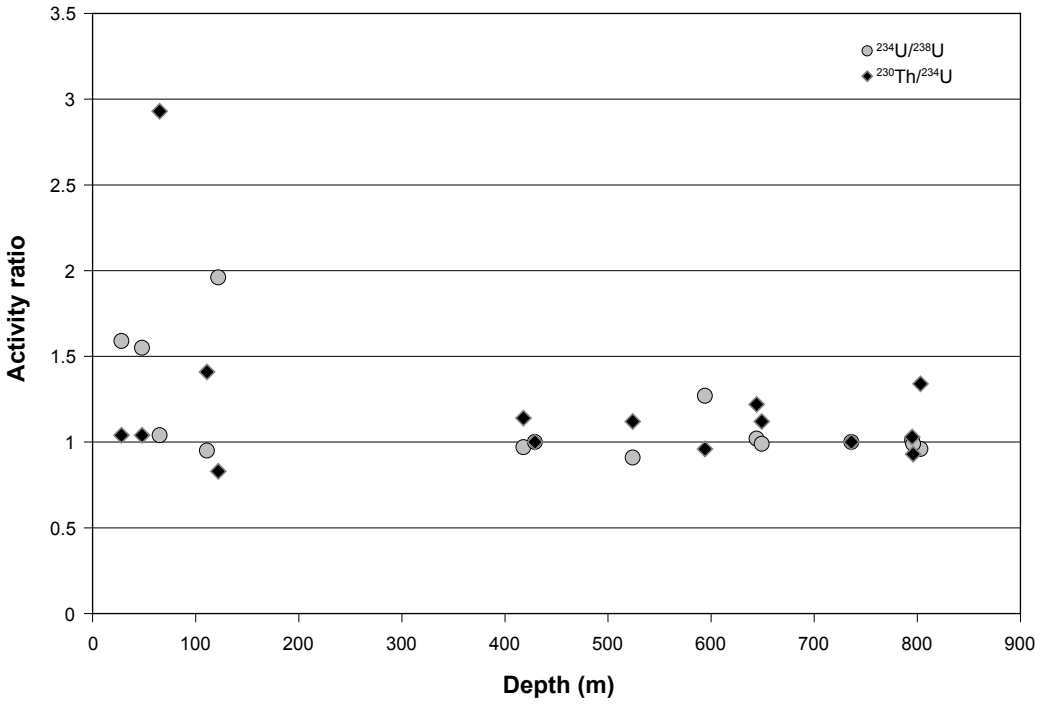

Figure 5-22. *Plots of $^{234}U/^{238}U$ and $^{230}Th/^{234}U$ activity ratios versus depth for fracture coatings samples from boreholes KFM01B, KFM03B, KFM03A, KFM05A, KFM06A, KFM07A and KFM08A.*

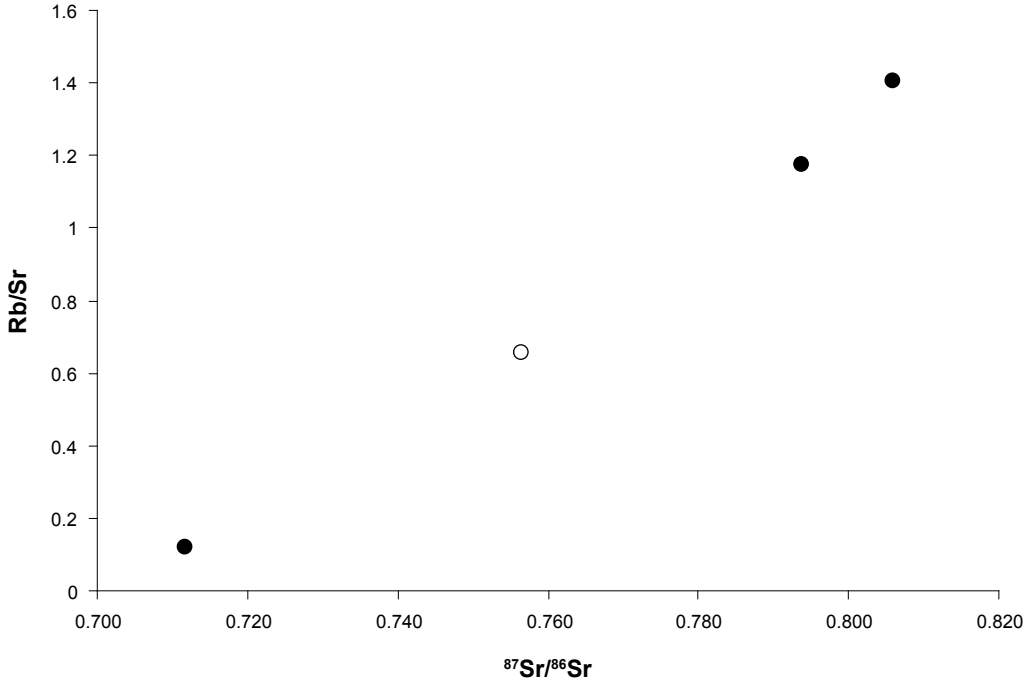

Figure 5-23. *$^{87}Sr/^{86}Sr$ versus Rb/Sr ratio for three of the analysed rock samples (granite to granodiorite, SKB rock code 101057. The unfilled circle represents data obtained from the Rb/Sr dating of a fracture filling /Sandström et al. 2006b/.*

Table 5-2. $^{87}Sr/^{86}Sr$ ratios for rock samples. Rb and Sr values from /Petersson et al. 2004/ and /Sandström and Tullborg 2006/.

Sample	Sample type	Rock type SKB code	$^{87}Sr/^{86}Sr$	±	Rb (ppm)	Sr (ppm)	Rb/Sr
KFM01B 416.50 m	Altered rock	101057	0.793821	23	88.9	75.6	1.176
KFM09A 150.67 m	Fresh rock	101057	0.752467	172	n.a.	n.a.	n.a.
KFM02A 712.05 m	Fresh rock	101057	0.805907	25	135.6	96.5	1.405
Ion exchanged 2 times	Fresh rock	101057	0.797451	54	135.6	96.5	1.405
KFM01A 521.10 m	Fresh rock	101051	0.711618	19	45.6	387.2	0.118

time the ion exchange procedure was repeated in order to better separate ^{87}Rb and ^{87}Sr. The results indicate that a somewhat too high value was obtained, from the samples which were ion exchanged only once, due to interference from ^{87}Rb.

5.5 Geochemistry of fracture fillings

The chemical composition of bulk fracture fillings are presented in Appendix 6 and in /Sandström and Tullborg 2005/ and are discussed below. No significant divergences from the trends described in /Sandström and Tullborg 2005/ have been found in the analysed fracture fillings in this report.

K, Rb, Ba, Cs

These elements are mainly hosted in K-feldspar, mica and clay minerals. From the chemical analyses it is obvious that K correlates with Ba (Figure 5-24), which indicates that most K is hosted in K-feldspar which preferably contains Ba and to lesser degree Rb and Cs. The latter

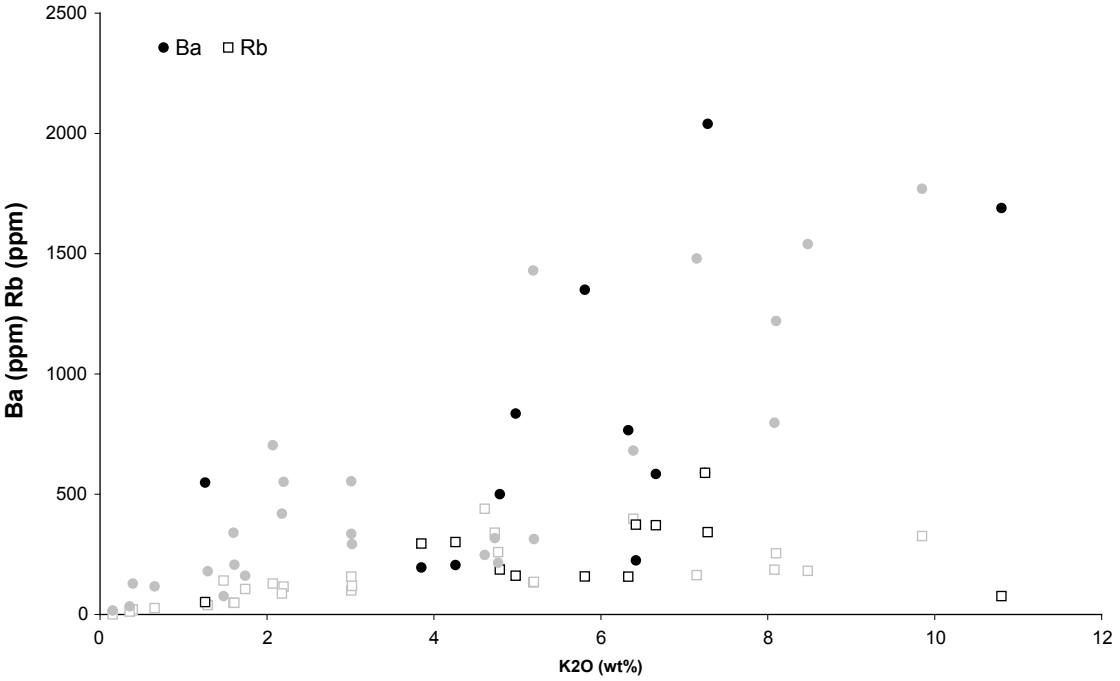

Figure 5-24. *Ba and Rb plotted versus K_2O for bulk samples of fracture fillings. Black symbols are from this study and grey symbols from /Sandström and Tullborg 2005/.*

elements are instead hosted together with K in clay minerals. Especially illite and mixed layer clays of illite/smectite type tend to enrich Rb and even more Cs.

The mean Cs content in the host rock is 0.8 ppm /Drake et al. 2006/, whereas the values in the fracture coatings are significantly higher (2.5 to 32.7 ppm in 25 of the 34 samples analysed for Cs with a mean of 6.86 ppm for all samples).

Na, Ca, Sr

The Sr content in the analysed fracture fillings varies between 16 and 490 ppm. A positive correlation between Sr and Ca is observed for the samples with CaO contents < 5 wt% (Figure 5-25) whereas the samples with the highest CaO contents (15 to 25 wt%) show relatively low Sr contents. The latter samples consist dominantly of prehnite, analcime and calcite, but also the apophyllite sample is amongst these. From ICP-MS analyses on calcite it is known that the Sr/CaO ratio /Sandström and Tullborg 2005/ in the calcites is very low. The minerals hosting most Sr are epidote /Sandström and Tullborg 2006/, laumontite and plagioclase.

Na shows a positive correlation with Sr in the samples with albite, whereas the analcime samples do not follow this trend.

Fe, Mg, Mn, Ti, V, Sc

Fe correlates with Mg in most samples (Figure 5-26), which is explained by the presence of chlorite and corrensite in the fracture fillings. As has been shown by SEM-EDS analyses, the Fe/Mg ratio in the chlorites of different generations varies /Sandström and Tullborg 2005/, which partly explains the variation in Fe/Mg ratio in the entire bulk samples. Additional contents of minerals containing Fe but no Mg is another explanation. The two samples with the highest Fe_2O_3 content also have high Cr and Ni content, indicating that part of the Fe in these samples can result from iron-rich debris produced during the drilling which may have soaked into the split-tube and penetrated the fractured drill core.

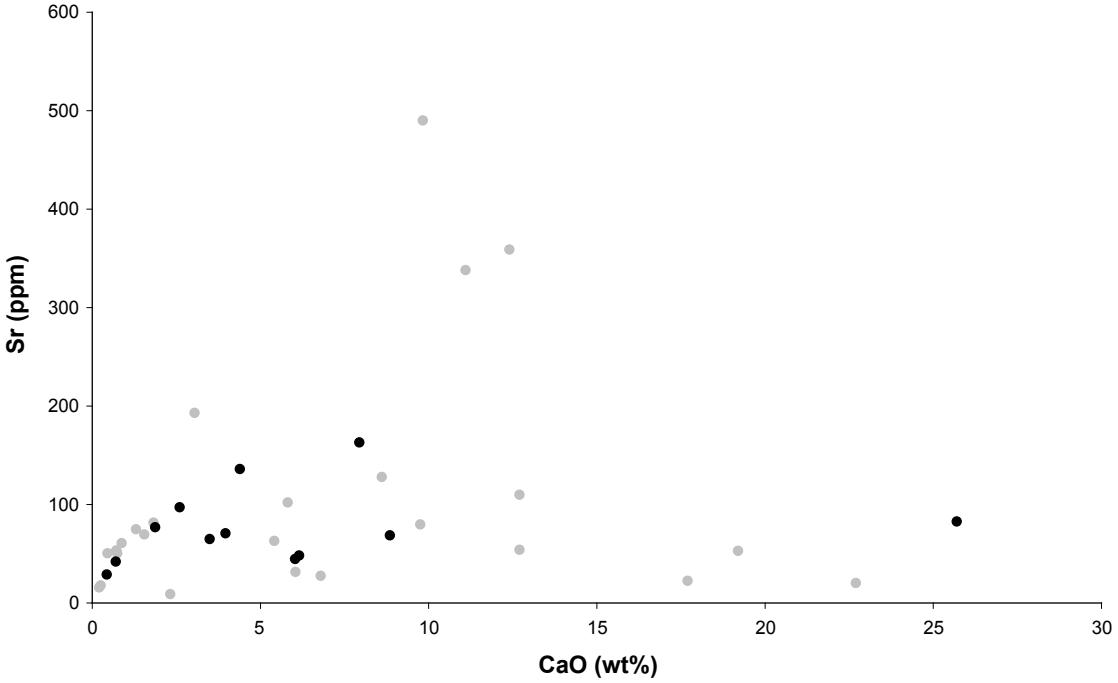

Figure 5-25. *CaO plotted versus Sr for bulk samples of fracture fillings. Black symbols are from this study and grey symbols from /Sandström and Tullborg 2005/.*

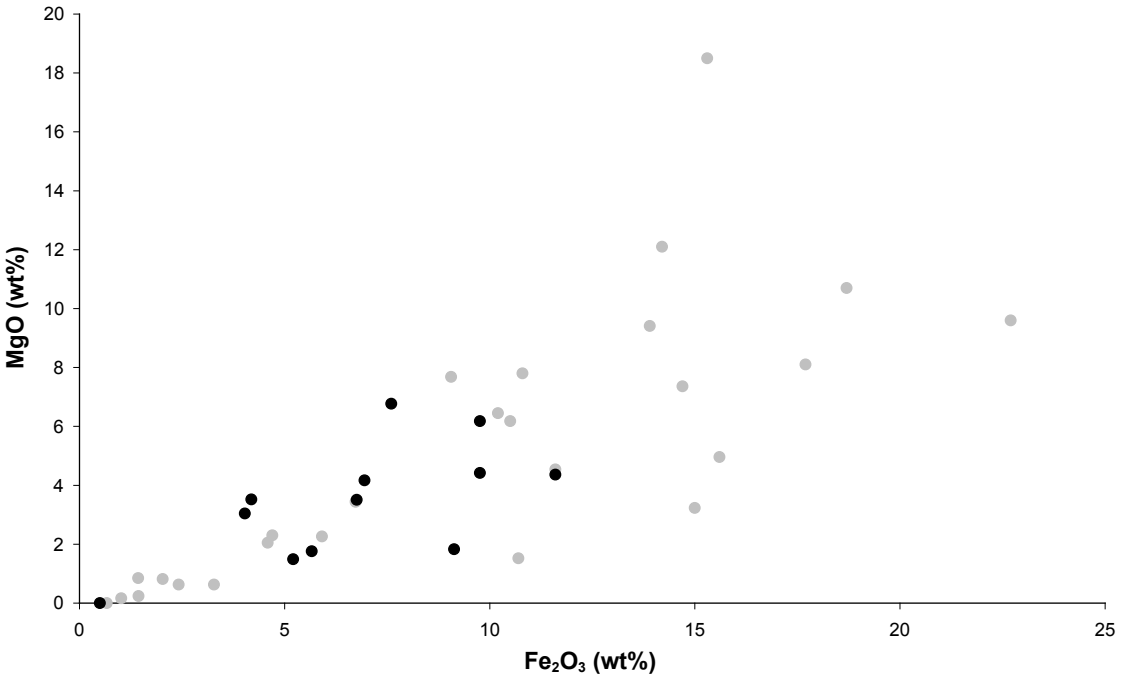

Figure 5-26. *Fe_2O_3 versus MgO for bulk samples of fracture fillings. Black symbols are from this study and grey symbols from /Sandström and Tullborg 2005/.*

Mn shows a significant positive correlation with Fe indicating its presence in chlorite and clay minerals. Ti, V and Sc generally show a positive correlation with Fe except for some prehnite and pyrite rich samples that display very low Ti, Sc and V contents.

U and Th

The U content varies between 0.46 and 164 ppm except in two samples from KFM03A 643.8–644.12 m and KFM03A 644.17 m which show U values of 2,200 and 2,310 ppm /Sandström and Tullborg 2005/. The Th values, in contrast, are all within the interval 0.2 to 14.7 ppm (Figure 5-27). The Th/U ratios are < 1 for all except five samples, indicating an enrichment of U in the fracture coatings compared to the fresh rock (Th/U usually > 2) /Drake et al. 2006/. This U enrichment has taken place during different periods of time; The USD analyses (cf, section 5.2) show possible ongoing mobilisation/deposition of U in a number of samples from the site. From the U/Th ratio it is however evident that U has been mobilised and inhomogenously deposited in the fracture system before the last 1 Ma detectable by the USD analyses. It is notable that the high U content in the fracture fillings correlate with high U content in water samples from the same depths /Drake et al. 2006/ indicating that at least part of the uranium is found in easily accessible sites.

Concerning the U in the fracture coatings no significant correlations with P, Ti or La can be seen.

REEs

Chondrite normalised REE curves from analysed fracture fillings are shown in Figure 5-28. The La/Yb ratios vary between 0.1 and 28, except for four samples with higher ratios out of 38 analysed samples. The higher ratios are 63, 91, 128 and 324. Most samples show negative Eu-anomalies, probably inherited from the host rock. A few samples from earlier boreholes /see Sandström and Tullborg 2005/ show Ce-anomalies (both positive and negative) which probably are related to (hydrothermal?) oxidation in these fractures. The overall trend for the fracture fillings is enrichment in REEs compared to the host rock. This enrichment is generally more pronounced for the LREEs than the HREEs. However, four samples show significantly high Yb values (from 22.7 to 30 ppm). Two of these are the uranium rich samples from KFM03A 644 m. The other two samples (KFM06C 149.54 m and KFM08A 495.13 m) do not share the high U values. These samples in contrast, show La/Yb ratio (< 1) and significantly high Y contents (520 to 600 ppm). Zr and Hf are not enriched in these samples.

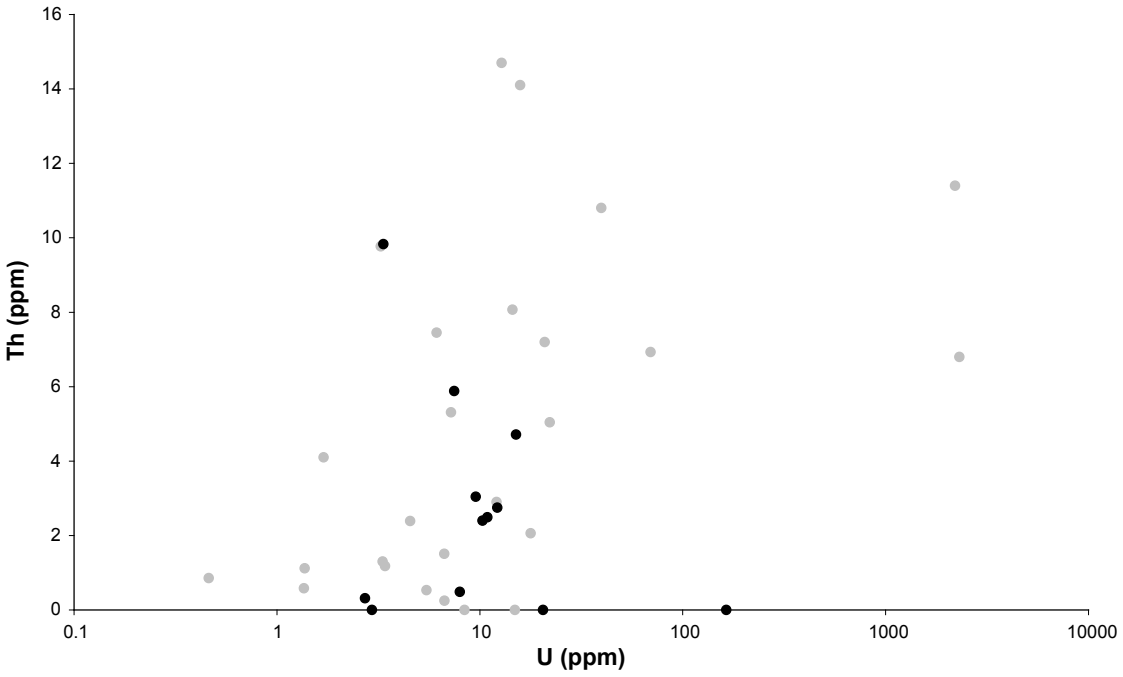

Figure 5-27. *U (ppm) versus Th (ppm) for bulk samples of fracture fillings. Black symbols are from this study and grey symbols from /Sandström and Tullborg 2005/.*

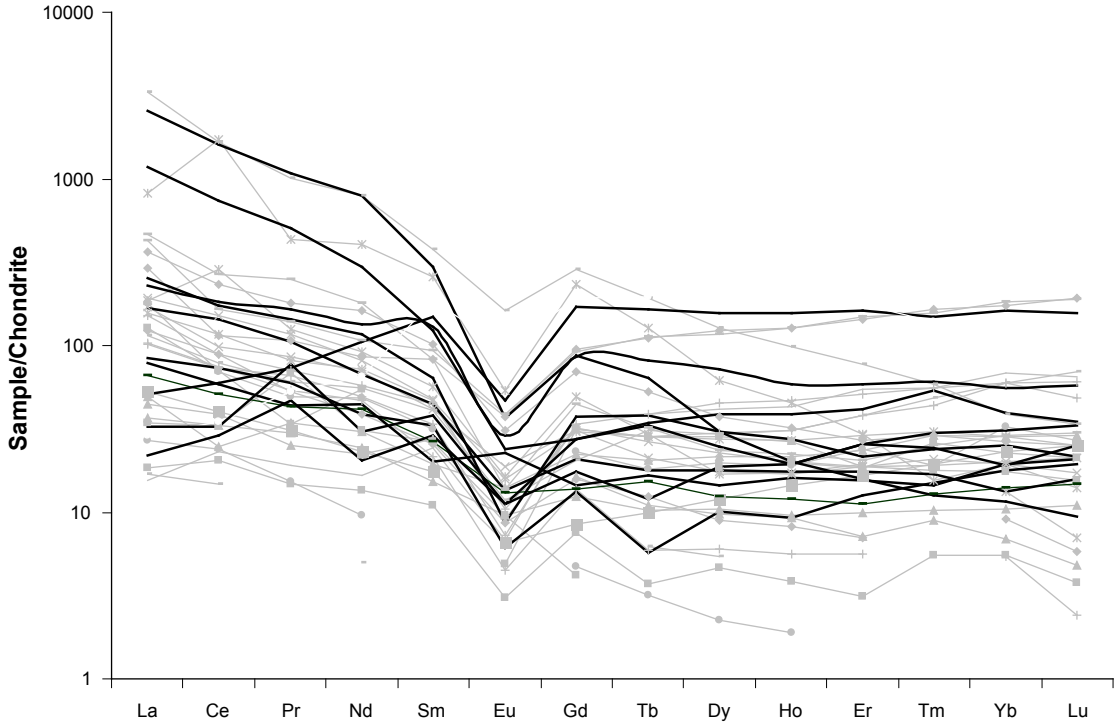

Figure 5-28. *Chondrite normalized REE curves for bulk samples of fracture fillings. Chondrite data from /Evansen et al. 1978/. Black lines are from this study and grey lines from /Sandström and Tullborg 2005/.*

6 Summary

The present fracture filling mineral study comprises results from boreholes KFM06B, KFM06C, KFM07A, KFM08A and KFM08B which are added to the earlier obtained results from KFM01A, KFM02A, KFM03A and KFM03B /Sandström et al. 2004/ and KFM01B, KFM04A, KFM05A, KFM06A /Sandström and Tullborg 2005/.

The relative sequence of fracture minerals described in /Sandström and Tullborg 2005/ has been strengthened although slightly modified due to more data. The main difference is the merge of three low-temperature generations (Generations 3, 4 and 5 in /Sandström and Tullborg 2005/) into one single Generation 3 based on textural relations and stable isotopic data. The sequence now consists of 4 generations; 1) Epidote-quartz-chlorite, 2) A sequence of hydrothermal minerals consisting of adularia, prehnite, laumontite and calcite. Both adularia and laumontite are red-stained due to micro-grains of hematite. 3) Low-temperature minerals consisting mainly of quartz, calcite, pyrite and, in the upper parts of the bedrock, asphaltite. Minor occurrences of e.g. analcime, flurite and galena also belong to this generation. 4) Clay minerals and thin precipitates of calcite which preferably occur in presently hydraulically conductive zones.

Generation 1 is believed to be older than 1,704–1,635 Ma based on the stability of epidote and the cooling history in the area based on $^{40}Ar/^{39}Ar$ dating of biotite by /Page et al. 2004/. The minerals of Generation 1 are preferably found in steep NW striking as well as subhorisontal fractures. **Generation 2** probably represents a complex and probably prolonged event of hydrothermal circulation and precipitation grading between temperatures of 280° and 150°C based on mineral stabilities. The orientation of most fractures with Generation 2 minerals is steep with a NE strike. **Generation 3** consists of minerals precipitated at low temperatures, and $\delta^{13}C$ values in calcite indicate influence of organic rich fluids. The presence of asphaltite with a confirmed organic origin /Sandström et al. 2006a/ further implies an organic rich source of the fluids responsible for the precipitation of Generation 3 minerals. Generation 3 minerals are found as coatings in older reactivated fractures, but there is also an increase in new horizontal to subhorisontal fractures during the same event that led to the precipitation of Generation 3 minerals. The clay minerals and calcite belonging to **Generation 4** have probably precipitated during a long period until present and U series analyses show possible mobility of uranium in many of these fractures during the last 1 Ma.

Geochemical analyses of fracture fillings corroborate the trends described in /Sandström and Tullborg 2005/, e.g. the trend of generally significantly higher U/Th ratios in the fracture fillings than in the wall rock remains, which indicates a mobility of U. This is also supported by the uranium series analyses (USD), which indicate a U redistribution during the last 1 Ma in many of the analysed samples. This redistribution is more significant in the uppermost 150 m of the bedrock, although some of the samples from deeper levels also indicate a possible late mobilisation of U.

7 Acknowledgements

We would like to thank Jesper Petersson, Anders Wängnerud, Göran Skogsmo (Vattenfall Power Consultants AB) and Christin Döse and Eva Samuelsson (Geosigma AB) for assistance during the drill core sampling. Assen Simeonov (SKB) and Michael Stephens (SGU) are thanked for support and constructive discussions, Allan Stråhle (Geosigma AB) for help with e.g. the BIPS-images, Owe Gustavsson (Göteborg University) for the stable C and O isotope analyses, Ulf Brising (Sweco) for the geological map and Henrik Drake (Göteborg University) for rewarding discussions concerning fracture mineralogy. Tony Fallick (SUERC) is acknowledges for the stable isotope analyses of pyrite. We would also like to thank Sven Åke Larson (Göteborg University) for reviewing the report.

8 References

Bird D K, Schiffman P, Elders W A, Williams A E, McDowell S D, 1984. Calc-silicate mineralization in active geothermal systems. Economic Geology, 79, 671–695.

Carlsten S, Jaana G, Mattsson H, Petersson J, Stephens M B, 2006. Forsmark site investigation. Geological singel-hole interpretation of KFM06C. SKB P-06-83, Svensk Kärnbränslehantering AB.

Cederbom C, Larson S Å, Tullborg E-L, Stiberg J-P, 2000. Fission track thermo-chronology applied to Phanerozoic thermotectonic events in central and southern Sweden. Tectonophysics, 316, 153–167.

Chacko T, Cole D R, Horita J, 2001. Equilibrium oxygen, hydrogen and carbon isotope fractionation factors applicable to geologic systems. Reviews in Mineralogy and Geochemistry, 43, 1–81.

Drake H, Sandström B, Tullborg E L, 2006. Mineralogy and geochemistry of rocks and fracture fillings from Forsmark and Oskarshamn: Compilation of data for SR-Can, R-report in progress. Svensk Kärnbränslehantering AB.

Drake H, Tullborg E-L, 2006. Oskarshamn site investigation. Fracture mineralogy of the Götemar granite. Results from drill cores KKR01, KKR02 and KKR03. SKB P-06-04, Svensk Kärnbränslehantering AB.

Evansen N M, Hamilton P J, O'Nions R K, 1978. Rare Earth Abundances in Chondritic Meteorites. Geochimica et Cosmochimica Acta, 42, 1199–1212.

Frey M, De Capitani C, Liou J G, 1991. A new petrogenetic grid for low-grade metabasites. Journal of Metamorphic Geology, 9, 497–509.

Hoefs J, 2004. Stable isotope geochemistry. 5th rev. and updated ed. Springer-Verlag. 244 pp.

La Pointe P R, Olofsson I, Hermansson J, 2005. Statistical model of fractures and deformations zones for Forsmark, preliminary site description Forsmark area – version 1.2. SKB R-05-26, Svensk Kärnbränslehantering AB.

Liou J G, 1971. Analcime equilibria. Lithos, 4, 389–402.

Liou J G, Kim H S, Maruyama S, 1983. Prehnite – epidote equilibria and their petrologic applications. Journal of Petrology, 24, 321–342.

Liou J G, Maruyama S, Cho M, 1985. Phase equilibria and mineral paragenesis of metabasites in low-grade metamorphism. Mineralogical Magazine, 49, 321–333.

Macaulay C I, Fallick A E, Haszeldine R S, Graham C M, 2000. Methods of laser-based stable isotope measurement applied to diagenetic cements and hydrocarbon reservoir quality. Clay minerals, 36, 313–322.

Möller C, Snäll S, Stephens M B, 2003. Forsmark site investigation. Dissolution of quartz, vug formation and new grain growth associated with post-metamorphic hydrothermal alteration in KFM02A. SKB P-03-77, Svensk Kärnbränslehantering AB.

Page L, Hermansson T, Söderlund P, Andersson J, Stephens M B, 2004. Forsmark site investigation. Bedrock mapping U-Pb, $^{40}Ar/^{39}Ar$ and (U-Th)/He geochronology. SKB P-04-126, Svensk Kärnbränslehantering AB.

Petersson J, Tullborg E-L, Mattsson H, Thunehed H, Isaksson H, Berglund J, Lindroos H, Danielsson P, Wängnerud A, 2004. Forsmark site investigation. Petrography, geochemistry, petrophysics and fracture mineralogy of boreholes KFM01A, KFM02A and KFM03A+B. SKB P-04-103, Svensk Kärnbränslehantering AB.

Sandström B, Savolainen M, Tullborg E-L, 2004. Forsmark site investigation. Fracture Mineralogy. Results from fracture minerals and wall rock alteration in boreholes KFM01A, KFM02A, KFM03A and KFM03B. SKB P-04-149, Svensk Kärnbränslehantering AB.

Sandström B, Tullborg E-L, 2005. Forsmark site investigation. Fracture mineralogy. Results from fracture minerals and wall rock alteration in KFM01B, KFM04A, KFM05A and KFM06A. SKB P-05-197, Svensk Kärnbränslehantering AB.

Sandström B, Tullborg E-L, 2006. Forsmark site investigation. Mineralogy, geochemistry, porosity and redox capacity of altered rock adjacent to fractures. SKB P-06-209, Svensk Kärnbränslehantering AB.

Sandström B, Tullborg E-L, de Torres T, Ortiz J E, 2006a. The occurence and potential origin of asphaltite in bedrock fractures, Forsmark, central Sweden. GFF, 128, 233–242.

Sandström B, Page L, Tullborg E-L, 2006b. Forsmark site investigation. $^{40}Ar/^{39}Ar$ (adularia) and Rb-Sr (adularia, prehnite, calcite) ages of fracture minerals. SKB P-06-213, Svensk Kärnbränslehantering AB.

Sharp Z D, 1990. A laser-based microanalytical method for in situ determination of oxygen isotope ratios in silicates and oxides. Geochimica et Cosmochimica Acta, 54, 1353–1357.

SKB, 2005. Hydrochemical evaluation. Preliminary site description Forsmark area – version 1.2. SKB R-05-17, Svensk Kärnbränslehantering AB.

SKB, 2006. Site descriptive modelling. Forsmark stage 2.1. Feedback for completing of the site investigation including input from safety assessment and repository engineering. SKB R-06-38, Svensk Kärnbränslehantering AB.

SKB GIS database, 2006. Svensk Kärnbränslehantering AB.

Strauss H, 1997. The isotopic composition of sedimentary sulphur through time. Palaeogeography, Palaeoclimatology, Palaeoecology, 132. 97–118.

Truesdell A H, Nathenson M, Rye R O, 1977. The effects of subsurface boiling and dilution on the isotopic compositions of Yellowstone thermal waters. Journal of Geophysical Research, 82, 3694–3704.

Tullborg E-L, 1997. Recognition of low-temperature processes in the Fennoscandian shield. Ph.D Thesis, Earth Sciences Centre, Göteborg University. A17.

Vernon R H, 2004. A practical guide to rock microstructure. Cambridge University Press. 594 pp.

Appendix 1

Sample descriptions

Sample: **KFM06B 55.52–55.65 m**
Rock type: Metagranite
Fracture: Crushed Zone
Orientation: 0187/08°
Deformation zone: ZFMNE00A2
Fracture orientation set: HZ
Fracture minerals: Clay minerals, asphaltite, calcite

Sample: **KFM06B 67.00–67.10 m**
Rock type: Metagranite
Fracture: Open fracture
Orientation: 074/25°
Deformation zone: ZFMNE00A2
Fracture orientation set: HZ
Fracture minerals: Clay minerals, asphaltite, calcite

Sample: **KFM06B 69.00–69.10 m**
Rock type: Metagranite
Fracture: Sealed fracture
Orientation: 042/62°
Deformation zone: ZFMNE00A2
Fracture orientation set: NE
Fracture minerals: Calcite, quartz, asphaltite

Ca 10 mm thick fracture sealing consisting of a mixture of calcite and quartz with large inclusions filled with asphaltite.

Sample: **KFM06B 90.60–90.85 m**
Rock type: Metagranite
Fracture: Open fracture
Orientation: 044/87°
Deformation zone: ZFMNE00A2
Fracture orientation set: NE
Fracture minerals: Calcite, quartz, asphaltite, clay minerals

Open fracture coated with a thin coating of euhedral quartz together with calcite and clay minerals. Hardened asphaltite droplets are found on this coating.

Sample: **KFM06B 98.50–98.60 m**
Rock type: Metagranite
Fracture: Sealed fracture
Orientation: No BIPS available
Deformation zone: No zone
Fracture orientation set: n.a.
Fracture minerals: Asphaltite, calcite, quartz

Thin fracture with asphaltite, calcite and quartz.

Sample: **KFM06C 103.19–103.28 m**
Rock type: Metagranite
Fracture: Partly open fracture
Orientation: 221/84°
Deformation zone: DZ1 (from single-hole interpretation)
Fracture orientation set: NE
Fracture minerals: Calcite, quartz, asphaltite

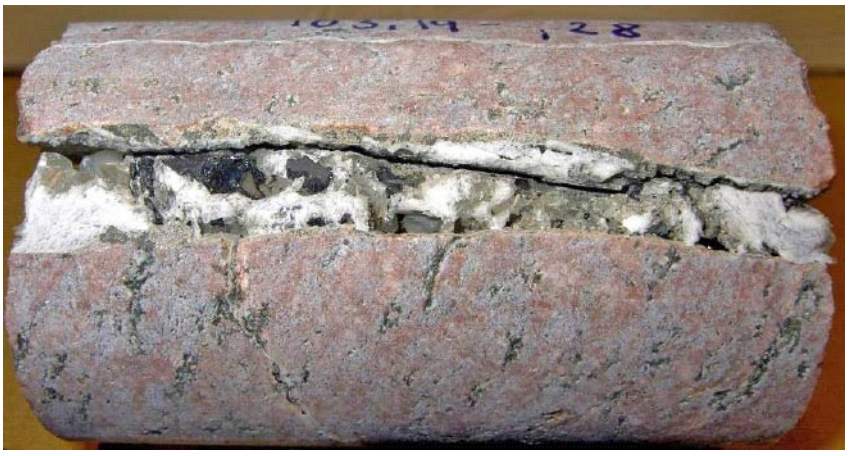

Partly open fracture with a mixture of euhedral calcite, small euhedral quartz crystals, asphaltite and small pyrite crystals.

Sample: **KFM06C 103.70–103.83 m**
Rock type: Metagranite
Fracture: Sealed fracture
Orientation: 221/84°
Deformation zone: DZ1 (from single-hole interpretation)
Fracture orientation set: NE
Fracture minerals: Calcite, quartz, asphaltite, pyrite, galena

Sequence of mineralizations:
1. Adularia, chlorite, hematite
2. Calcite, quartz, pyrite, galena, asphaltite

Older fracture sealed with hematite stained adularia and chlorite is cut by a cataclasite with small fragments of wall rock, pyrite and galena. The matrix consists of calcite and quartz and contains inclusions of asphaltite.

Sample: **KFM06C 132.35–132.43 m**
Rock type: Metagranite
Fracture: Open fracture
Orientation: 038/77°
Deformation zone: DZ1 (from single-hole interpretation)
Fracture orientation set: NE
Fracture minerals: Calcite, chlorite, hematite, adularia

Sample: **KFM06C 154.61–154.70 m**
Rock type: Metagranite
Fracture: Open fracture
Orientation: 184/88°
Deformation zone: DZ1 (from single-hole interpretation)
Fracture orientation set: NS
Fracture minerals: Quartz, calcite, pyrite

Sequence of mineralizations:
1. Quartz
2. Calcite + pyrite

Sample: **KFM06C 162.02–162.33 m**
Rock type: Metagranite
Fracture: Sealed fracture
Orientation: 010/84°
Deformation zone: DZ1 (from single-hole interpretation)
Fracture orientation set: NS
Fracture minerals: Fluorite, quartz, calcite, pyrite

Sequence of mineralizations:
1. Fluorite + pyrite
2. Quartz + calcite + pyrite

Fluorite and pyrite have crystallized enclosing wall rock fragments. Later quartz, calcite and pyrite have precipitated, the calcite has precipitated both as nails together with the quartz and after the quartz filling voids.

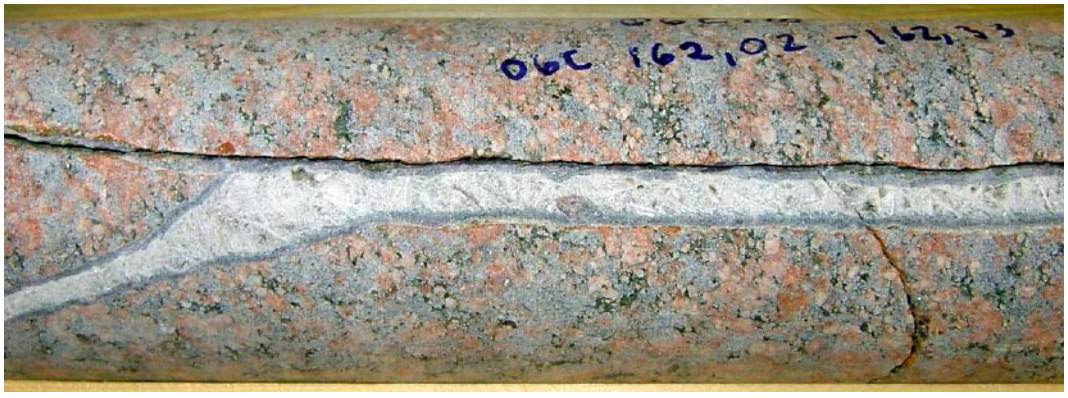

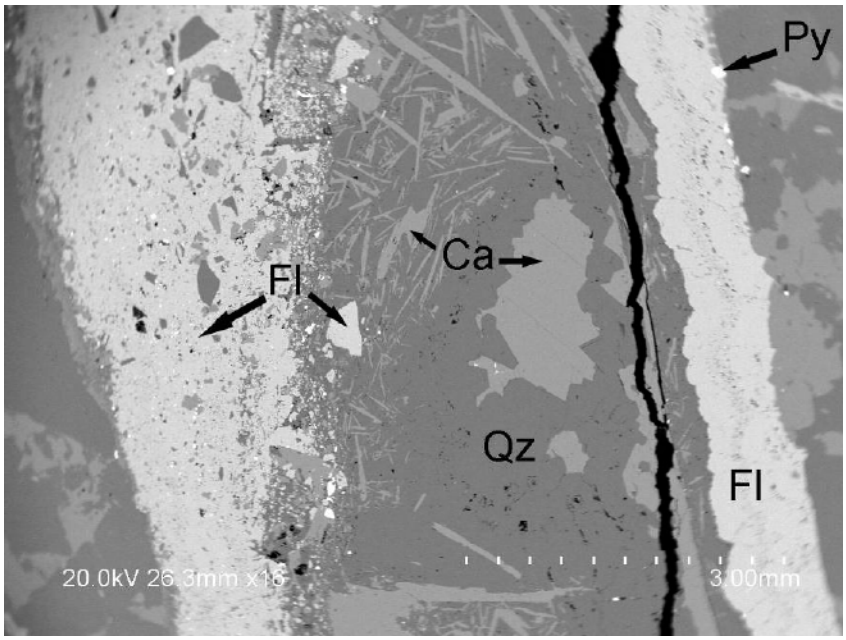

BSE image, Fl = fluorite, Ca = calcite, Qz = quartz, Py = pyrite.

Sample: **KFM06C 364.26–364.36 m**
Rock type: Metagranite
Fracture: Sealed fracture
Orientation: 030/88°
Deformation zone: DZ2 (from single-hole interpretation)
Fracture orientation set: NE
Fracture minerals: Adularia, hematite, chlorite, calcite

Sequence of mineralizations:
1. Adularia + hematite + chlorite
2. Calcite

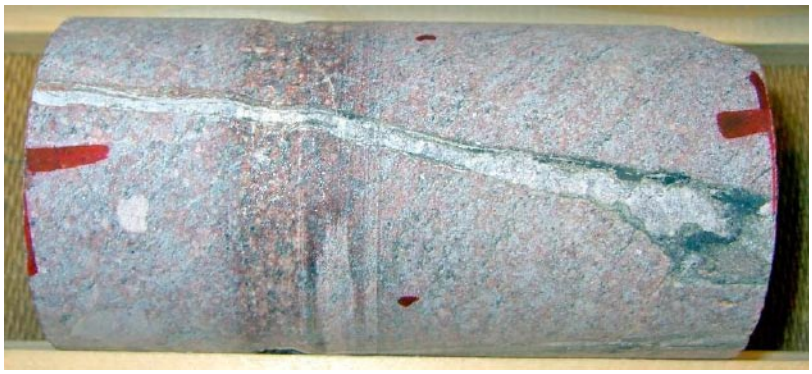

Sample: **KFM06C 442.48–442.52 m**
Rock type: Metagranite
Fracture: Sealed fracture
Orientation: 212/75°
Deformation zone: DZ3 (from single-hole interpretation)
Fracture orientation set: NE
Fracture minerals: Laumontite, calcite

Sequence of mineralizations:
1. Laumontite + calcite

Sample: **KFM06C 450.62–450.69 m**
Rock type: Metagranite
Fracture: Sealed fracture
Orientation: 229/75°
Deformation zone: DZ3 (from single-hole interpretation)
Fracture orientation set: NE
Fracture minerals: Chlorite, laumontite, calcite

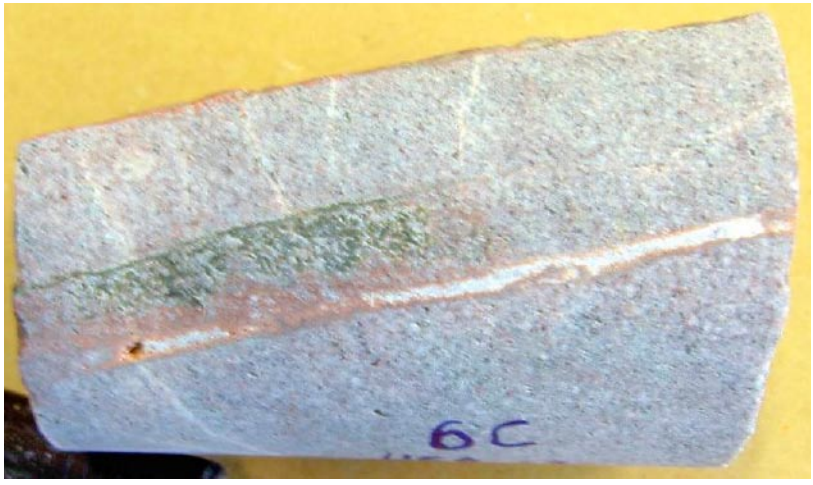

Sample: **KFM06C 451.64–451.82 m**
Rock type: Altered granite
Fracture: Open fracture and voids
Orientation: n.a.
Deformation zone: DZ2 (from single-hole interpretation)
Fracture orientation set: n.a.
Fracture minerals: (from XRD) Calcite, quartz, plagioclase, K-feldspar, illite, goethite

Sample: **KFM06C 453.84–454.04 m**
Rock type: Metagranite
Fracture: Sealed fracture
Orientation:223/89°
Deformation zone: DZ3 (from single-hole interpretation)
Fracture orientation set: NE
Fracture minerals: Adularia, hematite, calcite, chlorite

Sequence of mineralizations:
1. Adularia + hematite
2. Calcite + chlorite

Sample: **KFM06C 651.64–651.74 m**
Rock type: Metagranite
Fracture: Open fracture
Orientation: 022/89°
Deformation zone: DZ5 (from single-hole interpretation)
Fracture orientation set: NE
Fracture minerals: Adularia, albite, hematite, quartz, calcite, chlorite/corrensite

Sequence of mineralizations:
1. Adularia + albite + hematite + chlorite
2. Euhedral quartz
3. Calcite + chlorite/corrensite

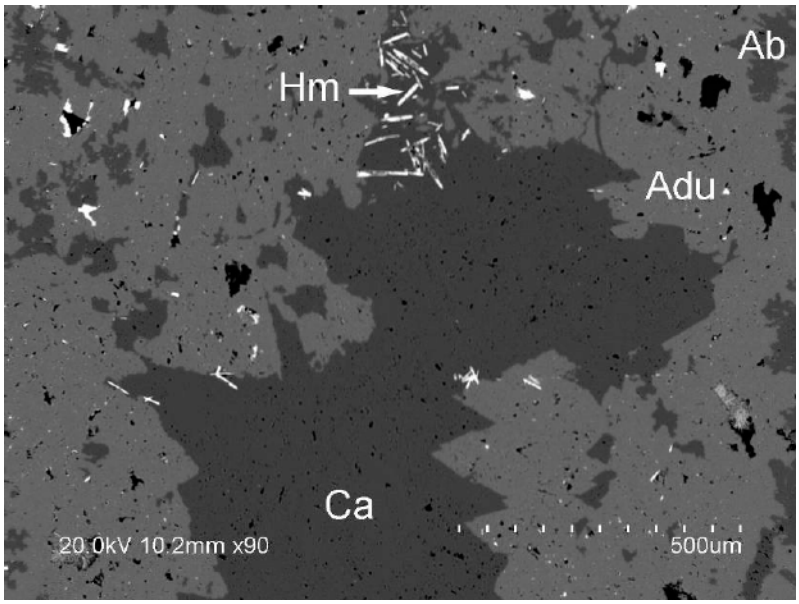

BSE image, Adu = adularia, Ab = albite, Ca = calcite, Hm = hematite.

Sample: **KFM06C 663.76–663.90 m**
Rock type: Metagranite
Fracture: Open fracture
Orientation: 224/85°
Deformation zone: DZ5 (from single-hole interpretation)
Fracture orientation set: NE
Fracture minerals: Chlorite, quartz, calcite, pyrite

Sequence of mineralizations:
1. Chlorite
2. Calcite + quartz + pyrite

Sample: **KFM06C 675.90–675.98 m**
Rock type: Metagranite
Fracture: Open fracture
Orientation: n.a.
Deformation zone: DZ5 (from single-hole interpretation)
Fracture orientation set: n.a.
Fracture minerals: Chlorite, prehnite, quartz, calcite, pyrite

Sample: **KFM06C 839.43–839.51 m**
Rock type: Metagranite
Fracture: Sealed fracture
Orientation: 010/84°
Deformation zone: No zone
Fracture orientation set: NS
Fracture minerals: Adularia, albite, hematite, quartz, calcite

Sequence of mineralizations :
1. Adularia + albite + calcite
2. Euhedral quartz + calcite

Sample: **KFM06C 939.15–939.39 m**
Rock type: Metagranite
Fracture: Partly open fracture
Orientation: n.a.
Deformation zone: No zone
Fracture orientation set: n.a.
Fracture minerals: Corrensite, hematite, mixed layer clay

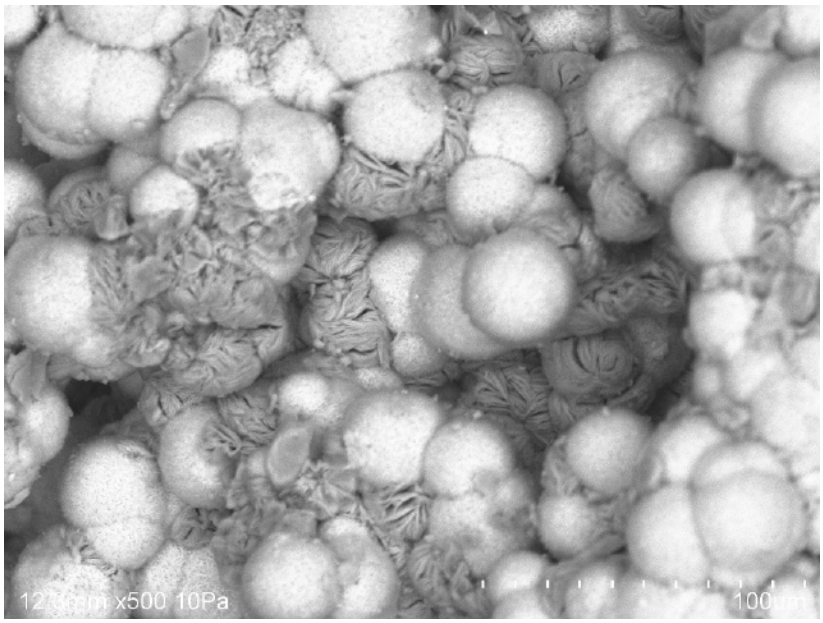

BSE image of spherical corrensite aggregates with brighter spherical hematite.

Sample: **KFM07A 112.34–112.42 m**
Rock type: Metagranite
Fracture: Crushed zone
Orientation: 006/11°
Deformation zone: ZFMNE1203
Fracture orientation set: HZ
Fracture minerals: Chlorite, clay minerals, pyrite

Sample: **KFM07A 118.18–118.31 m**
Rock type: Metagranite
Fracture: Open fracture
Orientation: 151/79°
Deformation zone: ZFMNE1203
Fracture orientation set: NW
Fracture minerals: Laumontite, chlorite/corrensite, apatite, titanite, zircon

Open fracture coated with a thin layer of chlorite/corrensite interlayered with laumontite. The fracture coating also contains small amounts of apatite, titanite and zircon.

Open fracture coated with mainly chlorite/corrensite and laumontite.

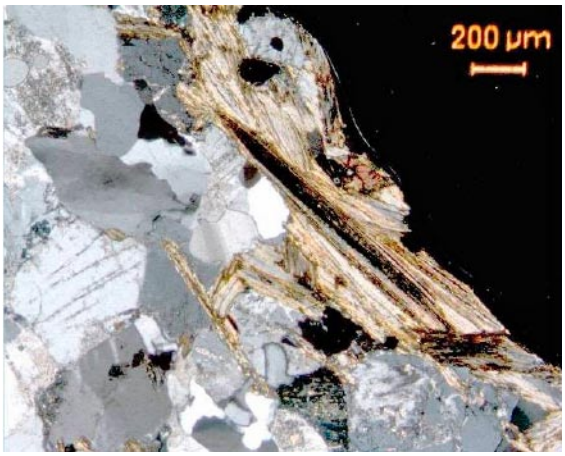

Photomicrograph (crossed polars) of chlorite/corrensite on fracture surface together with laumontite, titanite and apatite.

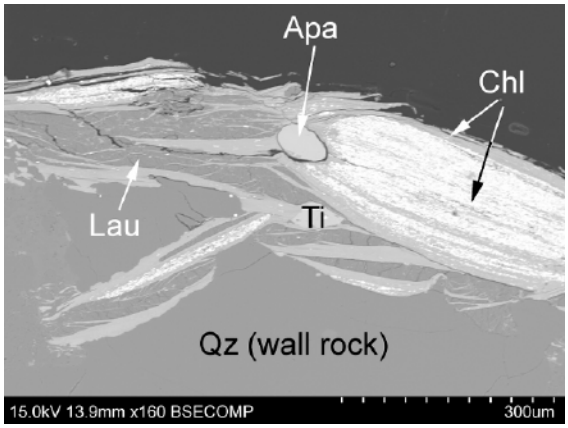

BSE image of chlorite/corrensite (Chl) interlayered with laumontite (Lau) and titanite (Ti) together with apatite (Ap).

Sample: **KFM07A 120.37–120.45 m**

Rock type: Metagranite

Fracture: Open fracture

Orientation: 081/11°

Deformation zone: ZFMNE1203

Fracture orientation set: HZ

Fracture minerals: quartz, adularia, titanite, Zn-silicate, pyrite

The fracture surface consists of biotite and K-feldspar from the wall rock together with small euhedral crystals of quartz and adularia. An unknown Zn-Fe silicate occurs as small black spots together with small amounts of titanite and pyrite.

Open fracture with thin greenish coating of quartz, adularia, pyrite and an unidentified Zn-silicate (small black spots). The diameter of the drill core is c 5 cm.

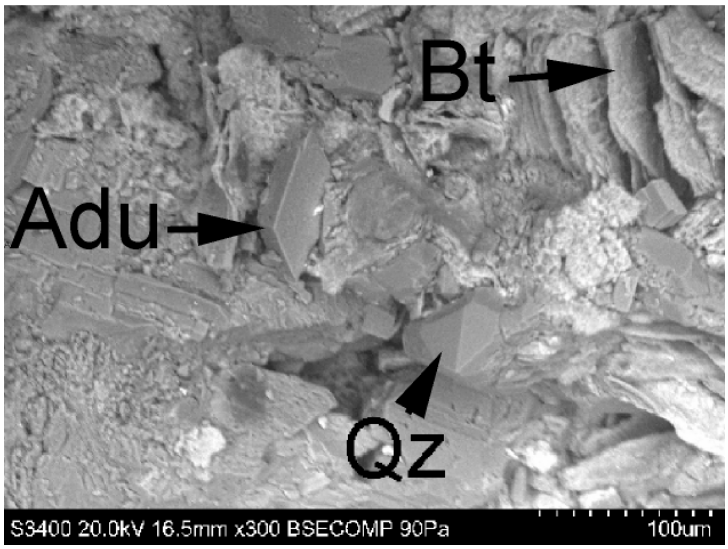

BSE image of fracture surface with biotite (Bt) from the wall rock and euhedral quartz (Qz) and adularia (Adu).

Sample: **KFM07A 121.47–121.63 m**

Rock type: Metagranite

Fracture: Sealed fracture + open fracture

Orientation: 348/82° (sealed) + 104/10° (open)

Deformation zone: ZFMNE1203

Fracture orientation set: NS (sealed) + HZ (open)

Fracture minerals: *Sealed fracture*: Quartz, prehnite, chlorite, mixed layer clay, illite, hematite, pyrite. *Open fracture*: Adularia, calcite, hematite, clay minerals, quartz

The sealed fracture is filled with large subhedral to euhedral quartz crystals. The space between the fractures has been filled with prehnite which has been partly or completely altered into chlorite and clay minerals (mixed layer clay, illite) and hematite and pyrite. The open fracture is coated with a thin layer of euhedral adularia with micro grains of hematite. Over the adularia calcite has precipitated. This open fracture is cut by another open fracture with a thin layer of adularia with small amounts of clay minerals, quartz and hematite.

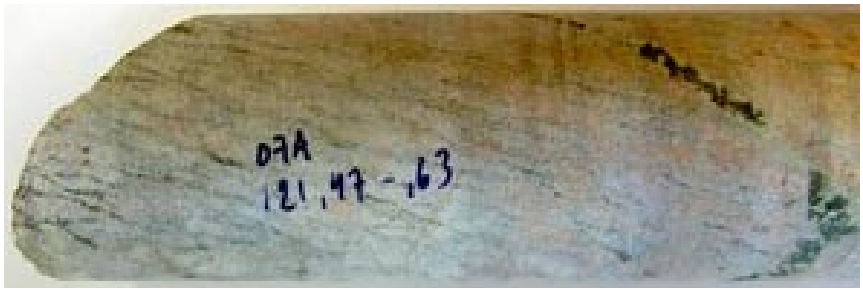

Sealed fracture with prehnite (bright) and prehnite altered into mainly clay minerals (dark). The left end of the drill core is an open fracture. The diameter of the drill core is c 5 cm.

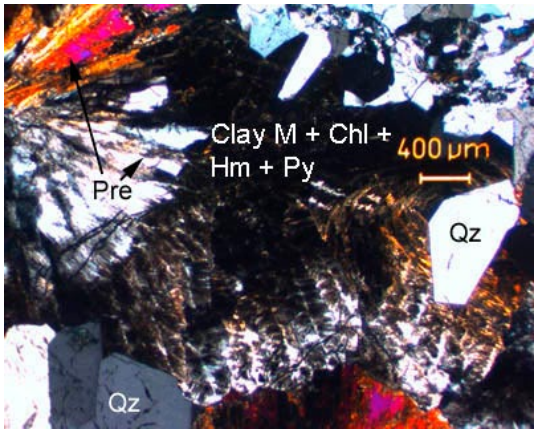

Photomicrograph of euhedral quartz and prehnite crystals partly and completely altered into chlorite, clay minerals, hematite and pyrite, crossed polars.

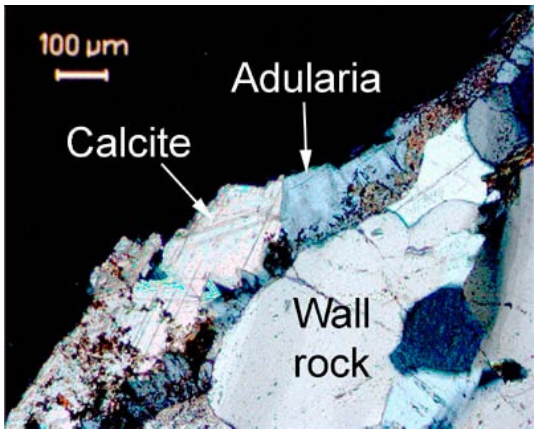

Photomicrograph of open fracture with euhedral adularia and later calcite, crossed polars.

Sample: **KFM07A 122.81–122.92 m**
Rock type: Metagranite
Fracture: Open fracture
Orientation: 083/16°
Deformation zone: ZFMNE1203
Fracture orientation set: HZ
Fracture minerals: As-Fe sulphide, pyrite, quartz, chlorite, clay mineral

Sample: **KFM07A 141.44–141.50 m**
Rock type: Metagranite
Fracture: Open fractures
Orientation: 251/26°
Deformation zone: ZFMNE1203
Fracture orientation set: HZ
Fracture minerals: Clay minerals, adularia, quartz

Striated open fracture with mainly clay minerals. The diameter of the drill core is c 5 cm.

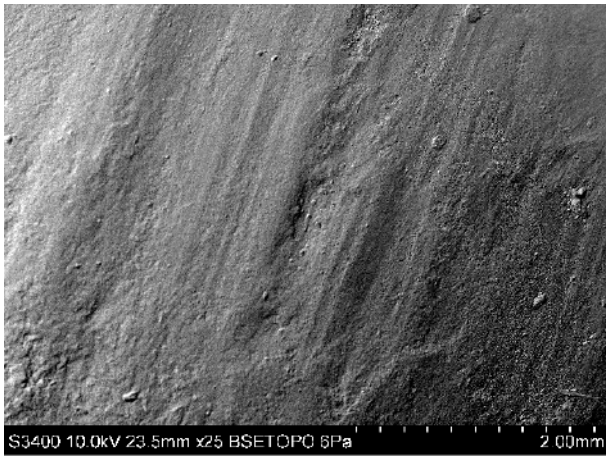

BSE (topographic) image of striation on fracture surface.

Sample: **KFM07A 151.90–152.20 m**

Rock type: Metagranite

Fracture: Sealed fracture

Orientation: Not defined in BIPS, parallel to drillcore

Deformation zone: ZFMNE1203

Fracture orientation set: n.a.

Fracture minerals: Laumontite, calcite, hematite, corrensite

Sequence of mineralizations:

1. Laumontite + hematite + calcite
2. Corrensite

Fracture sealed with laumontite and prismatic calcite crystals. Small amounts of corrensite have grown along the calcite planes. The calcite twins are generally straight and less than 10 µm thick. The calcite contains many small inclusions.

Sealed fracture with laumontite and calcite. The diameter of the drill core is c 5 cm.

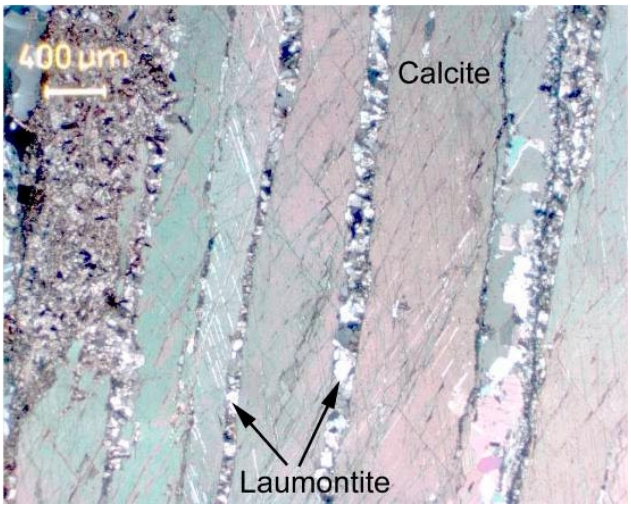

Photomicrograph of prismatic calcite crystals and laumontite.

Sample: **KFM07A 155.68–156.05 m**
Rock type: Metagranite
Fracture: Sealed fracture
Orientation: 255/88°
Deformation zone: ZFMNE1203
Fracture orientation set: NE
Fracture minerals: Laumontite, calcite, hematite

Sequence of mineralizations:
1. Laumontite + hematite + calcite

Fracture sealed with hematite stained laumontite and calcite.

Sealed fracture with laumontite and calcite. The diameter of the drill core is c 5 cm.

Sample: **KFM07A 166.07–166.35 m**
Rock type: Breccia
Fracture: Sealed breccia
Orientation: Not defined in BIPS
Deformation zone: ZFMNE1203
Fracture orientation set: n.a.
Fracture minerals: Laumontite, chlorite, hematite

Sequence of mineralizations:
1. Laumontite + hematite
2. Chlorite

Breccia sealed with hematite stained laumontite. The breccia is cut by a chlorite filled fracture.

Breccia sealed with hematite stained laumontite. The diameter of the drill core is c 5 cm.

Sample: **KFM07A 178.46–178.52 m**
Rock type: Metagranite
Fracture: Open fracture
Orientation: 252/24°
Deformation zone: ZFMNE1203
Fracture orientation set: NE
Fracture minerals: Chlorite/corrensite, calcite

Open fracture coated with chlorite/corrensite on which calcite has precipitated. The diameter of the drill core is c 5 cm.

Sample: **KFM07A 183.13–183.41 m**
Rock type: Metagranite
Fracture: Sealed fracture
Orientation: 254/20°
Deformation zone: No zone
Fracture orientation set: HZ
Fracture minerals: Adularia, chlorite/corrensite

Intense wall rock alteration adjacent to thin adularia and chlorite/corrensite sealed fracture. The diameter of the drill core is c 5 cm.

Sample: **KFM07A 193.77–193.90 m**
Rock type: Metagranite
Fracture: Open fracture
Orientation: 230/85°
Deformation zone: No zone
Fracture orientation set: NE
Fracture minerals: Quartz, calcite, corrensite, baryte

Sequence of mineralization:
1. Quartz
2. Calcite + corrensite + baryte + pyrite

Euhedral quartz crystals have precipitated on a fresh rock surface. Over the quartz calcite, corrensite, baryte and pyrite have crystallized. The corrensite occurs both massively and as spherical aggregates.

Open fracture with quartz, chlorite, corrensite, baryte and pyrite. The diameter of the drill core is c 5 cm.

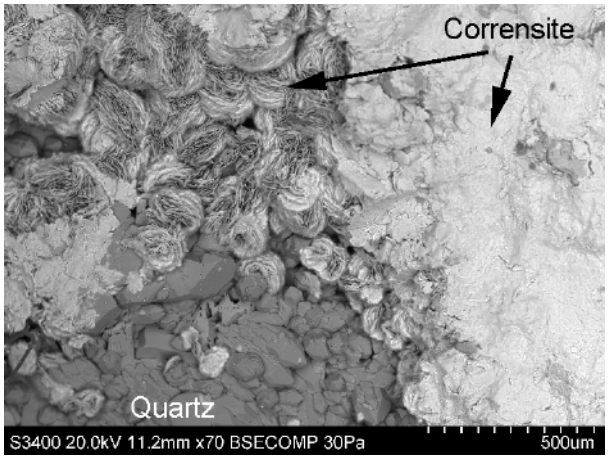

BSE image of fracture surface with euhedral quartz crystals partly covered with corrensite, occurring both massively and as small spherical aggregates.

Sample: **KFM07A 274.95–275.07 m**
Rock type: Metagranite
Fracture: Sealed fracture
Orientation: 065/86°
Deformation zone: No zone
Fracture orientation set: NE
Fracture minerals: Quartz, calcite, pyrite

Fracture sealed with euhedral quartz, calcite and some pyrite. Part of the fracture consists of brecciated wall rock sealed with quartz and calcite.

Fracture sealed with quartz, calcite and pyrite. The diameter of the drill core is c 5 cm.

Sample: **KFM07A 402.68–402.76 m**
Rock type: Metagranite
Fracture: Sealed fracture
Orientation: 112/87°
Deformation zone: No zone
Fracture orientation set: EW
Fracture minerals: Quartz, calcite, corrensite, allanite
1. Quartz + calcite
2. Allanite + corrensite

The fracture is coated with quartz and calcite on which small crystals of allanite and spherical aggregates of corrensite have grown. The allanite appears as a greenish gray coating in hand sample.

Open fracture coated with quartz and calcite (white), corrensite (dark green) and allanite (beige). The width of the sample is c 3 cm.

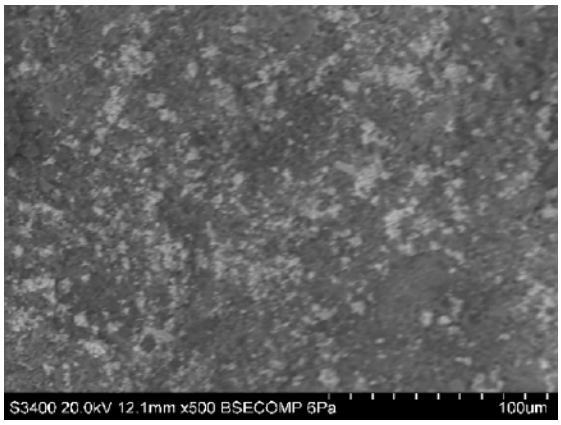

BSE image of fracture coating with small allanite crystals (white) on calcite coating.

Sample: **KFM07A 419.19–419.46 m**
Rock type: Metagranite
Fracture: Sealed fracture
Orientation: Fracture network
Deformation zone: ZFMNE0159
Fracture orientation set: n.a.
Fracture minerals: Prehnite, calcite, chlorite, clay minerals

The highly altered rock consists of epidote and amphibole, chlorite and recrystallized quartz. The rock is cut by veins with prehnite, calcite and clay minerals.

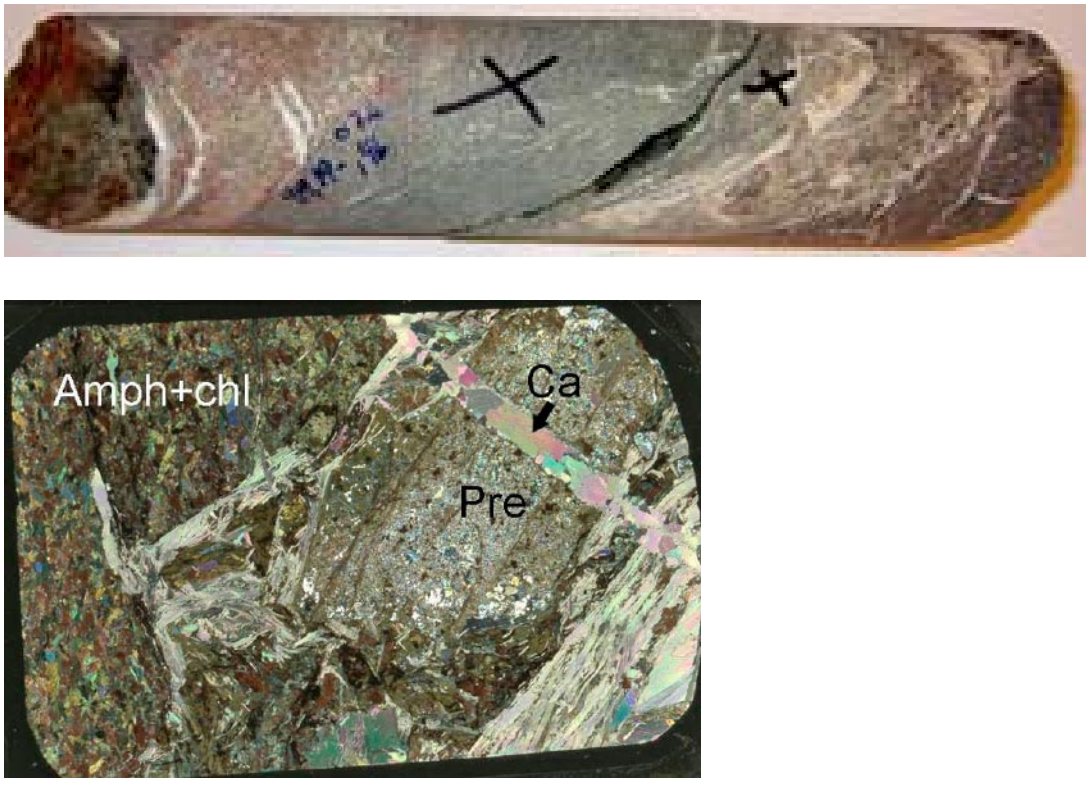

Scanned thin section, Amph = amphibole, chl = chlorite, Ca = calcite, Pre = prehnite. The base of the figure is c 3 cm.

Sample: **KFM07A 500.73–500.98 m**
Rock type: Metatonalite
Fracture: Sealed fractures
Orientation: 259/28° + 276/28°
Deformation zone: No zone
Fracture orientation set: HZ
Fracture minerals: Prehnite, chlorite

Thin sealed fractures with prehnite and chlorite surrounded with altered red-coloured wall rock. The diameter of the drill core is c 5 cm.

Sample: **KFM07A 569.73–569.94 m**
Rock type: Metatonalite
Fracture: Sealed fracture
Orientation: 039/78°
Deformation zone: No zone
Fracture orientation set: NE
Fracture minerals: Adularia, hematite, calcite

Thin sealed fracture with adularia, hematite and calcite surrounded with altered red-coloured wall rock. The dark bands are amphibolites. The diameter of the drill core is c 5 cm.

Sample: **KFM07A 797.83–797.89 m**
Rock type: Pegmatite
Fracture: Open fracture
Orientation: 238/74°
Deformation zone: No zone
Fracture orientation set: NE
Fracture minerals: Fe-oxide

Open fracture with black spots consisting of iron oxide. The diameter of the drill core is c 5 cm.

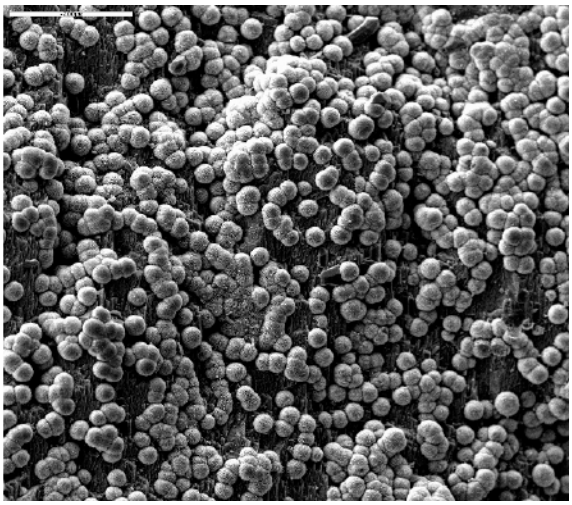

BSE image of spherical aggregates of iron oxide. The white bar is 200 µm.

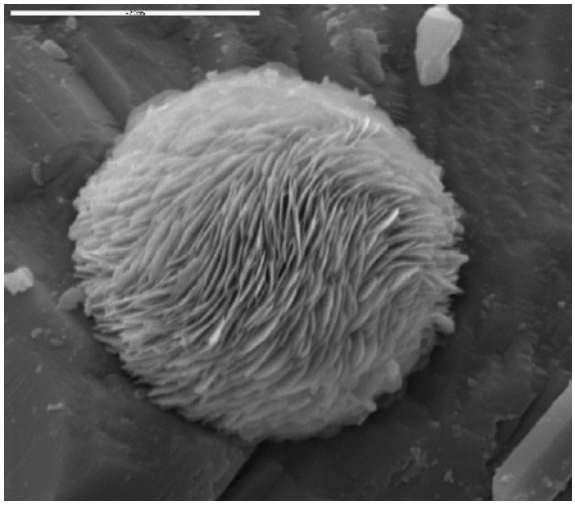

BSE image of a spherical aggregate of iron oxide. The white bar is 20 µm.

Sample: **KFM07A 804.41–804.54 m**
Rock type: Breccia
Fracture: Sealed breccia with open fracture
Orientation: 079/88°
Deformation zone: No zone
Fracture orientation set: NE
Fracture minerals: Laumontite, hematite, chlorite, quartz, pyrite, calcite

Sequence of mineralizations:
1. Laumontite
2. Chlorite
3. Euhedral quartz
4. Calcite + pyrite + chlorite/clay mineral

Breccia sealed with hematite stained laumontite. The drill core is cut by an open fracture which is coated with a thin layer of chlorite. Over the chlorite a thin coating of quartz has precipitated. The quartz occurs both massively and as small euhedral crystals. The last minerals to have precipitated in the open fracture are calcite, chlorite/clay mineral and small amounts of pyrite.

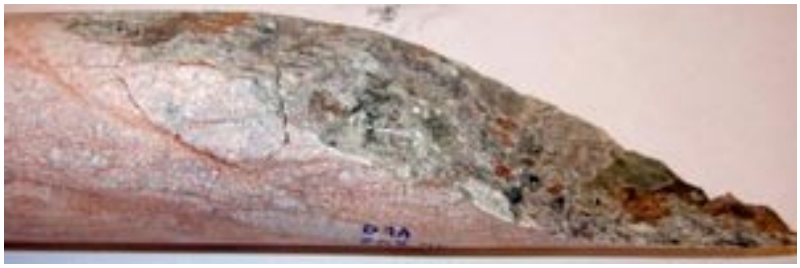

Laumontite sealed breccia with open fracture coated with chlorite, quartz, calcite and pyrite. The diameter of the drill core is c 5 cm.

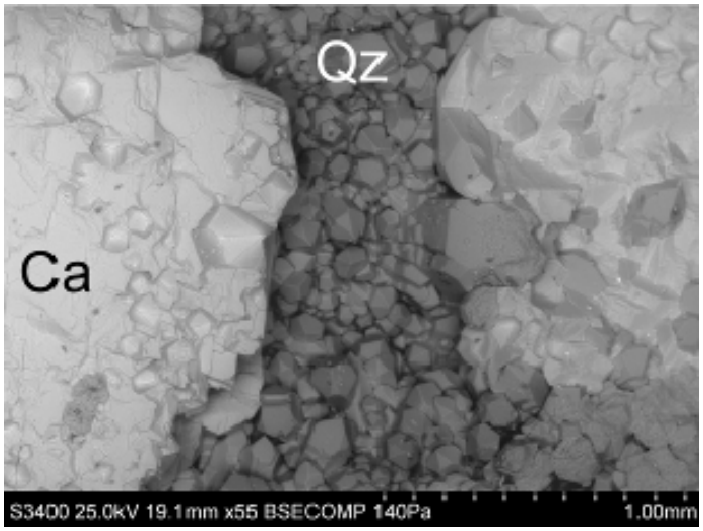

BSE image of euhedral quartz crystals with overgrowth of calcite. Observe the thin calcite coating on prismatic quartz crystals to the left in the picture.

Sample: **KFM07A 815.27–815.37 m**

Rock type: Altered metagranite

Fracture: Sealed fracture/mylonite

Orientation: 357/88°

Deformation zone: No zone

Fracture orientation set: NS

Fracture minerals: Quartz, epidote, hematite

Altered wall rock consisting of saussuritized plagioclase and epidote. The epidote occurs mostly symplectic with intergrowth of epidote and quartz. The thin section also contains a part dominated by polygonal epidote with crystals showing zonation.

The wall rock is cut by a fracture in which euhedral epidote has crystallized, quartz has later filled the fracture. Subgrain formation can be seen in the quartz due to later deformation.

The red colour of parts of the wall rock is due to small hematite grains in the saussuritized plagioclase.

Altered wall rock of mainly saussuritized plagioclase and epidote. The diameter of the drill core is c 5 cm.

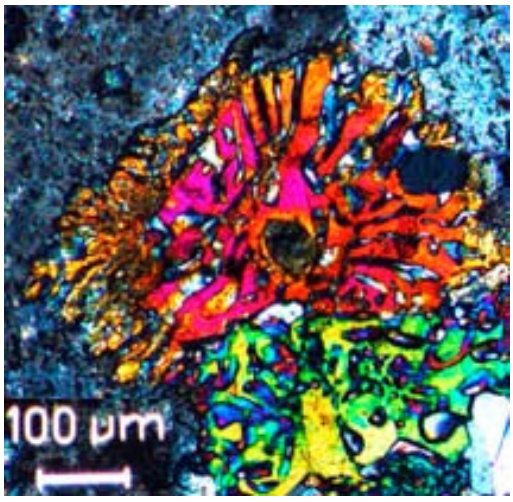

Symplectic intergrowth of epidote and quartz together with small apatite crystals. Photomicrograph with crossed polars.

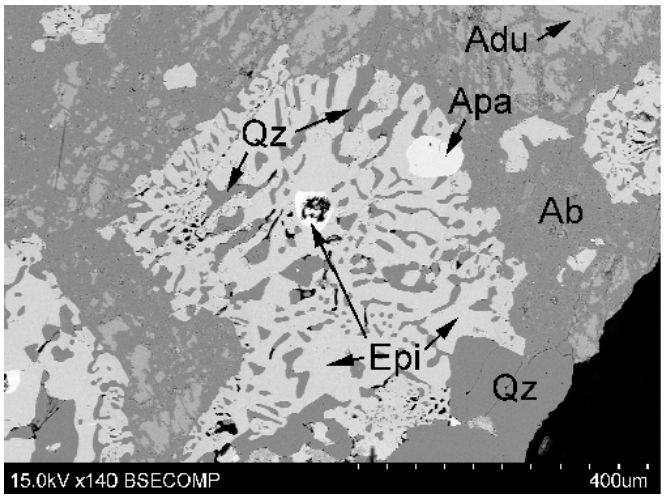

BSE image of the same area as in the precious figure of symplectic intergrowth of epidote and quartz together with quartz (Qz), apatite (Apa) and plagioclase altered into adularia (Adu) and albite (Ab).

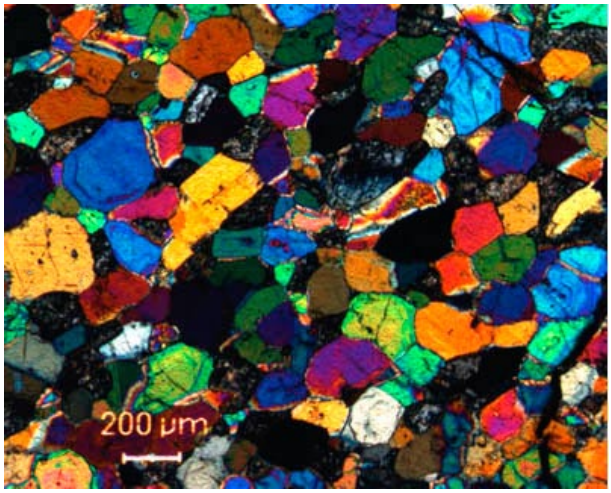

Polygonal crystallization of epidote. Zonation can be seen in some of the crystals. Photomicrograph with crossed polars.

Sample: **KFM07A 876.11–876.55 m**
Rock type: Metagranite
Fracture: Sealed and open fractures
Orientation: Fracture network
Deformation zone: ZFMNS0100
Fracture orientation set: n.a.
Fracture minerals: Calcite, quartz, adularia, hematite

A thin fracture is sealed with calcite. In the open voids large euhedral crystals of quartz and adularia have crystallized. The red colour is due to hematite staining of the quartz and adularia.

Thin fracture sealed with calcite. The diameter of the drill core is c 5 cm.

Open void with large euhedral crystals of quartz and adularia – red-stained of hematite. The diameter of the drill core is c 5 cm.

Sample: **KFM07A 882.49–882.83 m**
Rock type: Metabasite, highly altered
Fracture: Sealed fracture
Orientation: Fracture network
Deformation zone: ZFMNS0100
Fracture orientation set: n.a.
Fracture minerals: Quartz, epidote, chlorite, laumontite, fluorite, hematite

Sequence of mineralizations:
1. Quartz + epidote + chlorite
2. Laumontite + fluorite + hematite + chlorite

The highly altered rock consists of epidote with albite inclusions, Mg-rich chlorite, laumontite, fluorite and hematite. Most of the epidote crystals are highly altered and partly replaced by laumontite. Euhedral quartz and epidote nails have grown into voids which later have been filled with fluorite. The laumontite crystals occur fan-shaped and are probably pseudomorphs after prehnite. Both laumontite and fluorite occur as lenses in chlorite. The chlorite also contains bands of more Fe-rich chlorite and hematite. The sample is partly brecciated with fragments of mainly quartz in a matrix of laumontite, epidote and chlorite. The laumontite replacement of prehnite has probably occurred during the formation of the laumontite sealed breccia.

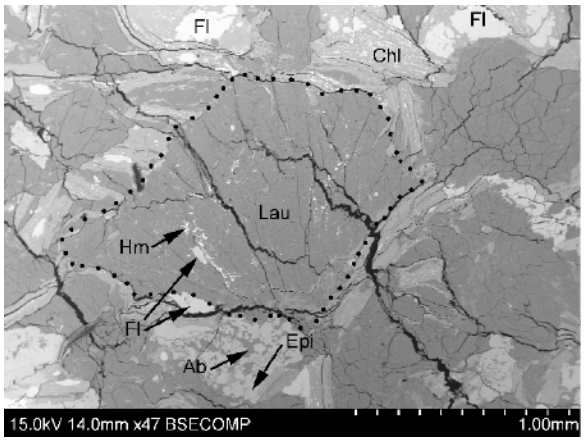

BSE image of fan-shaped pseudomorph after prehnite replaced by laumontite (Lau), hematite (Hm) and fluorite (Fl). Albite (Ab), chlorite (Chl) and epidote (Epi) also occur in the sample.

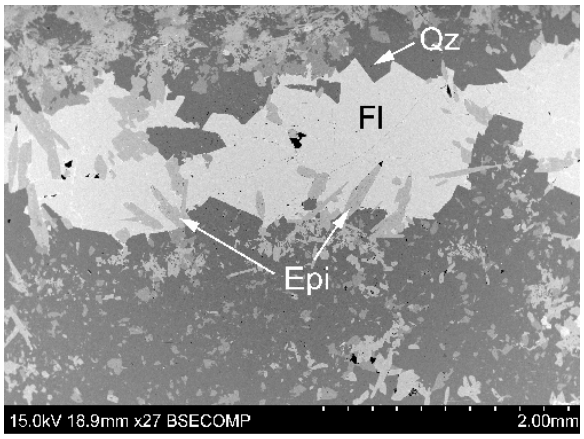

BSE image of euhedral epidote and quartz crystals which have grown into a void. The void has later been filled with fluorite.

Sample: **KFM07A 882.95–883.05 m**
Rock type: Metagranite
Fracture: Open fracture
Orientation: 236/67°
Deformation zone: ZFMNS0100
Fracture orientation set: NE
Fracture minerals: Quartz, pyrite, adularia

Sequence of mineralizations:
1. Quartz
2. Pyrite + adularia

Open fracture with coating of euhedral quartz, pyrite and adularia. The diameter of the drill core is c 5 cm.

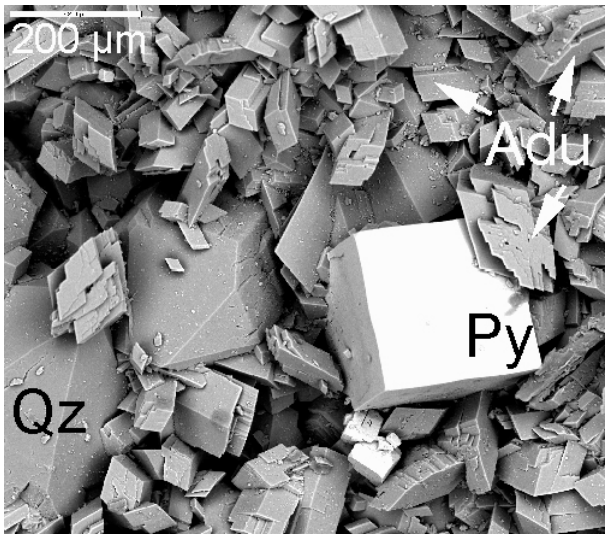

BSE image of euhedral crystals of quartz covered by euhedral pyrite and adularia.

Sample: **KFM07A 883.31–883.42 m**
Rock type: Metagranite
Fracture: Partly open fracture
Orientation: 078/77°
Deformation zone: No zone
Fracture orientation set: NE
Fracture minerals: Adularia, hematite, quartz, pyrite, calcite

Sequence of mineralizations:
1. Adularia + hematite
2. Quartz
3. Pyrite + calcite

A fracture sealed with adularia, hematite and quartz with an open void where the quartz has grown euhedral. Euhedral calcite and pyrite have precipitated on this quartz coating.

Open fracture coated with small euhedral quartz crystals. On this coating euhedral pyrite and calcite have precipitated. The diameter of the drill core is c 5 cm.

Sample: **KFM07A 883.57–883.63 m**
Rock type: Metagranite
Fracture: Sealed fracture
Orientation: 176/83°
Deformation zone: ZFMNS0100
Fracture orientation set: NS
Fracture minerals: Laumontite, chlorite/corrensite

Drill core sample penetrated by sealed laumontite filled fractures. The diameter of the drill core is c 5 cm.

Sample: **KFM07A 896.68–896.77 m**
Rock type: Metabasite
Fracture: Crushed zone
Orientation: ~ 180/80° (zone)
Deformation zone: ZFMNS0100
Fracture orientation set: NS
Fracture minerals: Chlorite/corrensite, laumontite, calcite, quartz, illite, mixed layer clay

Crushed zone in metabasite consisting of older laumontite and calcite and later chlorite/corrensite. The diameter of the drill core is c 5 cm.

Sample: **KFM07A 933.91–934.06 m**
Rock type: Metagranite
Fracture: Sealed fracture
Orientation: 154/80°
Deformation zone: ZFMNS0100
Fracture orientation set: NW
Fracture minerals: Quartz, adularia, chlorite, hematite, titanite

Sequence of mineralizations:
1. Quartz + adularia + chlorite + hematite + titanite
2. Chlorite/corrensite
3. Euhedral quartz + adularia

Breccia with fragments of wall rock with saussuritized plagioclase and deformed quartz. The matrix consists of quartz, adularia, alternating Mg and Fe rich chlorite, hematite and titanite. The breccia is cut by micro fractures with chlorite on which euhedral quartz and adularia have crystallized. The micro fractures have been reopened after the crystallization of these minerals.

Breccia sealed with quartz, adularia, chlorite, hematite and titanite. The diameter of the drill core is c 5 cm.

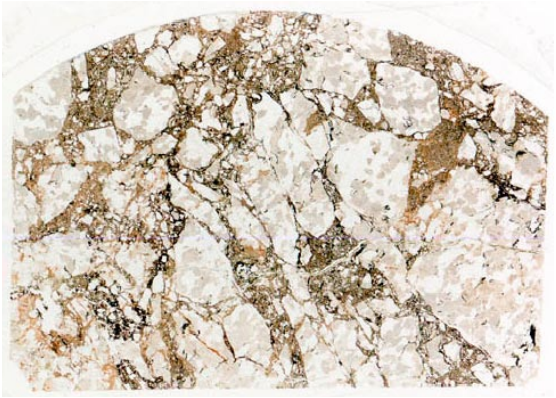

Scanned thin section of breccia sealed with quartz, adularia, chlorite, hematite and titanite. The base of the figure is c 35 mm.

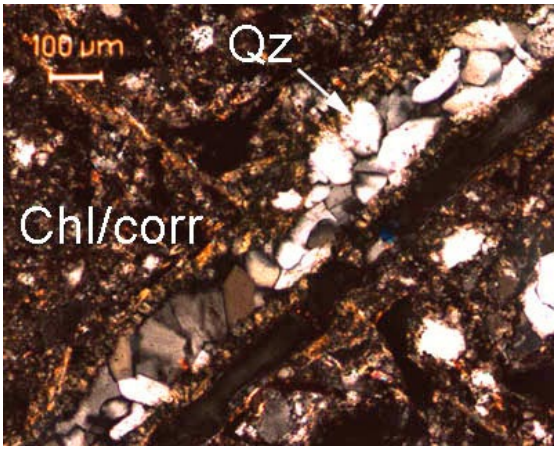

Chlorite/corrensite (Chl/corr) cut by thin fracture sealed with euhedral quartz. Photomicrograph with crossed polars.

Sample: **KFM07A 944.58–944.78 m**
Rock type: Metagranite
Fracture: Open fracture
Orientation: 244/42°
Deformation zone: ZFMNS0100
Fracture orientation set: NE
Fracture minerals: Clay minerals

Open fracture with clay minerals. The diameter of the drill core is c 5 cm.

Sample: **KFM07A 969.68–969.80 m**
Rock type: Metagranite
Fracture: Open fracture
Orientation: 162/86°
Deformation zone: ZFMNS0100
Fracture orientation set: NS
Fracture minerals: Quartz, adularia, plagioclase, chlorite, illite

According to XRD, the sample contains mainly quartz and adularia together with some plagioclase and chlorite. The fine fraction contains illite, chlorite, quartz, adularia and plagioclase.

Open fracture with quartz, adularia, plagioclase, chlorite and illite. The diameter of the drill core is c 5 cm.

Sample: **KFM07A 974.16–974.22 m**
Rock type: Metagranite
Fracture: Open fracture
Orientation: 164/71°
Deformation zone: ZFMNS0100
Fracture orientation set: NS
Fracture minerals: Adularia, hematite, chlorite/corrensite, calcite, pyrite

Sequence of mineralizations:
1. Adularia + hematite
2. Chlorite/corrensite
3. Calcite + pyrite

Open fracture coated with chlorite/corrensite on which calcite and small pyrite crystals have precipitated. The diameter of the drill core is c 5 cm.

Sample: **KFM07A 988.83–988.94 m**
Rock type: Metagranite
Fracture: Sealed fracture
Orientation: not visible in BIPS
Deformation zone: ZFMNS0100
Fracture orientation set: n.a.
Fracture minerals: albite, adularia, calcite, hematite

Fracture sealed with albite, adularia, hematite and calcite. The diameter of the drill core is c 5 cm.

Sample: **KFM07A 998.92–999.13 m**
Rock type: Metagranite
Fracture: Open fracture
Orientation: n.a.
Deformation zone: ZFMNS0100
Fracture orientation set: n.a.
Fracture minerals: Quartz, calcite, corrensite

Sequence of mineralizations:
1. Quartz
2. Calcite + corrensite

Open fracture coated with euhedral quartz on which calcite and corrensite have precipitated. The diameter of the drill core is c 5 cm.

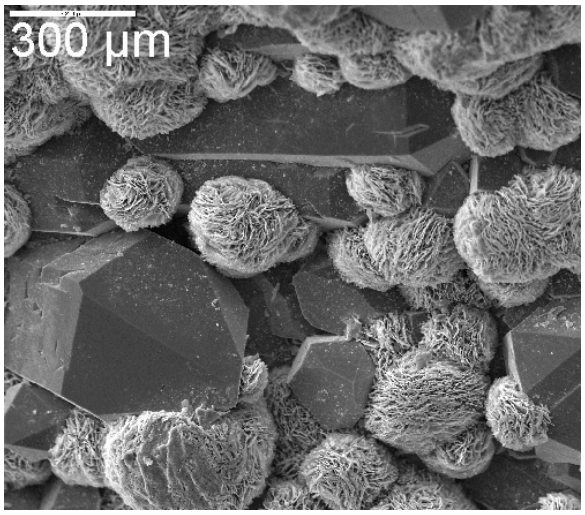

BSE image of euhedral quartz crystals covered with spherical aggregates of corrensite.

Sample: **KFM08A 107.42–107.57 m**
Rock type: Metagranite
Fracture: Sealed breccia
Orientation: 221/86°
Deformation zone: No zone
Fracture orientation set: NE
Fracture minerals: Prehnite, quartz, calcite

Sequence of mineralizations:
1. Prehnite
2. Quartz + calcite

Prehnite sealed fracture later reactivated with accompanying breccia formation of the wall rock which is sealed with calcite and quartz.

Quartz and calcite sealed breccia. The grey-green filling to the right of the breccia in the picture is the older prehnite sealing. The diameter of the drill core is c 5 cm.

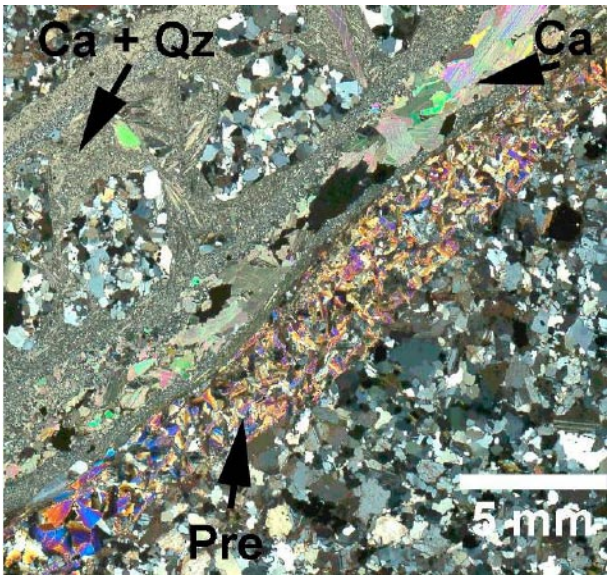

Scanned thin section with crossed polars of prehnite sealed fracture adjacent to calcite and quartz sealed breccia with wall rock fragments.

Sample: **KFM08A 183.77–183.88 m**
Rock type: Metagranite
Fracture: Sealed fracture
Orientation: 026/75°
Deformation zone: ZFMNE1061
Fracture orientation set: NE
Fracture minerals: Quartz, albite, adularia, prehnite, calcite, fluorite

Sequence of mineralizations:
1. Prehnite + adularia + quartz + fluorite
2. Prehnite
3. Albite
4. Calcite

Sealed fracture with adularia, quartz, fluorite, hematite, prehnite and calcite. The diameter of the drill core is c 5 cm.

Sample: **KFM08A 193.01–193.07 m**
Rock type: Metagranite
Fracture: Sealed fracture
Orientation: 031/84°
Deformation zone: ZFMNE1061
Fracture orientation set: NE
Fracture minerals: Adularia, hematite, pyrite, calcite, quartz

Sequence of mineralizations:
1. Adularia + calcite + quartz + hematite + pyrite
2. Calcite + quartz

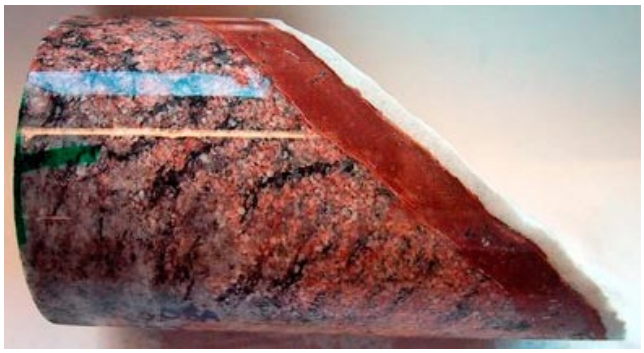

Sample: **KFM08A 197.65–197.88 m**
Rock type: Metagranite
Fracture: Crush zone
Orientation: 203/12°
Deformation zone: ZFMNE1061
Fracture orientation set: HZ
Fracture minerals: (from XRD) Calcite, quartz, plagioclase, K-feldspar, chlorite, illite, corrensite

Sample: **KFM08A 245.46–245.59 m**
Rock type: Metagranite
Fracture: Open fracture
Orientation: 039/84°
Deformation zone: ZFMNE1061
Fracture orientation set: NE
Fracture minerals: Quartz, calcite, pyrite, adularia, analcime

Sequence of mineralizations:
1. Calcite + pyrite + quartz + adularia + analcime

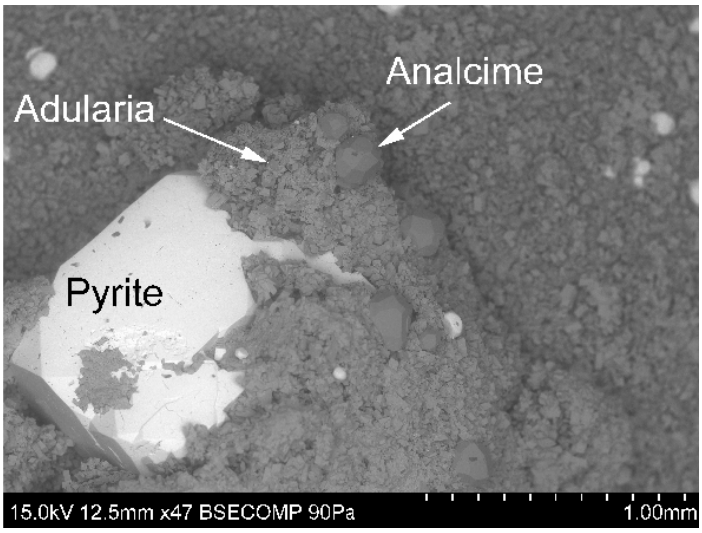

BSE image.

Sample: **KFM08A 246.11–246.35 m**
Rock type: Metagranite
Fracture: Open fracture
Orientation: 217/90°
Deformation zone: ZFMNE1061
Fracture orientation set: NE
Fracture minerals: Chlorite, quartz, calcite, adularia, pyrite, analcime

Sequence of mineralizations:
1. Chlorite
2. Adularia + calcite + quartz
3. Pyrite + analcime

Open fracture coated with quartz and adularia on which euhedral crystals of pyrite and analcime have precipitated. The diameter of the drill core is c 5 cm.

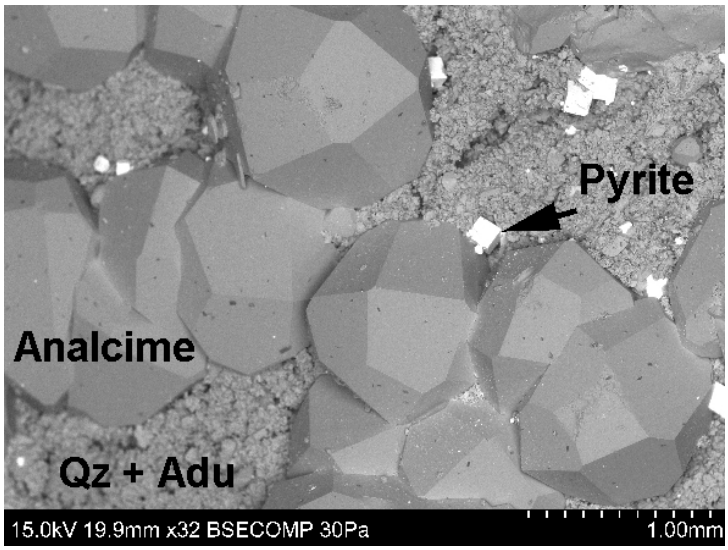

BSE image of Trapezohedral analcime and cubic pyrite crystals precipitated on fracture coating of quartz (Qz) and adularia (Adu).

Sample: **KFM08A 247.58–247.71 m**
Rock type: Metagranite
Fracture: Sealed fracture
Orientation: Fracture network
Deformation zone: ZFMNE1061
Fracture orientation set: n.a.
Fracture minerals: Laumontite, calcite

Sample: **KFM08A 304.57–304.60 m**
Rock type: Metagranite
Fracture: Sealed fracture
Orientation: 070/35°
Deformation zone: ZFMNE1061
Fracture orientation set: HZ
Fracture minerals: chlorite/corrensite, calcite, adularia

Sequence of mineralizations:
1. Chlorite/corrensite + adularia
2. Calcite

Sample: **KFM08A 410.60–411.04 m**

Rock type: Episyenite

Fracture: n.a.

Orientation: n.a.

Deformation zone: No zone

Fracture orientation set: n.a.

Fracture minerals: Hematite, calcite, corrensite

Sequence of mineralizations:

1. Hematite
2. Corrensite
3. Calcite

Episyenite with quartz dissolution. The voids have later been filled with nail-shaped hematite crystals, spherical aggregates of corrensite and massive calcite. Some re-crystallization has also occurred along the margins of the wall rock K-feldspar crystals.

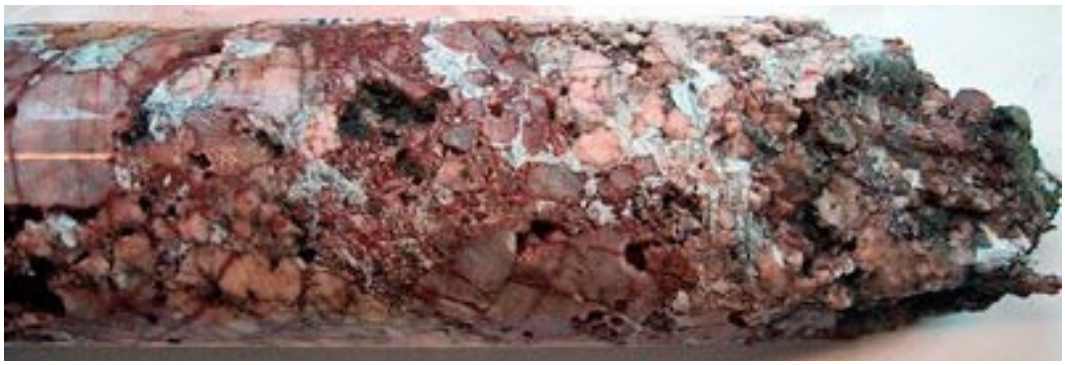

Episyenite where the quartz has been dissolved. The voids have later been filled with calcite (white in figure). The diameter of the drill core is c 5 cm.

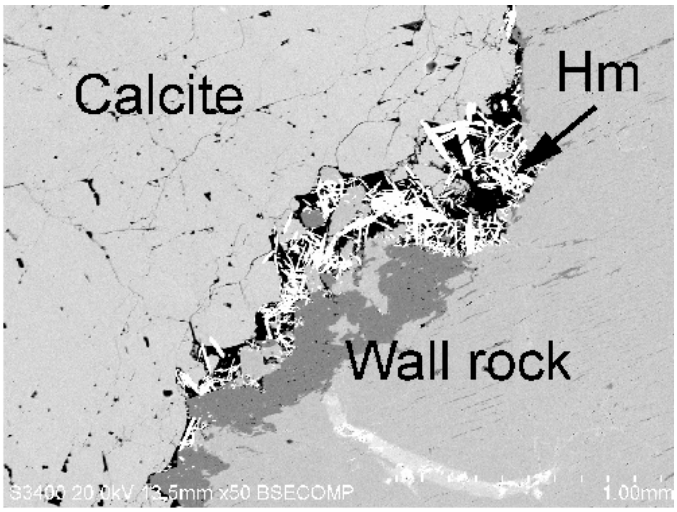

BSE image of calcite filled void in episyenite, nail-shaped hematite crystals have precipitated on the surface of the void.

Sample: **KFM08A 411.55–411.68 m**
Rock type: Episyenite
Fracture: Open fractres
Orientation: 014/56°; 005/60°; 226/35°
Deformation zone: No zone
Fracture orientation set: NS and HZ
Fracture minerals: calcite, chlorite, clay minerals, adularia, hematite

Three open fractures, the one facing left in the figure is orientated 005/60° and the one facing towards the viewer is orientated 226/35°. The main fracture coating on the two fractures dipping 56 and 60° are chlorite, clay minerals and calcite. The more horizontal fracture is coated with a thin layer of adularia and hematite. The diameter of the drill core is c 5 cm.

Sample: **KFM08A 480.30–480.52 m**
Rock type: Pegmatite
Fracture: Open fracture
Orientation: n.a. in BIPS, subparallel to drill core
Deformation zone: ZFMNS1204
Fracture orientation set: n.a.
Fracture minerals: Quartz, pyrite

Sequence of mineralizations:
1. Euhedral quartz + pyrite

Open fracture in pegmatite with small euhedral quartz crystals and pyrite as fracture minerals. The diameter of the drill core is c 5 cm.

Sample: **KFM08A 492.90–493.01 m**
Rock type: Metabasite
Fracture: Open fracture
Orientation: 216/86°
Deformation zone: ZFMNS1204
Fracture orientation set: NE
Fracture minerals: Adularia, hematite, calcite, chlorite/corrensite

Sequence of mineralizations:
1. Adularia + hematite + calcite
2. Chlorite/corrensite

Sealed fracture with adularia, hematite and calcite reactivated with precipitation of chlorite/corrensite in an open fracture. The diameter of the drill core is c 5 cm.

Sample: **KFM08A 495.07–495.37 m**
Rock type: Metagranite
Fracture: Open fractures
Orientation: 145/36°; 224/89°
Deformation zone: ZFMNS1204
Fracture orientation set: HZ; NE
Fracture minerals: Calcite, quartz, pyrite, adularia, illite, chlorite, prehnite

According to XRD analysis, the sample consists mainly of quartz and adularia with some illite, chlorite and prehnite. The fine fraction consists of the same minerals but is dominated by illite and chlorite.

Open fracture with quartz, calcite, pyrite, chlorite and illite (orientation 224/89°). The diameter of the drill core is c 5 cm.

Open fracture coated with mainly quartz, adularia, illite and chlorite (orientation 145/36°).
The diameter of the drill core is c 5 cm.

Sample: **KFM08A 529.50–529.50 m**
Rock type: Metatonalite
Fracture: Sealed fracture
Orientation: Many small fracture close to 020/65°
Deformation zone: No zone
Fracture orientation set: NE
Fracture minerals: Adularia, hematite

Thin fracture sealed with hematite stained adularia surrounded with altered red-coloured wall rock.
The diameter of the drill core is c 5 cm.

Sample: **KFM08A 605.08–605.16 m**
Rock type: Metagranite
Fracture: Sealed fracture
Orientation: 011/37°
Deformation zone: No zone
Fracture orientation set: HZ
Fracture minerals: Epidote, calcite

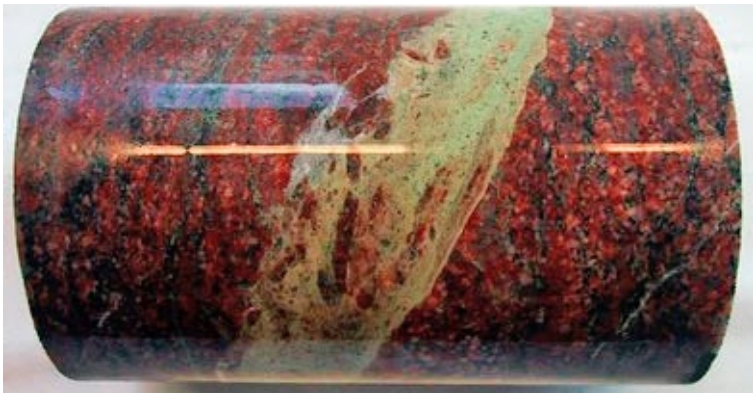

Epidote and calcite sealed fracture. The diameter of the drill core is c 5 cm.

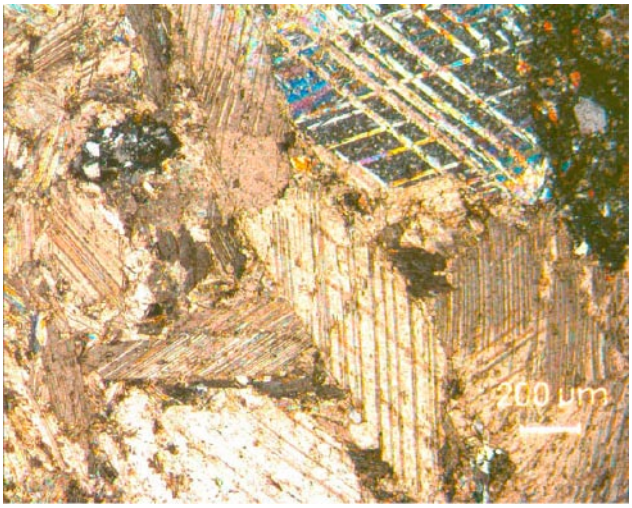

Photomicrograph with crossed polars of calcite crystals with thick twins.

Sample: **KFM08A 623.02–623.35 m**
Rock type: Metagranite
Fracture: Open fracture
Orientation: 224/80°
Deformation zone: No zone
Fracture orientation set: NE
Fracture minerals: prehnite, chlorite/corrensite

Open fracture coated with prehnite and chlorite/corrensite. Extensive red-coloured wall rock alteration adjacent to the fracture. The diameter of the drill core is c 5 cm.

Sample: **KFM08A 686.59–686.84 m**
Rock type: Metagranite
Fracture: Open fracture
Orientation: 350/13°
Deformation zone: No zone
Fracture orientation set: HZ
Fracture minerals: Muscovite, calcite, quartz, mixed layer clay

According to XRD analysis, the sample consists mainly of calcite, muscovite and some quartz and chlorite. The fine fraction is dominated by muscovite together with minor amounts of calcite, mixed layer clay (probably smectite and/or vermiculite components with some illite sheets).

The diameter of the drill core is c 5 cm.

Sample: **KFM08A 689.08–689.12 m**
Rock type: Pegmatite
Fracture: Open fracture
Orientation: 247/15°
Deformation zone: No zone
Fracture orientation set: HZ
Fracture minerals: Adularia, hematite, clay mineral

The diameter of the drill core is c 5 cm.

Sample: **KFM08A 789.42–789.50 m**
Rock type: Metagranite
Fracture: Open fractures
Orientation: 176/83°; 284/74°
Deformation zone: No zone
Fracture orientation set: NS and EW
Fracture minerals: Chlorite/corrensite, calcite, pyrite, hematite

Two open fractures, the one facing left in figure has an orientation of 284/74° and is coated with calcite, clay minerals and pyrite, and the one facing right in the figure has an orientation of 176/83° and is coated with chlorite/corrensite and hematite. The diameter of the drill core is c 5 cm.

Sample: **KFM08A 918.53–919.85 m**
Rock type: Breccia
Fracture: Crush zone
Orientation: ~ 110/60°
Deformation zone: No zone
Fracture orientation set: HZ
Fracture minerals: Quartz, plagioclase, calcite, laumontite, chlorite, hematite, illite

According to XRD analysis, the main minerals in the sample are quartz, plagioclase, calcite, laumontite, chlorite, hematite and illite. The fine fraction contains laumontite, quartz, hematite, chlorite, illite and mixed layer clay (smectite and/or vermiculate and possibly illite).

Crush zone with quartz, plagioclase, calcite, laumontite, chlorite, hematite and illite. The diameter of the drill core is c 5 cm.

Sample: **KFM08A 919.32–919.36 m**
Rock type: Metabasite
Fracture: Open fracture
Orientation: 095/60°
Deformation zone: No zone
Fracture orientation set: HZ
Fracture minerals: Laumontite, chlorite/corrensite, calcite

Open fracture with slickensides, the fracture minerals are laumontite, chlorite/corrensite and calcite.

Sample: **KFM08A 940.00–940.14 m**
Rock type: Metagranite
Fracture: Sealed fracture
Orientation: 207/71°
Deformation zone: No zone
Fracture orientation set: NE
Fracture minerals: Adularia, hematite, prehnite

Thin fractures sealed with adularia-hematite (red) and prehnite (green). The diameter of the drill core is c 5 cm.

Sample: **KFM08A 967.44–967.48 m**
Rock type: Metabasite
Fracture: Open fracture
Orientation: n.a.
Deformation zone: No zone
Fracture orientation set: n.a.
Fracture minerals: Chlorite/corrensite, epidote

Open fracture with chlorite/corrensite and epidote. The diameter of the drill core is c 5 cm.

Sample: **KFM08A 972.65–972.76 m**
Rock type: Metabasite
Fracture: Open fracture
Orientation: n.a.
Deformation zone: No zone
Fracture orientation set: n.a.
Fracture minerals: Chlorite/corrensite, laumontite, pyrite

Open fracture with chlorite/corrensite, laumontite and pyrite. The diameter of the drill core is c 5 cm.

Sample: **KFM08A 975.50–975.66 m**
Rock type: Metabasite
Fracture: Open fractures
Orientation: n.a.
Deformation zone: No zone
Fracture orientation set: n.a.
Fracture minerals: Laumontite, chlorite/corrensite, epidote, clay minerals

Open fractures coated with laumontite, chlorite/corrensite, epidote and clay minerals. The diameter of the drill core is c 5 cm.

Sample: **KFM08B 7.40–7.45 m**
Rock type: Metagranite
Fracture: Open fracture
Orientation: 048/86°
Deformation zone: No zone
Fracture orientation set: NE
Fracture minerals: Calcite, goethite, clay mineral

Sample: **KFM08B 8.18–8.29 m**
Rock type: Metagranite
Fracture: Open fracture
Orientation: 220/89°
Deformation zone: No zone
Fracture orientation set: NE
Fracture minerals: Chlorite, calcite, clay minerals

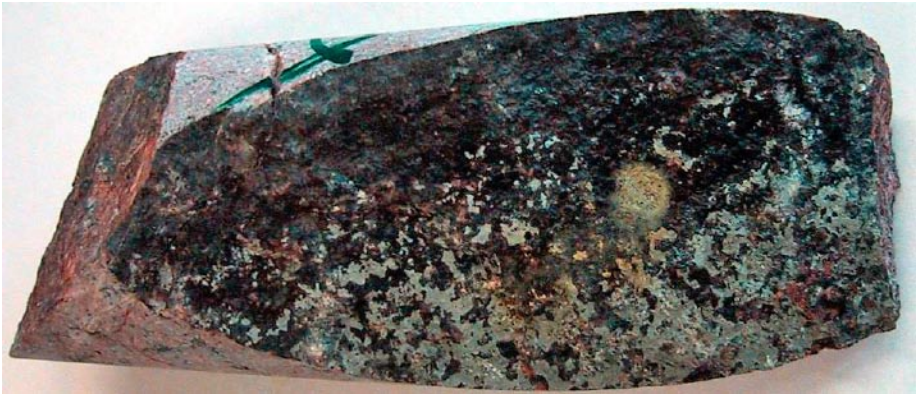

Sample: **KFM08B 13.19–13.23 m**
Rock type: Metagranite
Fracture: Open fracture
Orientation: 143/09°
Deformation zone: No zone
Fracture orientation set: HZ
Fracture minerals: Chlorite, calcite, clay minerals, adularia

Sample: **KFM08B 14.30–14.37 m**
Rock type: Metagranite
Fracture: Open fracture
Orientation: 242/54°
Deformation zone: No zone
Fracture orientation set: NE
Fracture minerals: Chlorite, calcite, adularia, quartz

Sample: **KFM08B 16.44–16.49 m**
Rock type: Metagranite
Fracture: Open fracture
Orientation: 033/85°
Deformation zone: No zone
Fracture orientation set: NE
Fracture minerals: Chlorite, clay mineral, calcite, quartz

Sample: **KFM08B 20.47–20.63 m**
Rock type: Metagranite
Fracture: Open fracture
Orientation: 068/81°
Deformation zone: No zone
Fracture orientation set: NE
Fracture minerals: Chlorite, clay mineral, calcite, quartz

Sample: **KFM08B 21.69–21.76 m**
Rock type: Metagranite
Fracture: Open fracture
Orientation: 272/16°
Deformation zone: No zone
Fracture orientation set: HZ
Fracture minerals: Chlorite, clay mineral, calcite, quartz

Sample: **KFM08B 26.42–26.58 m**
Rock type: Metagranite
Fracture: Crushed Zone
Orientation: 252/02°
Deformation zone: No zone
Fracture orientation set: HZ
Fracture minerals: Chlorite, clay mineral, pyrite, calcite

Sample: **KFM08B 30.72–30.92 m**
Rock type: Metagranite
Fracture: Open fracture
Orientation: 282/84°
Deformation zone: No zone
Fracture orientation set: EW
Fracture minerals: Clay mineral, calcite, pyrite

Sample: **KFM08B 41.98–42.11 m**
Rock type: Metagranite
Fracture: Open fracture
Orientation: 084/71°
Deformation zone: No zone
Fracture orientation set: EW
Fracture minerals: Clay mineral, quartz, adularia, calcite, pyrite, asphaltite

Sample: **KFM08B 43.50–43.54 m**
Rock type: Metagranite
Fracture: Open fracture
Orientation: 020/73°
Deformation zone: No zone
Fracture orientation set: NE
Fracture minerals: Chlorite, calcite, quartz, asphaltite, pyrite

Sample: **KFM08B 43.71–43.80 m**
Rock type: Metagranite
Fracture: Open fracture
Orientation: 050/85°
Deformation zone: No zone
Fracture orientation set: NE
Fracture minerals: Calcite, quartz, adularia, pyrite, asphaltite

Sample: **KFM08B 54.45–54.54 m**
Rock type: Metagranite
Fracture: Open fracture
Orientation: 164/81°
Deformation zone: No zone
Fracture orientation set: NS
Fracture minerals: Calcite, quartz, adularia, pyrite, asphaltite

Sample: **KFM08B 61.10–61.16 m**
Rock type: Metagranite
Fracture: Open fracture
Orientation: 051/05°
Deformation zone: No zone
Fracture orientation set: HZ
Fracture minerals: Quartz, adularia

Sample: **KFM08B 78.46–78.47 m**
Rock type: Metagranite
Fracture: Open fracture
Orientation: 038/74°
Deformation zone: No zone
Fracture orientation set: NE
Fracture minerals: Calcite, adularia

Sample: **KFM08B 91.36–91.58 m**
Rock type: Metagranite
Fracture: Open fracture
Orientation: 064/88°
Deformation zone: No zone
Fracture orientation set: NE
Fracture minerals: Calcite, quartz, asphaltite, pyrite

Sample: **KFM08B 97.37–97.43 m**
Rock type: Metagranite
Fracture: Open fracture
Orientation: 052/76°
Deformation zone: No zone
Fracture orientation set: NE
Fracture minerals: Calcite, quartz, clay mineral, pyrite

Appendix 2

Pyrite, sulphur isotopes

Sample	$\delta^{34}S$ (‰ CDT)	Laboratory
KFM01A 146.77B	7.5	IFE
KFM01A 267.00–267.20A	14.9	SUERC
KFM01A 267.00–267.20C	7.6	IFE
KFM01B 439.95–440.14	5.2	IFE
KFM04A 295.67–295.81A	–0.4	SUERC
KFM04A 295.67–295.81B	1.9	IFE
KFM04A 306.40–306.65	16.1	SUERC
KFM04A 415.30–415.35A	4.0	IFE
KFM04A 415.30–415.35B	15.3	SUERC
KFM04A 415.30–415.35C	12.3	SUERC
KFM05A 146.40–146.57	10.5	SUERC
KFM06A 331.88	14.1	SUERC
KFM06A 332.62	9.7	SUERC
KFM06A 356.33	7.0	SUERC
KFM06A 743.39	12.5	SUERC
KFM06A 743.39	–2.8	SUERC
KFM06B 90.6	14.0	SUERC
KFM06C 663.76A	20.4	SUERC
KFM06C 663.76B	21.7	SUERC
KFM06C 675.90	22.7	SUERC
KFM07A 274.95	11.1	SUERC
KFM08A 495.07	–1.3	SUERC

Appendix 3

Calcite, stable isotopes

Sample	$\delta^{13}C$ (‰ PDB)	$\delta^{18}O$ (‰ PDB)	$^{87}Sr/^{86}Sr$	Comment
KFM06A 794.78	–6.601	–12.553		
KFM06C 651.64A	–10.863	–13.225		Large euhedral on quartz
KFM06C 364.26	–1.59	–9.486		Chlorite
KFM06C 162.02	–20.256	–11.251		Later than fluorite
KFM06C 442.48	–3.148	–18.534		with laumonite
KFM06C 663.76	–13.19	–14.356		with quartz and pyrite
KFM06C 154.61	–17.925	–13.012		Large euhedral on quartz
KFM06C 450.62	–4.036	–18.216		with laumonite
KFM06C 103.19	–46.362	–12.078		With asphaltite
KFM06C 839.43	–1.625	–23.877		With red adularia
KFM06C 651.64A	–10.671	–13.165		
KFM06C 103.70	–33.392	–12.434		With asphaltite
KFM06C 453.84	–2.181	–23.888		With chlorite and adularia
KFM06C 675.90	–10.827	–14.122		With pyrite
KFM07A 112.34	–11.005	–7.945	0.716605	Water conductive zone
KFM07A 151.90	–1.835	–10.542		with laumonite
KFM07A 155.68	–2.179	–11.057	0.707695	with laumonite
KFM07A 178.46	–10.555	–14.168	0.715337	On chlorite/corrensite
KFM07A 193.77	–14.194	–12.019		On quartz and corrensite
KFM07A 274.95A	–13.319	–13.957		Massive
KFM07A 419.19	–4.972	–17.086		With chlorite
KFM07A 803.31	–11.115	–12.009	0.715776	clear scalenohedral
KFM07A 804.41	–12.57	–13.065		On quartz
KFM07A 876.11	–6.589	–8.561	0.712888	Cuts epidote and quartz
KFM07A 882.95	–10.339	–11.33		euhedral on quartz, clear
KFM07A 896.68A	–2.202	–9.387		with laumonite
KFM07A 896.68B	–1.789	–9.755		In zone
KFM07A 974.16	–14.775	–12.133		Equant
KFM07A 938.83	–4.255	–18.44		with laumonite
KFM07A 998.92	–10.605	–12.819		On quartz and corrensite
KFM08A 107.42	–16.504	–13.564		Breccia sealing
KFM08A 183.77	–14.598	–13.098		With prehnite
KFM08A 193.01	–13.716	–12.968		
KFM08A 245.46A	–13.781	–12.568		Late
KFM08A 245.46B	–18.899	–10.169		Late euhedral
KFM08A 246.11	–16.21	–9.624		On quartz and pyrite
KFM08A 274.58A	–5.247	–18.581		With laumontite
KFM08A 274.58B	–12.639	–13.211		With chlorite
KFM08A 304.57	–17.664	–12.432		Euhedral
KFM08A 410.60	–3.979	–20.903		Episyenite
KFM08A 411.55B	–4.28	–19.905		Episyenite
KFM08A 480.30	–21.632	–11.43		Equant
KFM08A 492.90A	–7.114	–15.242		With adularia
KFM08A 495.07	–16.391	–13.076		With pyrite and clay minerals

Sample	$\delta^{13}C$ (‰ PDB)	$\delta^{18}O$ (‰ PDB)	$^{87}Sr/^{86}Sr$	Comment
KFM08A 605.08	–2.811	–15.625		With epidote
KFM08A 919.32	–3.543	–18.026		With laumontite and chlorite/corrensite
KFM08B 7.40	–9.251	–12.497		thin layer
KFM08B 8.18	–12.367	–11.458		thin layer
KFM08B 13.19	–4.576	–9.575		With clay minerals
KFM08B 14.30	–4.106	–9.823		With clay minerals
KFM08B 16.44	–5.12	–21.721		With clay minerals
KFM08B 20.47	–4.392	–12.321		With clay minerals
KFM08B 21.69	–8.016	–8.119		With clay minerals
KFM08B 41.98	–40.65	–10.332		With clay minerals and asphaltite
KFM08B 43.50A	–53.102	–10.204		Scalenohedral with asphaltite
KFM08B 43.50B	–48.423	–11.736		Scalenohedral with asphaltite
KFM08B 54.50	–20.046	–11.845		With clay minerals and asphaltite
KFM08B 43.71	–18.065	–10.584		On quartz and asphaltite
KFM08B 78.46	–14.961	–11.048		
KFM08B 97.37	–17.746	–12.375		Thin layer

Appendix 4

Quartz, oxygen isotopes

Sample	$\delta^{18}O$ (‰ SMOW)
KFM06A 352.27	19.66
KFM06A 356.53	18.37
KFM07A 876.11	15.59
KFM06C 103.19	21.90

Appendix 5

XRD analyses of fracture fillings

	Ca	Qz	Plag	K-fsp	Pre	Lau	MLC	Chl	Bi	Hm	Ill	X
KFM06A												
357.81 m		xx	xx					xx	xx			Amp(xx)
fine fraction						x	xx	xx				
KFM06B												
55.52 m	xx	xx	xx	xx				x			xx	
Fine fraction	x	x	x				x	xx			xx	
KFM06C												
132.35 m	xx	xx	xx	xx			x	x				
fine fraction	xx	x	x	x			x					
149.54 m	xx	xx	x	x				xx			x	Apo(x)
fine fraction							x	x			x	Ver(xx)
398.2 m		xx	xx	xx				xx			xx	Mus(xx)
fine fraction							xx	xx			xx	Sme(x)
451.64 m	x		xx	xx								Go(x)
fine fraction	xx	xx	xx	xx							x	
482.94 m	xx	xx	x	x				xx			xx	Mus(xx)
fine fraction								xx			xx	Sme(x)
939.15 m	xx						xx	x				Corr(xx)
fine fraction	x						xx	x				Corr(xx)
KFM07A												
896.68 m	x	xx				x		x			x	
fine fraction							x	x			xx	
969.68 m	xx		x	xx				x				
fine fraction		x	x	x				xx			xx	
KFM08A												
197.65 m	xx	xx	xx	xx				xx			x	
fine fraction			x					x			x	Corr(x)
495.07 m		xx		xx	x			x			x	
fine fraction		x		x	x			xx			xx	
686.59 m	xx	x						x				Mus(xx)
fine fraction	x						x					Mus(xx)
918.53 m	xx	xx	xx			xx		xx		x	x	
fine fraction		xx				xx	xx	xx		xx	xx	
975.50 m		xx	xx	xx				xx			xx	Mus(xx)
fine fraction								xx			xx	

xx = main minerals, x = minor minerals, Amp = Amphibole, Apo = Apophyllite, Bi = Biotite, Ca = Calcite, Chl = Chlorite Corr = Corrensite, Go = Goethite, Hm = Hematite, Ill = Illite, K-fsp = K-feldspar (Adularia), Lau = Laumontite, MLC = Mixed layer clay, Mus = Muscovite, Plag = Plagioclase (Albite) Pre = Prehnite, Sme = Smectite, Sc = Swelling clay, Ver = Vermiculite, Qz = Quartz.

Appendix 6

Chemical analyses of fracture fillings

Sample		KFM06A 357.81	KFM06B 55.52	KFM06C 132.35	KFM06C 149.54	KFM06C 398.20	KFM06C 451.64	KFM06C 482.94
Minerals (XRD)		Amp,Bi,Pl, Qz, Chl MLC	Ca,Qz,Pl K-fsp,MLC Chl,Ill	Ca, Qz, Pl K-fsp,MLC Chl	Ca, Qz, Pl K-fsp,MLC Chl,Ill,Apo	Qz, Pl K-fsp,MLC Chl,Ill	Ca, Qz, Pl K-fsp,Ill	Ca, Qz, Pl K-fsp,Ill,Mus Chl,Sme
SiO_2	%	42.9	46.3	49.6	50.6	51.1	65.4	26
Al_2O_3	%	12.8	12.6	14.1	14.3	22	18.7	8.24
CaO	%	5.41	3.96	8.85	6.03	2.6	1.87	25.7
Fe_2O_3	%	18.7	9.13	5.21	11.6	6.95	0.499	9.76
K_2O	%	3.01	4.98	10.8	4.79	6.42	6.33	1.26
MgO	%	10.7	1.83	1.49	4.36	4.17	< 0.02	4.42
MnO	%	0.458	0.0563	0.0371	0.112	0.0474	0.0057	0.197
Na_2O	%	1.12	0.905	0.221	0.435	0.262	6.66	0.358
P_2O_5	%	0.185	0.0612	0.0104	0.0067	0.0079	0.0163	0.0227
TiO_2	%	0.782	0.279	0.0341	0.052	0.0376	0.108	0.261
Summa	%	96.1	80.1	90.4	92.3	93.6	99.6	76.2
Ba	mg/kg	335	835	1,690	500	225	766	548
Be	mg/kg	2.96	3.44	4.67	16.3	16.7	1.23	13.8
Co	mg/kg	39.9	8.65	< 9	< 6	< 6	68.7	< 6
Cr	mg/kg	896	26.4	< 20	< 10	< 10	< 10	< 10
Cs	mg/kg	4.35	8.49	< 0.2	4.39	11.6	< 0.1	0.443
Cu	mg/kg	8.11	21.7	19.3	11.5	10.8	6.07	9.94
Ga	mg/kg	13.4	22.2	28.8	26.7	38	8.49	16.4
Hf	mg/kg	2.1	4.19	1.19	1.09	0.559	4.55	2.26
Mo	mg/kg	< 2	10.2	< 4	< 2	< 2	< 2	< 2
Nb	mg/kg	32.8	8.51	2.57	5.94	3.71	13	13.4
Ni	mg/kg	144	< 10	< 20	< 10	< 10	< 10	< 10
Rb	mg/kg	157	161	76.5	187	373	157	51.1
Sc	mg/kg	52.4	10.7	7.2	3.85	3.15	2.72	16.2
Sn	mg/kg	22.8	2.06	31.3	12.7	5.66	2.45	7.49
Sr	mg/kg	63	70.8	68.7	44.7	97.2	76.9	82.7
Ta	mg/kg	4.97	0.69	0.202	0.51	0.285	1.35	1.15
Th	mg/kg	< 0.1	5.88	2.49	2.75	0.312	9.83	4.71
U	mg/kg	14.9	7.48	10.9	12.2	2.72	3.35	15.1
V	mg/kg	234	55.1	46.6	49.5	39	2.4	75.4
W	mg/kg	1.64	2.35	1.85	0.533	< 0.3	0.516	0.991
Y	mg/kg	73.1	39.5	42.2	600	61.8	19.4	136
Zn	mg/kg	287	179	46	65.9	46.2	< 10	176
Zr	mg/kg	39.6	169	26.3	97.1	16.8	201	96.2
La	mg/kg TS	28.2	40.8	622	7.04	5.35	20.5	55.7
Ce	mg/kg TS	50.4	91	1,020	22.3	18.5	47.1	116
Pr	mg/kg TS	5.8	10.1	105	5.11	4.52	5.76	15.9
Nd	mg/kg TS	26.4	32	376	30.6	9.61	18.4	63.5
Sm	mg/kg TS	6.27	6.85	45.3	28.7	4.45	5.12	19.8
Eu	mg/kg TS	0.68	0.787	2.13	5.63	0.649	0.355	1.68
Gd	mg/kg TS	4.21	4.25	17.8	39.1	3.57	2.73	17.6
Tb	mg/kg TS	1.15	0.673	2.41	7.34	0.445	0.213	3.03
Dy	mg/kg TS	7.41	4.5	7.67	48	4.74	2.58	18.2
Ho	mg/kg TS	1.76	0.995	1.15	9.89	1.11	0.522	3.35
Er	mg/kg TS	6.37	2.93	2.63	29.2	4.25	2.09	9.79
Tm	mg/kg TS	1.24	0.431	0.324	3.56	0.764	0.381	1.56
Yb	mg/kg TS	9.91	2.18	1.92	22.7	5.11	2.96	9.19
Lu	mg/kg TS	1.76	0.4	0.237	3.53	0.841	0.495	1.47

Sample		KFM07A 896.86	KFM08A 197.65	KFM08A 495.07	KFM08A 686.59	KFM08A 918.53	KFM08A 975.50
Minerals (XRD)		Qz,Lau Ca,Chl,Ill MLC	Ca,Qz,Pl K-fsp,Ill Corr,Chl	Qz,K-fsp Ill,Chl,Pre	Ca,Mus Qz,Chl MLC	Qz,Pl,Ca Lau,Chl,Hm Ill,MLC	Qz,Pl,Lau K-fsp,MLC Mus,Chl,Ill
SiO_2	%	64.8	45.5	60.5	46.9	51.4	57.1
Al_2O_3	%	14.7	14.6	16.6	21.9	16.5	22.1
CaO	%	3.49	7.94	0.702	6.15	4.39	0.435
Fe_2O_3	%	4.03	7.6	6.76	5.66	9.76	4.19
K_2O	%	4.26	5.81	7.25	7.28	3.85	6.66
MgO	%	3.04	6.77	3.51	1.76	6.18	3.52
MnO	%	0.0481	0.158	0.0556	0.0696	0.145	0.0418
Na_2O	%	0.229	0.699	0.319	1.17	1.12	0.276
P_2O_5	%	0.114	0.0118	0.025	0.0116	0.176	0.0157
TiO_2	%	0.421	0.0881	0.165	0.356	0.883	0.109
Summa	%	95.1	89.2	95.9	91.3	94.4	94.4
Ba	mg/kg	205	1350	589	2040	195	584
Be	mg/kg	1.91	7.71	4.2	9.81	7.04	6.96
Co	mg/kg	< 6	< 6	< 6	< 6	18.3	< 6
Cr	mg/kg	17.7	13.9	26.4	258	85.1	< 10
Cs	mg/kg	8.25	0.344	6.12	17.6	12.1	8.48
Cu	mg/kg	9.4	47.8	18.2	73.5	17.1	8.49
Ga	mg/kg	< 1	35.8	18.9	35.7	< 1	21.9
Hf	mg/kg	3.07	1.03	2.89	1.56	2.09	3.29
Mo	mg/kg	< 2	< 2	< 2	< 2	< 2	< 2
Nb	mg/kg	6.36	3.81	12.9	10.5	6.3	14.3
Ni	mg/kg	< 10	< 10	< 10	< 10	15	< 10
Rb	mg/kg	301	158	589	342	295	371
Sc	mg/kg	11	13.6	11.2	13.9	34.8	3.05
Sn	mg/kg	3.27	28.4	3.89	13.1	20.3	11.5
Sr	mg/kg	64.9	163	42.1	48.2	136	28.9
Ta	mg/kg	0.88	0.476	3.21	0.585	0.555	1.05
Th	mg/kg	< 0.1	2.4	0.486	< 0.1	< 0.1	3.04
U	mg/kg	2.94	10.3	7.97	164	20.5	9.56
V	mg/kg	55.4	32.5	87	93.8	187	7.76
W	mg/kg	68.3	0.713	48.4	68.6	7.75	1.45
Y	mg/kg	25.9	53.2	521	62.4	37.4	118
Zn	mg/kg	54.8	131	77.2	51.9	109	42.3
Zr	mg/kg	129	28.4	80.4	73.4	92.7	177
La	mg/kg TS	16.1	286	12.5	62.3	19.2	8
Ce	mg/kg TS	32.3	469	37.9	110	37.2	20.9
Pr	mg/kg TS	4.17	48.8	7.08	13.8	4.22	7.45
Nd	mg/kg TS	19.7	141	50.1	55	20.9	14.3
Sm	mg/kg TS	4.06	19	23	9.87	3.11	5.85
Eu	mg/kg TS	0.759	1.38	2.71	0.503	1.31	0.651
Gd	mg/kg TS	2.79	5.58	34.6	7.59	2.95	5.57
Tb	mg/kg TS	0.572	1.25	6.2	1.42	0.623	1.29
Dy	mg/kg TS	3.16	6.26	40	7.68	3.71	9.88
Ho	mg/kg TS	0.679	1.11	8.92	1.55	0.907	2.2
Er	mg/kg TS	1.86	4.25	27	3.55	2.59	6.85
Tm	mg/kg TS	0.331	0.619	3.79	0.616	0.373	1.38
Yb	mg/kg TS	2.33	3.13	26.9	4.16	3.23	6.54
Lu	mg/kg TS	0.377	0.638	3.97	0.545	0.529	0.879

Ab = albite, Amp = amphibole Ana = analcime, Apo = apophyllite, Asph = asphaltite, Chl = chlorite, Corr = corrensite, Hm = hematite, Ill = illite, K-fsp = K-feldspar, Lau = laumontite, MLC = Mixed layer clay, Mus = muscovite, Pl = plagioclase, Pre = prehnite, Qz = quartz, Sme = smectite.

Appendix 7

Uranium series analyses

Sample	^{238}U (Bq/kg)	±	^{235}U (Bq/kg)	±	^{234}U (Bq/kg)	±	^{230}Th (Bq/kg)	±	^{232}Th (Bq/kg)	±	^{234}U/^{238}U	^{230}Th/^{234}U	^{234}U/^{238}U
KFM01B 28.65–28.70 m	201	2.3	7.6	0.42	319	3	331	6.7	66	2.1	1.59	1.04	1.59
KFM01B 47.9–48.0 m	237	2.5	9.5	0.46	367	3.2	382	8.1	24.2	1.2	1.55	1.04	1.55
KFM01B 418.29–43 m	72	0.68	2.7	0.12	70	0.67	80	1.6	3.2	0.18	0.97	1.14	0.97
KFM03B 65.2–65.25 m	174	1.3	7	0.25	181	1.3	531	11	47	1.8	1.04	2.93	1.04
KFM03A 643.8–644.17 m	25,300	374	940	21	25,700	380	31,300	656	69	3.8	1.02	1.22	1.02
KFM03A 803.85–804.05 m	134	1.2	5.2	0.23	129	1.2	173	3.5	26	0.9	0.96	1.34	0.96
KFM05A 111.56–111.60 m	34.8	0.47	1.4	0.09	33	0.47	46.5	1	19	0.5	0.95	1.41	0.95
KFM06A 145.62–145.73 m	169.8	1.6			333	2.3	275.1	4.6	11.2	0.5	196.00	1.22	1.96
KFM06A 622.31–622.36 m	60.5	0.8			55	0.8	61.6	2.4	23.5	1.3	91.00	1.12	0.91
KFM06A 770.32–770.42 m	241.9	1.9			239.1	1.9	268	5.5	92.6	2.4	99.00	1.12	0.99
KFM07A 896.68–896.77 m	34.9	0.4			35.1	0.4	35	1.2	48.6	1.4	1.00	1.00	1.00
KFM07A 969.68–969.80 m m	350.30	2.70			354.40	2.70	364.10	6.5	151.60	3.20	1.01	1.03	1.01
KFM08A 495.07–495.37 m	92.00	1.40			92.00	1.40	91.00	1.90	39.00	0.90	1.00	1.00	1.00
KFM08A 686.59–686.84 m	1,450.00	24.00			1,844.00	27.00	1,778.00	38.00	22.00	2.30	1.27	0.96	1.27
KFM08A 918.53–918.85 m	283.00	3.30			281.00	3.30	262.00	2.50	34.00	6.60	0.99	0.93	0.99